CERAMIDE SYNTHASE 6 IN METABOLIC RESPONSE TO
DIETARY FAT AND FOLIC ACID

Keri Anne Barron

A dissertation submitted to the faculty at the University of North Carolina at Chapel Hill in partial fulfillment of the requirements for the degree of Doctor of Philosophy in the Department of Nutrition in the Gillings School of Global Public Health.

Chapel Hill
2020

Approved by:

Natalia Krupenko

Sergey Krupenko

Folami Ideraabdullah

Susan Smith

Stephen Hursting

ABSTRACT

Keri Anne Barron: Ceramide Synthase 6 in Metabolic Response to Dietary Fat and Folic Acid
(Under the direction of Natalia Krupenko)

Ceramides, a class of bioactive lipids, are important regulators of cellular metabolism mediating response to nutrient stress. Recent work from our laboratory demonstrated that, in cultured cells, folate stress response is mediated by ceramide synthase 6 (CerS6), a sphingolipid enzyme producing C_{16}-ceramide. To test the hypothesis that alterations in dietary FA will induce a CerS6-dependent response in mice, we evaluated the sphingolipid and metabolomic responses in WT and CerS6 KO mice. We also investigated the role of dietary fat in the response to folate stress in WT and KO mice. This dissertation sought to characterize the sphingolipid and metabolomic responses in wild type (WT) and CerS6 knockout (KO) mice to both short-term alterations in dietary FA as well as to long-term changes in dietary FA combined with high fat diet.

As expected, CerS6 KO mice compared to WT mice exhibited significant differences in liver sphingolipids, free fatty acids and phosphatidylethanolamines, among other lipids. Inducing folate stress resulted in changes to sphingolipid pools in the liver with significantly different responses between sexes. Because folate has been shown to influence lipid metabolism, we further challenged CerS6 KO and WT mice by altering folate levels in a high fat diet. We found that the low FA, high fat diet led to increased weight gain, hepatic lipid droplet accumulation, and elevated plasma sphingolipid species in male WT mice only. CerS6 KO mice were mostly

protected from diet-induced weight gain and lipid droplet accumulation. Additionally, they exhibited significantly lower levels of many plasma sphingolipid species indicating that CerS6 plays a critical role in shaping the plasma sphingolipid profile. Interestingly, the presence of too little or too much FA was similarly detrimental in male WT mice whereas female mice demonstrated a protection on the FD diet.

In summary, our studies demonstrate that dietary FA affects hepatic and plasma sphingolipid profiles after short- and long-term consumption and that CerS6 is involved in the whole-body response to folate stress. These results underscore the role of ceramides in mediating nutrient challenges as well as the need to investigate the effects of FA supplementation on tissue metabolomes.

To my parents, Jim, Stephanie, Kaity, Andy, and Kalie for supporting me in every way, believing in me when I was unable to see the end, and encouraging me daily. I wouldn't have gotten here without all of you.

ACKNOWLEDGEMENTS

To my advisor, Natalia Krupenko, for her mentoring, support, encouragement and taking me in as a student when I needed a lab. Thank you for listening to my input on the studies we planned, always hearing me out, and telling me to calm down when I needed it most.

To the original Bennett lab members- the people who first welcomed me into the NRI family and taught me the basics of science I would need for the future. Specifically, thank you to Jody and Melissa for becoming friends and family down here. You never gave up on me and were always willing to listen to me stress and vent. Melissa- thank you for only ever giving me 50% of a protocol but helping me figure it out when everything didn't work. Jody- thank you for always being a friend even through the hard times. And for cleaning up your side of our bench from time to time. Brian- thank you for always pushing me to be better and learn more, except for learning R. That was dumb and I hated every minute of it. And thank you for buying me a brownie when mine was wrongfully consumed.

To Kristen and Madeline- thanks for being supportive and optimistic even when I was miserable, for helping me out with lab work especially all of the terrible westerns, and for always being down to get coffee, shamrock shakes, and anything else that sounded delicious. Additionally, to both Krupenko labs for the laughs in lab meetings, encouragement, and constructive criticism that helped me become a better scientist.

Finally, I want to thank my Refuge Church family- my Vertical girls and co-leaders over the years that have watched me stress and always remained supportive and unwaveringly

PREFACE

In addition to the work conducted and included in this dissertation I have co-authored 2 papers related to CerS6. The first is a comparative study of CerS6 using bioinformatic approaches and the second is a review of the literature on possible CerS6-related mechanisms in the link between alcohol and development of cancers:

Holmes RS, Barron KA, Krupenko NI. Ceramide Synthase 6: Comparative Analysis, Phylogeny and Evolution. *Biomolecules.* 2018 Oct; 8(4). PMID: 30297675

Barron K*, Jeffries KA*, Krupenko NI. Sphingolipids and the link between alcohol and cancer. *Chem. Biol. Interact.*, In press.

Additionally, I contributed to a collaborative study with members of the nutrition department which is not related to the work presented in this dissertation.

Xu X, Drobna Z, Voruganti VS, Barron K, Gonzalez-Horta C, Sanchez-Ramirez B, Ballinas-Casarrubias L, Ceron RH, Moralles DV, Terrazas FAB, Ishida MC, Gutierrez-Torres DS, Saunders RJ, Crandell J, Fry RC, Loomis D, Garcia-Vargas GG, Del Razo LM, Styblo M, Mendez MA. Association between variants in arsenic (+3 oxidation state) methyltransferase (*AS3MT*) and urinary metabolites of inorganic arsenic: Role of exposure level. *Toxicol Sci.* 2016 Sept; 153(1):112-123. PMID: 27370415

* co-first authors.

TABLE OF CONTENTS

LIST OF TABLES

LIST OF FIGURES

LIST OF ABBREVIATIONS

CerS6   Ceramide Synthase 6

FA   Folic acid

WT   Wild-type

KO   Knock-out

Cer   Ceramide

THF   Tetrahydrofolate

5-MTHF   5-methyl-tetrahydrofolate

SAM   S-adenosyl-methionine

DNA   deoxyribonucleic acid

RNA   ribonucleic acid

SAH   S-adenosyl-homocysteine

MTHFR   Methylenetetrahydrofolate reductase

DHFR   Dihydrofolate reductase

HFD   High fat diet

mRNA   messenger ribonucleic acid

PPARδ   Peroxisome proliferator-activated receptor gamma

MCP-1   monocyte chemoattractant protein 1

TNFα   Tumor necrosis factor alpha

BMI   Body mass index

IR   Insulin resistance

AMPK   5' AMP-activated protein kinase

RFC   Reduced folate carrier

Sph   Sphingosine

SM   Sphingomyelin

GlucCer	Glucosyl-Ceramide
CoA	Coenzyme A
SPT	Serine palmitoyl transferase
CerS	Ceramide Synthase
dhCer	Dihydroceramide
S1P	Sphingosine-1-phosphate
ER	Endoplasmic reticulum
SMase	Sphingomyelinase
CERT	Ceramide transferase protein
GlucCerS	Glucosylceramide synthase
siRNA	small interfering ribonucleic acid
HexCer	Hexosyl-ceramide
IL	Interleukin
WAT	White adipose tissue
BAT	Brown adipose tissue
DIO	Diet-induced obesity
PKCζ	Protein kinase c zeta
ASO	Antisense oligonucleotide
ALDH1L1	Aldehyde dehydrogenase 1 family member L1
IFNγ	interferon-gamma
SNP	Single nucleotide polymorphism
ATP10D	ATPase Phospholipid Transporting 10D (Putative)
GCase	glycosidases
FD	Folate deficient
Ctrl	Control

FS	Folate over-supplemented
HPLC-MS/MS	High-performance liquid chromatography- tandem mass spectrometry
SEM	Standard error of measurement
FIGLU	Formiminoglutamate
7,8-DHF	7,8-dihydrofolate
PCFT	Proton-coupled folate transporter
ATP	Adenosine triphosphate
HF	High fat
RER	Respiratory exchange ratio
NAFLD	Non-alcohol fatty liver disease

CHAPTER 1: INTRODUCTION

Ceramides (Cer) are bioactive lipids regulating multiple cellular processes and they have been implicated in the development and progression of several disease states [1]. As such, they are gaining attention as potential biomarkers for diseases including atherosclerosis [2] and colorectal cancer [3]. Ceramide analogs and inhibitors are also being developed as potential treatment modalities for conditions including obesity and insulin resistance [4, 5]. While these studies are producing promising data about the effectiveness of these new therapeutic strategies, the effect of diet on ceramide metabolism and therapeutic interventions cannot be ignored.

In this dissertation, we have specifically focused on the role of Ceramide Synthase 6 (CerS6), one the six enzymes producing ceramides. CerS6 generates C_{14}- and C_{16}-ceramides and is expressed in most tissues at low levels. C_{16}-ceramide is considered to be a lipotoxic mediator of metabolic stress based on a plethora of evidence indicating the detrimental role it plays in both cells and rodent models [6]. As a result, suppression of C_{16}-ceramide production is often viewed as a strategy for overcoming negative impact of stressors. However, the role of CerS6 in cellular homeostasis is not well defined and knocking out CerS6 can provide important information about the functions of this enzyme and its product C_{16}-ceramide at the whole-body level. Ceramides are known to respond to nutrient stress, including withdrawal of magnesium [7, 8], treatment with a synthetic retinoid [9] or vitamin E metabolite, γ-tocotrienol [10], and increased supply of fatty acids [11]. Changes in ceramide levels in response to the aforementioned nutrients occur via several mechanisms including upregulation of *de novo* ceramide biosynthesis as indicated by increased dihydroceramide species [9, 10] and through alterations of the activity

of enzymes involved in sphingolipid metabolism [7]. Furthermore, CerS6 is directly involved in the cellular response to folate stress, including folate withdrawal [12]. The removal of folate from cell culture media resulted in elevation of CerS6 and increased cellular C_{16}-ceramide concentrations, as well induction of apoptosis [12].

Since most of the data on ceramide response to nutrient stress were obtained in cultured cells, we sought to determine the ceramide response to dietary folate stress in an animal model. In Chapter III, we investigate the metabolic alterations resulting from short-term dietary exposure to both low and high folate supplementation in CerS6 knockout (KO) and wild-type (WT) mice. We hypothesized that C_{16}-Cer levels would increase in wild type mice after exposure to a folate-deficient diet, congruent to the cell culture findings, but also that CerS6 KO mice would have reduced C_{14}- and C_{16}-Cer that will not change due to folate supplementation and may be compensated by increases of other ceramide species. Our metabolomics results revealed that both loss of CerS6 and dietary folate supplementation that was too high or too low resulted in significant changes of several lipid classes, including sphingolipids. In Chapter IV, we sought to characterize the role of CerS6 in response to HFD in mice by comprehensively examining body composition, indirect calorimetry, food and water intake, plasma ceramide concentrations, as well as liver and plasma metabolomes. Based on results of published studies, we hypothesized that CerS6 KO mice would be protected from high fat diet-induced weight gain with further protection demonstrated in the metabolomes of liver and plasma tissues indicating an overall protective effect of lowering C_{16}-Cer levels beyond sphingolipids. In Chapter V, we investigated plasma ceramide response to either low or high folate intake combined with a high fat diet to evaluate the effects of long-term exposure to suboptimal folate supplementation and high fat in plasma. This allowed us to understand dietary influence of the ceramide profile of WT mice but

also begin to assess how diet may affect the efficacy of ceramide-related inhibitors or drugs designed to lower C_{16}-Cer levels through studying the effects of folate stress in CerS6 KO mice, which lack the ability to respond to nutrient stress through C_{16}-Cer. We hypothesized that a high fat diet combined with low folate intake would increase plasma ceramide levels in addition to causing greater weight gain and fat mass accumulation. The results revealed differential effects of folate consumption between male and female mice, however CerS6 KO mice, regardless of sex, were protected from many of the detrimental effects of high fat diet consumption.

This is the first study to directly investigate micronutrient alterations in an animal model with the goal of evaluating compensatory ceramide response. Our data provide valuable information about the response of plasma ceramides to dietary intervention, which is critical if ceramides are going to be utilized as biomarkers or as therapeutics for common diseases. Taken together, these results indicate that both hepatic and plasma ceramide pools respond to dietary folate consumption and that response is sexually dimorphic. These results warrant further investigation of ceramide response to other nutrients, as well as call for human studies to determine reference ceramide intervals for each sex before plasma ceramides could be used as a biomarker or disease risk scores.

CHAPTER 2: BACKGROUND

Background

Folate function and its link to multiple metabolic pathways

Folate, one of the B-vitamins, is a generic name for a family of chemically similar

compounds that function as carriers of one-carbon groups and are involved in the biosynthesis of

nucleotides and the metabolism of amino acids [13, 14]. A folate molecule consists of a pterine

ring conjugated to p-aminobenzoic acid which is linked via amide bond to one or multiple

glutamic acid residues linked by peptide bonds via γ-carboxyl groups [13]. It is an essential

micronutrient as humans are unable to synthesize folate *de novo* and therefore must acquire it

from their diet [13]. In nutritional sciences the term folate is used for a group of natural

compounds related to folic acid which are found in green leafy vegetables, whereas folic acid

(FA) is the name for the synthetic vitamer which contains a single glutamic acid residue and has

pterine ring in the oxidized state [13]. FA is not an active coenzyme and must undergo several

conversion steps within the cell in order to become a coenzyme [14], but FA is highly stable and

bioavailable, which explains its wide use as a pro-vitamin [15, 16]. Folate ingested from the diet

mainly exists as polyglutamates and must be hydrolyzed to monoglutamates in the intestinal

mucosa before being transported for further metabolism [14]. Several different species of folate

are important in one carbon metabolism, each differing in the presence and oxidation state of the

one-carbon group attached to the N5 and/or N10 positions of the tetrahydrofolate (THF)

backbone [13]. Folate has important roles in the synthesis of purine and pyrimidine precursors of

nucleic acids [14], the metabolism of methionine, serine, glycine and histidine, and for the

formation of methyl group donors which are required for normal metabolism and gene regulation [14]. 10-formyl-THF is used in two reactions of *de novo* purine biosynthesis, and 5-methyl-THF (5-MTHF) supports methylation reactions. The methyl group on 5-methyl-THF is transferred to homocysteine to produce methionine which is converted to S-adenosyl-methionine (SAM), a universal methyl group donor. SAM can then methylate proteins, lipids, and nucleic acids (deoxyribonucleic acid (DNA) and ribonucleic acid (RNA)), in addition to providing methyl groups for biosynthetic reactions such as the synthesis of hormones and other small molecules [17]. As SAM donates a methyl group to its target, it becomes S-adenosyl-homocysteine (SAH) which is further metabolized to homocysteine. 5-MTHF can remethylate homocysteine to methionine, which is further converted to SAM, which can be used for next methylation. Thus 5-MTHF completes the cycle and prevents accumulation of homocysteine and possibly the harmful effects associated with homocysteine accumulation [14]. Thus, folate is a critical piece to several metabolic pathways including nucleotide biosynthesis, amino acid metabolism, and methylation reactions via supporting adequate SAM/SAH levels [17]. Therefore, maintaining an adequate supply of folate is required for normal cell function, and suboptimal folate supply is linked to adverse health effects [18]. An overview of folate metabolism and its links to other metabolic pathways are shown in Figure 2.1.
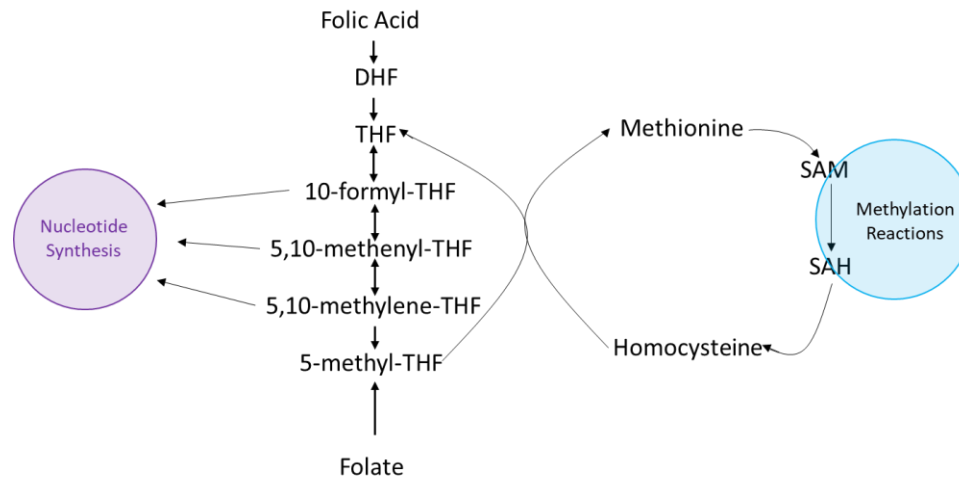
Figure 2.1 Folate and folic acid in one-carbon metabolism

Folate deficiency affects many cellular processes

Inadequate intake of folate results in folate deficiency which has widespread effects due to its role in many cellular processes. Folate deficiency can lead to altered protein expression [19-21], increased DNA damage and chromosomal fragility [22, 23], impaired cellular division [24], and even altered melatonin secretion [25] and disturbances in circadian rhythm [26]. Folate inadequacy induces both DNA hypomethylation and DNA strand breaks hyperhomocysteinemia as homocysteine generated by SAH hydrolysis cannot be remethylated to methionine [26], and this is associated with an increased risk of vascular disease [23, 27]. Hyperhomocysteinemia can also result in reduction of SAM levels and impaired DNA methylation [28-30]. Folate deficiency perturbs lipid metabolism, leading to accumulation of triglycerides in the liver [31] and changes in expression of genes involved in cholesterol biosynthesis [32] and fatty acid metabolism [26]. Folate deficiency is also considered a public health issue because inadequate consumption of folate during pregnancy significantly increases the risk of neural tube defects in the developing fetus [33].

Severe folate deficiency is not a common micronutrient deficiency in industrialized nations [34], however, there are several conditions under which folate is not metabolized correctly or efficiently which can result in functional deficiency. Poor absorption in the intestines may result in significantly reduced levels of folate being delivered to the liver [14]. Additionally, if the pH of the intestine is altered, there could be incomplete deconjugation of folate which would reduce its absorption [35, 36]. Therefore, despite adequate folate consumption, the downstream alterations in digestion, absorption and transport of folate could result in significantly decreased levels of folate in the liver and other tissues [14]. Additionally, increased demand such as during physical activity or pregnancy can cause deficiency if intake is not appropriately increased [14]. Pathological liver conditions, drug interactions, and genetic mutations also contribute to functional folate deficiency [14]. The most studied genetic polymorphism in folate metabolism is 677C→T in methylenetetrahydrofolate reductase (MTHFR) which catalyzes the reaction producing 5-methyl-THF. The TT genotype *in vitro* enzyme activity was reduced by 75% compared to that of wild-type enzyme [14]. This mutation affects 5-20% of the populations studied [37]. There is also a 19-base pair deletion in dihydrofolate reductase (DHFR) gene which can alter folate metabolism [14] and up to 5-fold differences in the activity of DHFR has been reported among individuals [38]. Functional folate deficiency can also arise from inadequate intake of other B-vitamins which are involved in one carbon metabolism, including B_2, B_6 and B_{12}. As such, if folate levels are low this can also affect the metabolism of B_2, B_6 and B_{12} [34]. Alternatively, if levels of these vitamins are insufficient, it could result in altered folate metabolism. Mild inadequacies of these B-vitamins commonly occur in industrialized nations and depletion of one often leads to biochemical phenotypes characteristic of the deficiencies of the others [34], meaning inadequate intake of B_{12} could cause

functional folate deficiency in liver tissue. Approximately 18-25% of adolescents and adults have blood indicators of B_6 status that fall below the accepted lower limits in US and western Europe while 15-20% of elderly populations are thought to have marginal B_{12} status [34]. Despite presumed adequate folate intake, it is possible that these groups may experience functional folate deficiency.

Adverse effects of excessive folate intake

Mandatory fortification of grain foods with FA began in the United States in the 1990s [39] to help reduce the incidence of neural tube defects. This effort was unique in that the target population for the fortification is many times smaller than the population affected by folic acid fortification. There are serious concerns regarding the consequences of excessive consumption of folic acid. While consumption of the natural form of folate is rarely above the upper limit, a combination of fortified foods, supplements, and multivitamins has been shown to result in significant accumulation of unmetabolized FA in cells [38]. Data from the National Health and Nutrition Examination Survey found that approximately 25% of children and 5% of adults over 50 years of age consume more than the recommended upper limit for FA [40-42]. Excessive folic acid intake can alter the flux through one carbon metabolic pathways and gene expression patterns, all of which can result in liver injury [37], as liver is the primary site of folate metabolism and the site of most folate-dependent enzymes [43]. As such, alterations in folate metabolism are likely to affect the liver before other tissues. Studies have found that excessive intake of FA increases the incidence of certain cancers [44, 45] potentially through overwhelming folate-metabolizing pathways, resulting in increased production of nucleotides which allows cells to divide rapidly. It is also possible that increased blood levels of unmetabolized FA may interfere with folate transport and metabolism or competitively inhibit natural folates from binding to enzymes and carrier proteins [46]. High intake of FA may also

lead to the accumulation of dihydrofolate which inhibits thymidylate synthase and MTHFR, leading to decreased levels of thymidylate and 5-MTHF. This shortage of thymidylate can impair DNA integrity and cellular division and the lack of 5-MTHF decreases methionine biosynthesis which can affect DNA methylation. Christensen et al. found that MTHFR activity was reduced in the liver of mice fed a high folic acid diet [37], confirming findings from early studies indicating that unmetabolized folic acid may contribute to MTHFR deficiency by inhibiting its activity [47]. High FA consumption may alter the expression of genes involved in one-carbon metabolism and lipid metabolism [37, 48]. Studies have also found a link between circulating unmetabolized FA levels and lower cognitive test scores [49] and impaired immune function in humans [50]. In many ways, excessive folic acid consumption is metabolically similar to folate deficiency [51, 52].

Folic acid affects lipid metabolism

Folate is at the center of one carbon metabolism, including nucleotide biosynthesis and methylation reactions, but it also affects lipid metabolism. Studies have found both negative and positive effects of FA supplementation on mitigating the consequences of a high fat diet (HFD). When mice were fed HFD that was supplemented with FA, they had lower blood glucose concentrations, decreased inflammation, reduced serum cytokines, and altered adipose tissue gene expression [53]. It was suggested that FA supplementation may alter adipocyte function and insulin resistance by changing DNA methylation and messenger RNA (mRNA) expression of obesity-relevant genes. Sid et al. reported that FA supplementation had no effect on HFD-induced body weight gain in mice [54]. However, it did attenuate the increase in blood glucose levels and reduced total and free cholesterol without changing triglyceride content of the liver [54]. Furthermore, FA supplementation along with HFD has been shown to protect against liver injury and preserve the structural integrity of the liver [55].

In contrast to studies demonstrating a positive effect of FA in reducing detrimental effects of HFD, several studies have demonstrated negative effects of folic acid supplementation. Kelly et al. found that excess FA on HFD increased weight gain, adipose tissue mass, and markers of inflammation compared to adequate FA intake [48]. These effects were not seen with excess FA on a low-fat diet. In cell culture models, FA increased triglyceride accumulation in 3T3-L1 cells, which can differentiate into adipose tissue, by inducing peroxisome proliferator-activated receptor gamma (PPARγ), a key regulator of adipogenesis and promoter of lipid storage [56]. Furthermore, rats fed HFD with excess FA exhibited impaired glucose clearance, increased adipocyte size, increased mRNA levels of triglyceride synthetic genes, and increased expression of PPARγ in adipose tissue, but there were no differences in plasma triglycerides or cholesterol in rats [48]. Monocyte chemoattractant protein 1 (MCP-1) levels, a marker of inflammation, along with protein and mRNA levels of tumor necrosis factor alpha (TNFα) were also higher in the adipose tissue of rats fed a high fat-excess folic acid diet [48]. In a separate study, FA supplementation in rats decreased PPARγ promotor methylation in the liver leading to increased PPARγ gene expression [57]. The authors concluded that excess dietary FA exacerbates fat mass gain, adipose tissue inflammation and systemic glucose intolerance in rats fed HFD. The differential effects of FA in rodent models may be due to the life stage, animal model, duration and amount of FA, dietary composition, or specific tissues being investigated. However it should be noted that translating findings in rodents to humans is difficult because rodents can efficiently metabolize folic acid and may be able to tolerate higher doses compared to humans [54].

The relationship between FA and lipid metabolism has been studied in humans in addition to the aforementioned *in vivo* and *in vitro* studies. Obese patients demonstrated low

folate levels in circulation [58-60], independent of dietary intake [61] and studies have found an inverse association between serum folate levels and body mass index (BMI) [62]. Low maternal folate levels were also associated with an increased risk of obesity, insulin resistance (IR), and type 2 diabetes in the offspring later in life [63, 64]. Folic acid supplementation has also been found to decrease IR and plasma levels of homocysteine while improving blood glucose control in obese patients with type 2 diabetes [65-67]. As such, decreased folate concentrations may influence susceptibility to metabolic syndrome [68, 69]. Interestingly, there are studies supporting the beneficial effects of supplementation on marginally adequate populations. When 97 young adult Caucasian individuals were grouped according to their folate intake (<40% versus 40-90% Reference Daily Intake), FA supplementation reduced total cholesterol levels in both groups [70]. Folic acid supplementation also resulted in significantly improved kidney function in the group with low folate in their diet indicating beneficial effects of mild FA supplementation [70]. In patients with metabolic syndrome, folate supplementation improved IR and endothelial dysfunction while decreasing homocysteine levels [68, 69]. It is likely that the benefits of FA supplementation may be lessened or absent in people that have adequate levels of folate. Elucidating the mechanisms connecting folate and lipid metabolism should be prioritized as folate may counteract the negative effects of HFD. Consumption of HFD contributes to the development of obesity and metabolic syndrome which affects nearly 40% of US adults [71]. Therefore, if folate is proven to be a safe and effective way to restore proper metabolism, it could significantly help many at-risk individuals.

Mechanisms connecting folate and lipids

The mechanisms linking folate to lipid metabolism are not fully known, but several pathways have been suggested. Phospho-5' AMP-activated protein kinase (AMPK) protein levels were markedly reduced in the liver of mice fed a high fat diet, while total AMPK protein

levels remained unchanged indicating inactivation of AMPK under high fat feeding [54]. Supplementation with FA increased AMPK phosphorylation and consequently its activation in the liver. The authors provided results from both animal and cell culture models indicating a role of FA in activating AMPK. They also found that FA supplementation increased levels of AMP which could further activate AMPK, a known regulator of glucose and cholesterol metabolism [54]. Another study also found that methyl donor supplementation increased activity of AMPK and suggested that AMPK may bind SAM directly and therefore act as a SAM-sensor [72].

Several possible mechanisms connecting folate to a negative effect on lipid metabolism have been suggested. Feeding mice HFD for 8 weeks resulted in hepatic lipid accumulation and decreased folate transporter via downregulation of NRF-1 [73]. There was also a significant downregulation of reduced folate carrier (RFC) protein in the liver of mice fed HFD, whereas expression of other transporters was not affected. Excessive FA may induce pseudo-MTHFR deficiency which may render hepatocytes more sensitive to phospholipid and lipid disturbances, leading to liver injury [37]. It is also possible that excessive FA promotes lipid accumulation by impairing fatty acid oxidation through decreased expression of carnitine palmitoyl transferase 1 (*cpt1a*)[74], an enzyme essential for fatty acid oxidation. Choline, a contributor to one carbon metabolism, may also be an important connection between folate and lipids. Folate deficiency may reduce hepatic phosphocholine biosynthesis which activates sterol regulatory element-binding protein 1a (SREBP1a) to stimulate *de novo* fatty acid synthesis [75]. Supporting this notion, the consequences of FA deficiency are also more evident when methionine and choline are also depleted in the diet [76].

Sphingolipid metabolism

Sphingolipids, a class of lipid molecules having a sphingoid base in their structure, comprise one of the major classes of membrane lipids [77, 78]. Ceramides, sphingosine (Sph), sphingomyelins (SM) and glucosyl-ceramides (GlucCer), among others, are members of this class (Fig 2.2) [78-80].
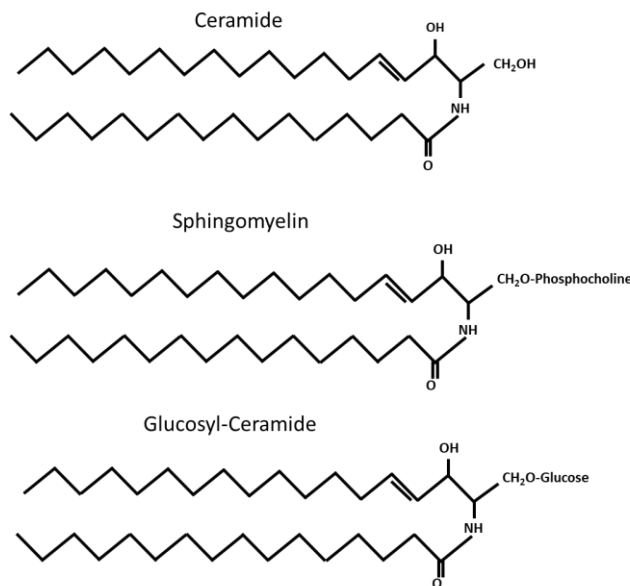
Figure 2.2 Basic structure of ceramide, sphingomyelin and glucosyl-ceramide

In the past, significance of these lipids was linked purely to their role as structural components of biological membranes. Changes in the membrane lipid composition were shown to affect many cellular functions including vesicular trafficking, cell-to-cell communication and signal transduction [81]. In addition to their role as structural components of cellular membranes [78, 82], sphingolipids are increasingly studied as bioactive signaling molecules and as important players in the development and progression of diseases, including cancer, type 2 diabetes, and Alzheimer's disease [80, 83, 84]. Sphingolipids are currently recognized as regulators of key cellular processes such as growth, differentiation, survival, senescence, immune cell trafficking and apoptosis [1]. The significance of sphingolipids is further underscored by the fact that

silencing of genes or proteins in sphingolipid metabolism results in embryonic lethal phenotypes in mouse models, including knocking out glucosyl-ceramide synthase [85], both isoforms of SPT [86], or CERT, the ceramide transfer protein [87].

Ceramide synthesis and isoforms of ceramide synthases

Ceramides are considered the building blocks of sphingolipids because they can be modified and converted to other sphingolipid species [77, 88, 89]. Ceramides are formed from a sphingoid-base connected to an acyl chain via an amide bond. There are two pathways by which ceramides are synthesized- the *de novo* pathway and the salvage pathway. In *de novo* biosynthesis, serine and palmitoyl-coenzyme A (CoA) are combined via a condensation reaction by serine palmitoyl transferase (SPT) to produce 3-ketosphinganine which is then reduced to sphinganine via 3-ketosphinganine reductase. Sphinganine is acylated via sphinganine N-Acyl transferase/Ceramide Synthase (CerS) to produce dihydroceramide (dhCer) which is further reduced to ceramide via dihydroceramide desaturases. Acyl-CoA-dependent ceramide synthesis was first described in 1966, however more than 30 years passed before the genes responsible for dhCer and Cer synthesis were identified in yeast [90, 91]. Additionally, ceramides can be generated through the salvage pathway which converts sphingosine-1-phosphate (S1P) to sphingosine then to ceramide, also via CerS. These multiple pathways converge at ceramide which serves as a hub in metabolism [1] (Fig 2.3). Over 28 distinct enzymes act on ceramide either as a substrate or product [78, 92], and the combinatorial synthesis with several enzymes collaborating to produce more than 200 distinct mammalian ceramides indicates a high degree of specialization and regulation within ceramide metabolism [1]. *De novo* ceramide synthesis occurs primarily in the endoplasmic reticulum (ER) [93-99], however ceramides can be generated in the plasma membrane [100], lysosome [101] and mitochondria [102] via the action of sphingomyelinases (SMase) and neutral glucocerebrosidases [103-105]. Variation is

14

introduced into ceramide species through the chain length and degree of saturation in the acyl chain that is linked via SPT [99, 106].
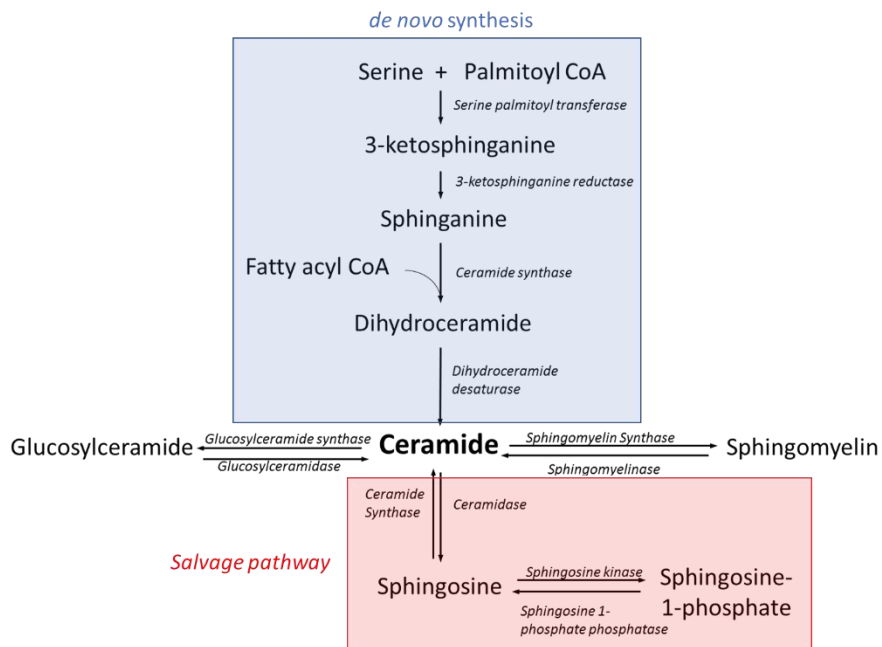
Figure 2.3 Ceramide is the hub of the sphingolipid pathway, formed *de novo* and through the salvage pathway

Furthermore, each ceramide synthase isoform, of which there are 6, exhibits a high specificity toward the acyl CoA chain length used for N-acylation, creating unique species [77, 80, 97-99, 107-109] with different functions. The preferred acyl chain length for each CerS isoform is shown in Table 2.1. Ceramides can be transported from the ER, where they are primarily synthesized, to other compartments including the mitochondria or the Golgi apparatus for further processing through vesicular transport or by the ceramide transfer protein (CERT) [96]. However, CERT has a defined specificity towards different acyl chain ceramides [110], indicating a further level of regulation which determines the availability and presence of certain ceramide species.

Isoform	Acyl-Chain length preference
CerS1	C_{18}
CerS2	C_{20-26}
CerS3	C_{22-26}
CerS4	C_{18-20}
Cers5	C_{16}
CerS6	C_{14-16}

Table 2.1 The acyl chain length specificity of the six isoforms of ceramide synthase

Ceramide Synthases are multi-spanning membrane proteins [97-99] with several similarities but also distinct differences [107, 111]. The six isoforms of Ceramide Synthases (CerS1-6) carry out the same chemical reaction, but differ in their affinity for the specific acyl-CoA used as highlighted in Table 2.1 [77]. Each tissue has a unique expression profile of the isoforms which can change upon stimulus [80]. CerS expression profiles have been investigated in humans and mice. CerS1 is primarily expressed in the brain [98, 99, 112] and skeletal muscle [109] and functions in cancer development, regulating sensitivity to chemotherapeutic drugs [113, 114], and promoting insulin resistance in skeletal muscle [109]. CersS2 is widely distributed in human tissues [115], producing very-long-chain ceramides, and appears to have diverse functions including regulation of ER stress [116], control of adipocyte signaling and amino acid metabolism [117], and triggering lung inflammation [84]. CerS2 has also been suggested to be critical for maintaining liver homeostasis [117] and may act more similar to a house keeping gene than a stress response gene [106]. CerS3 is expressed primarily in skin and testis [118, 119] and is important in maintaining the water permeability barrier of skin [120]. CerS4 is expressed highest in skin, leukocytes, heart, and liver [112] and was elevated in a

16

mouse model of Alzheimer's disease [121]. CerS5 synthesizes C_{16}-Cer and is highly expressed in the lung and brain [77]. Finally, CerS6, which is highly homologous to CerS5, also produces C_{14}- and C_{16}-Cer. CerS6 has been found to be expressed in most tissues at low levels [99, 112, 122] but is elevated upon stress stimuli [11, 123-125].

Regulation of ceramide synthesis

Because of the diverse nature of ceramides and their many functions, a high degree of regulation is required to maintain proper cellular-, tissue-, and whole-body homeostasis. Ceramide Synthase mRNA expression is not always correlated with protein levels, indicating that post-transcriptional and post-translational mechanisms affect protein levels [80, 82, 126, 127]. Correspondingly, the respective ceramide species also do not correlate with CerS mRNA levels, indicating further regulatory mechanisms [99, 112, 128]. Ceramide Synthase proteins may also be phosphorylated or glycosylated depending on the tissue being examined [82, 129], although glycosylation is dispensable for CerS6 activity [99]. CerS2-6 were found to be phosphorylated at the cytoplasmic C-terminal regions [129] and phosphorylation was important for the catalytic activity of CerS2 but only slightly increased the activities of CerS3-6. It is possible that hyperactivation of CerS by phosphorylation may worsen conditions in which sphingolipid species are already elevated, such as obesity and IR [130]. Interestingly, the phosphorylation sites in the C-terminal regions of CerS2-6 are mostly conserved between mouse and human proteins [129] and the catalytic components of yeast ceramide synthases, longevity-assurance gene 1 (Lag1) and its homolog longevity-assurance gene cognate 1 (Lac1), are also phosphorylated by casein kinase 2 at their C-terminal regions [131], similar to the human and mouse CerS. This suggests that CK2-dependent phosphorylation of CerS is an evolutionarily conserved mechanism to regulate CerS [129]. However, yeast Lac1 and Lag1 are also

phosphorylated at the N-terminal regions via the actions of a separate kinase [132] which was not found to affect mouse and human CerS proteins [129].

De novo ceramide synthesis can be regulated by substrate availability, the quantity of CerS mRNA and protein, and the activity of CerS [82]. Additionally, the availability of the acyl-CoA substrate may be less important in determining the ceramide composition of a specific cell/tissue because CerS expression and activity may compensate for any lack or overabundance of availability [82]. An exploratory study seeking to better understand ceramide metabolism in mice measured ceramide species in several tissues, along with mRNA and protein expression [82]. They found highest total ceramide levels in the brain and lowest total ceramide levels in the heart, lung, and spleen. Dihydroceramides were equally low in all tissues investigated and there was a clear difference in the distribution of long-chain (C_{14-20}) and very-long-chain (C_{22-26}) ceramides in tissues such that long-chain ceramides were most abundant in the brain and intestines whereas very-long-chain ceramides were most abundant in the lung, heart, kidney, liver, and spleen. This suggests that each tissue has a distinct ceramide composition, and it is possible that different cell types within a tissue also have a unique ceramide distribution [82]. Interestingly, most tissues had similar levels of $C_{24:0}$-dhCer but $C_{24:0}$-Cer level differed significantly between tissues, indicating that ceramide levels are a product of de novo synthesis but the salvage pathway and breakdown of complex sphingolipids may contribute substantially to the ceramide profile. These studies provide excellent data but are only a brief snapshot of metabolism as ceramides are substrates for synthesis of complex sphingolipids which have their own distinct functions and mechanisms of action. The authors concluded that each tissue in the mouse model seems to have its own specific ceramide equilibrium between the multiple ceramide species and that destabilization of this equilibrium is associated with various

pathological conditions [82]. Indeed, the ceramide steady state status of a cell or tissue is determined by the activity of enzymes that produce ceramides with different acyl chain lengths but also by those that utilize ceramides as substrates such as glucosylceramide synthase (GlucCerS) and SMase [82].

Dimerization is an important regulatory mechanism of CerS proteins

Ceramide metabolism is also regulated via oligomerization of CerS proteins [133]. Laviad et al. provide compelling data for the role of dimer formation in regulating CerS activity [133].While post-translational modifications provide a rapid avenue to change CerS activity upon exposure to stimuli or stressful conditions, it is possible that CerS2, CerS5, and CerS6 may exist as heterocomplexes in some cell lines [124]. This mode of regulation exists in addition to the protein phosphorylation and glycosylation which also alter the activity of CerS [82, 99, 133]. It has been proposed that the activity of one member of the heterodimer depends upon and can be modulated by the activity of the other. A dimer consisting of a CerS5 monomer attached via transmembrane domain to a CerS2 monomer resulted in 3-fold higher activity of CerS2 using C_{22}-CoA as a substrate [133]. This led the authors to conclude that optimal CerS2 activity depends on an interaction with a catalytically active form of CerS5 [133]. Interestingly, it was found that two monomers of CerS5 directly attached to each other via the N-terminus of one monomer to the C-terminus of the second monomer displayed no catalytic activity [133]. However, the insertion of a transmembrane domain between those two monomers resulted in a catalytically active dimer which had approximately 6-fold higher activity than the CerS5 monomer [133]. This indicated that the N and C termini of CerS are located on opposite sides of the ER and that CerS may exist in an equilibrium between monomers and dimers in different locations. Formation and dissociation of these dimers could be an extremely important mechanism of regulating activity [133].

Dimerization as a method of regulation also provides explanation of the fact that the acyl chain composition of ceramides does not reflect the CerS expression pattern in some tissues [133]. The ceramide composition likely depends on the expression of different CerS but also their ability to interact with each other. For example, investigation of different cell lines has found that co-transfection of CerS2 with CerS4 or CerS6 enhanced the activity of CerS2 [96]. Interestingly, CerS2 has the lowest *in vivo* activity[134], but the widest tissue distribution [82, 112, 133]. It was further suggested that CerS splice variants, which do not possess activity themselves [107], may act in a dominant-negative manner to regulate CerS activity [133]. More work is needed to better understand the molecular and structural details of how exactly CerS proteins interact, the mechanisms or signals that drive formation of homodimers or heterodimers, and the implications of such interactions. Dimerization is a rapid mechanism to increase ceramide levels under various physiological conditions or in response to cellular stress which relies on ceramides as signaling molecules [133].

Studies investigating the effects of knocking down or silencing CerS enzymes separately or together have provided valuable insight into the interconnectedness and regulation of these enzymes [135]. Knocking down individual CerS enzymes via small-interfering ribonucleic acid (siRNA) in MCF-7 breast adenocarcinoma cells resulted in a wide range of effects on nontargeted CerS expression. This change caused both increases and decreases in select sphingolipid species resulting in little change in total ceramide levels. Knockdown of CerS2 resulted in increased mRNA levels of CerS4, CerS5, and CerS6. Treatment with siCerS6 elevated levels of CerS5 mRNA by approximately 2-fold and siRNA for both CerS2 and CerS4 caused upregulation of CerS6 mRNA. At the protein level, knocking down CerS3, CerS4 or CerS5 caused an elevation in CerS2 protein and knocking down CerS2 or CerS4 also caused an

elevation of CerS6 protein. Interestingly, the authors found that knocking down CerS enzymes individually did not produce a significant increase in sphingoid base levels and that cells were able to maintain overall SM levels despite changes in acyl chain composition. The ability of cells to resist changes in ceramides due to knocking down CerS enzymes may be explained by nontargeted CerS compensation [135]. In addition to knocking down individual CerS proteins, the investigators also treated cells with siCerS2/5/6 to silence all three genes. There were no overall changes in Cer or SM levels but there was a shift in chain length distribution, particularly among medium and long-chain species. Total dhCer and hexosyl-ceramide (HexCer) levels increased as did Sph and S1P levels suggesting that knocking down three isoforms of CerS was sufficient to cause an accumulation of sphingoid bases. The changes in sphingolipids that were observed suggests the presence of a counter-regulatory mechanism whereby Cer and SM levels are maintained at the expense of accumulation of dhCer and HexCer species.

Ceramides in cellular signaling

Ceramides, the precursors for most complex sphingolipids [136], regulate and activate a variety of cellular pathways including autophagy, senescence, apoptosis, proliferation, p53 signaling, and inflammation [137-143], and are produced in response to many extracellular and intracellular stimuli including ultraviolet radiation, ionizing radiation, endotoxins, cytokines, serum deprivation, retinoic acid, folate withdrawal and chemotherapeutic agents [12, 92, 144-149]. Moreover, different stress stimuli evoke a response to produce specific acyl chain length ceramides during different physiological and pathological conditions which will differentially affect signaling pathways [150, 151]. In human colon and breast cancer cells, accumulation of long-chain ceramides induces apoptosis and inhibits cell cycle progression leading to inhibition of cell proliferation and ultimately cell death [152]. Abnormal ceramide signaling has also been found in lung diseases including acute lung injury, cystic fibrosis and chronic obstructive

pulmonary disease [84]. Ceramides have also been found to play a role in Toll-like receptor 4 protein (TLR4)-induced IR [153] as well as TNFα-induced IR, disturbed insulin secretion and pancreatic β-cell apoptosis [154]. Hamada et al. found that *de novo* synthesis of ceramides significantly contributes to the palmitate-stimulation of Interleukin (IL)-6 and MCP1 secretion from adipocytes and is involved in the interaction between adipocytes and macrophages and the mediation of pro-inflammatory adipokines [154].

The balance between sphingolipid species has also been shown to determine cellular response to various stimuli. Elevated C_{16}-Cer levels in tandem with loss of C_{24}-Cer has been implicated in triggering oxidative stress, apoptosis, alterations of inflammatory cell trafficking and alteration of host-environment interactions in lung tissue [84]. An important discovery in this area was that the balance between C_{16} and C_{24}-Cer is important for the induction of apoptosis [150]. CerS2, which produces C_{24}-Cer, is now thought to function as a house keeping gene whereas other CerS enzymes can be activated under stress situations to increase ceramide synthesis [107, 112, 117, 133]. The actions of ceramides in signaling is also likely countered by S1P. Ceramide and S1P have been found to play opposing roles in cell proliferation, migration, and survival indicating the importance of balancing these two specific sphingolipid species and an imbalance between these metabolites is likely to have significant pathological and physiopathological consequences [155-157].

CerS6 and C_{16}-ceramide metabolism

Ceramide Synthase 6, the protein of interest in this dissertation, is expressed at low levels in most tissues [82, 112], synthesizes C_{14}- and C_{16}-Cer, and has been studied extensively for its role in modulating ER stress and apoptosis[11, 124, 125, 158-162]. C_{16}-CoA which is used in production of C_{16}-ceramide, is one of the most abundant acyl-CoAs, used at two different steps in ceramide *de novo* synthesis, and also serves as a precursor for other lipids [82]. Currently, the

long-chain ceramides, especially C_{16}-Cer, are considered to be generally pro-apoptotic while very-long-chain ceramides, primarily C_{24}-Cer, are anti-apoptotic [124, 163]. The coordinated function of CerS2, 5, and 6 may result from association of these enzyme in a complex and the combined activity of the three isoforms determines the outcome for the cells based on the balance between pro- and anti-apoptotic species [124]. It is also likely that a change in single specific ceramide is not the only factor determining cellular outcome, but rather the ratio of several ceramide species. Specifically, the ratio of C_{16}-Cer to C_{24}-Cer is thought to be responsible for induction of apoptosis and tumor development [164].

In animal models, alterations of CerS6 activity affected sphingolipid pools. Specifically in brain tissue, inactivation of CerS6 led to a 70% reduction in incorporation of palmitoyl-CoA into C_{16}-Cer in the forebrain and cerebellum [122]. The kidneys were also affected by CerS6 inactivation as were the intestines, but to a lesser extent [122]. Nearly all tissues investigated showed a decrease in C_{16}-containing sphingolipids upon CerS6 inactivation. Interestingly, heterozygous mice also had reduced activity of CerS6 in incorporating palmitoyl-CoA, indicating that one allele is insufficient to maintain normal sphingolipid metabolism. CerS6 KO mice also exhibited behavioral abnormalities including impaired behavioral habituation toward a new environment which was attributed to an impaired ability to encode and maintain spatial information [122].

Altered CerS6 expression has been detected in several human diseases. CerS6 is involved in human alcoholic steatosis [165] and likely plays a role in psychosocial stress [166]. Additionally, both CerS2 and CerS6 mRNA were significantly elevated in breast cancer tissue with [167] approximately half of the affected individuals demonstrating elevated CerS2 and CerS6 mRNA levels [167]. Elevated C_{16}-Cer levels have also been found in breast cancer tissue

[168]. Because CerS mRNA levels do not necessarily reflect CerS protein expression or enzyme activity, and there are multiple modes of CerS activity regulation [107], caution should be used in the interpretation of expression data or their evaluation as prognostic or diagnostic biomarkers.

Ceramides in obesity and insulin resistance

There is strong evidence supporting a relationship between ceramide metabolism and obesity and IR. In human studies investigating CerS, only CerS6 expression was positively correlated with BMI, body fat content, and hyperglycemia [169] and ceramide levels are often elevated in skeletal muscle and plasma among other tissues in obese humans [109, 170, 171]. Animal models have indicated that there are significant changes in the sphingolipid profiles of mice fed a HFD [136, 169, 172-174].

There are few animal studies further investigating the relationship between ceramide metabolism and development of obesity and/or diabetes. Gosejacob et al. [173] fed CerS5 KO and WT mice a high fat diet until 24 weeks of age to analyze changes in energy homeostasis. They found a reduction of C_{16}-Cer but there were no alterations in ceramide species of different acyl chain lengths. Additionally, C_{16}- and C_{18}-Cer were reduced in the CerS5 KO mice fed a HFD. At a phenotypic level, CerS5 KO mice gained less weight on a HFD compared to WT mice, had lower levels of circulating leptin and lower accumulation of triacylglycerols, non-esterified fatty acids, and were protected from becoming severely glucose intolerant after HFD feeding, in contrast to their WT controls. Mice performed similarly during a glucose-tolerance test when on a low-fat diet but after HFD feeding only the KO mice retained their insulin sensitivity, indicating an interaction between ceramide metabolism and the development of diabetes. Additionally, CerS1 KO mice fed a high fat diet were protected from weight gain, fat mass accumulation, glucose intolerance and several other markers of metabolic syndrome. They also exhibited significantly lower ceramide levels, specifically C_{18}-Cer. [109]. These effects were

also seen in a skeletal muscle knockout model of CerS1. Interestingly, no protection was found when CerS5 and CerS6 were knocked down in skeletal muscle, thus indicating that CerS1 is important to skeletal muscle ceramide regulation [109].

The specific role of CerS6 in high fat diet feeding

In a whole-body and tissue-specific knockout models of CerS6, investigators found reduced C_{16}-Cer levels in white adipose tissue (WAT), brown adipose tissue (BAT) and liver after mice were challenged with a high fat diet [169]. CerS6 KO mice were also protected from diet-induced obesity (DIO), exhibiting reduced body weight, decreased body fat content, reduced adipocyte size, and lower serum leptin concentrations compared to their littermate controls. The authors suggested that this could be due to increased energy expenditure, although this was not further investigated. Mechanistically, the authors suggested that because the brown adipocytes from CerS6 KO mice showed unaltered utilization of glycolytic substrates but had increased mitochondrial beta-oxidative capacity, CerS6 may play a role in regulating BAT mitochondrial beta-oxidative capacity, thereby increasing energy expenditure and improving systemic glucose homeostasis. Deletion of CerS6 also protected the mice from macrophage infiltration and activation of pro-inflammatory WAT gene expression. Insulin action in the liver was improved, pointing to a system-wide role for CerS6 in protection from diet induced obesity [169].

Lipotoxic actions of ceramides

Based on the strength of the data presented in rodent and human studies investigating ceramide metabolism and high fat feeding, ceramide is considered to be an important nutrient metabolite that accumulates in obesity and results in alterations of cellular metabolism, contributing to hallmarks of metabolic disease [175]. Several studies have found that increasing ceramide levels inhibits insulin signaling and causes IR [109, 136, 169, 173, 175-177]. Ceramides and their derivatives have been found to antagonize insulin signaling, induce

25

oxidative stress, and inhibit glucose uptake and storage, which may initiate many of the molecular defects that contribute to IR [136]. Specifically, palmitate, which is used to form C_{16}-Cer, has been found to have detrimental effects on β-cell function including impairment of glucose-induced insulin release [178, 179], suppression of insulin gene expression [180-182] and induction of β-cell apoptosis [183-186]. Additionally, a cell-permeant analogue of ceramide has been found to impair insulin production in β-cells [187] and pharmacological inhibitors of ceramide synthesis have been found to prevent some of the detrimental effects of palmitate [181].

Several possible mechanisms have been suggested to explain the lipotoxic effects of ceramides. First, oversupply of saturated fatty acids from the diet induces ceramide accumulation [175, 188] which leads to activation of several downstream pathways. Specifically, ceramide metabolism appears to be closely linked to adipokine and cytokine signaling, further providing a link between ceramides and type 2 diabetes. Patient studies have found a strong correlation between plasma Cer, circulating cytokines and IR [169, 171, 189, 190]. It has also been found that ceramide metabolism plays a prominent role in leptin, TNFα, adiponectin and resistin activation and signaling [191-198]. Several studies have suggested that ceramide blocks the activation of protein kinase B (Akt/PKB) pathways thus impairing the translocation of glucose transporter type 4 (GLUT4) to the plasma membrane [199-203]. Ceramide accumulation decreases the activity of Akt/PKB both directly, via dephosphorylation of protein phosphatase 2, and indirectly by blocking translocation of Akt via protein kinase C zeta (PKCζ) [204], all of which affect cellular glucose uptake. In obesity, CerS6-derived $C_{16:0}$-Cer was found to be responsible for the inhibition of mitochondrial beta-oxidation in the liver and brown adipose tissue [205]. However, it is not clear how physiologically relevant these mechanisms are or how

the pathways work together in an animal model. Other studies, while lacking mechanistic understanding, have found that adipocytes are highly sensitive to glycosylated sphingolipids and that the antagonistic effects of TNFα can be negated by depleting cells of glycosylated ceramides [175]. These could be important pathways linking ceramide metabolism to the development and progression of metabolic diseases. Koves et al. [206] outlined a potential mechanism linking ceramides to diabetes whereby impairment of mitochondrial lipid oxidation leads to the build-up of toxic lipids including ceramide, causing a compensatory impairment of glucose utilization. A role for ER stress, in addition to mitochondrial stress, has also been proposed for its connection to ceramide metabolism [11, 159, 177]. However, the exact role of ceramide is not always clear. For example, one study in β-cell lines implicated ceramide as both a cause and effect of ER stress [207].

Due to the plethora of evidence supporting a relationship between sphingolipids and metabolic disturbances at both the cellular- and whole-body level, studies are underway to investigate therapeutic targets to reduce C_{16}-Cer levels. Raichur et al. [4] treated ob/ob (leptin-deficient) mice and HFD-fed mice with a CerS6 antisense oligonucleotide (ASO) to investigate the efficacy of targeting CerS6 without genetically modifying the mice. They found increased levels of $C_{16:0}$-Cer in ob/ob and HFD fed mice which were decreased upon treatment with ASO. Treatment also restored expression levels of CerS6 to that of controls whereas CerS6 expression remained elevated in obese mice. Treatment with CerS6 ASO restored glucose sensitivity and plasma adiponectin levels. A common conclusion in the studies investigating ceramides in obesity and IR is that the lipotoxic role is due to C_{16}-ceramide specifically. A mouse model of heterozygous CerS2 KO found similar impairment of glucose tolerance, altered plasma cholesterol, liver damage, and other markers common to obesity. These effects were explained

27

by the fact that knocking down CerS2 led to a concomitant increase in C_{16}-Cer due to decreased C_{24}-Cer [130]. This provides strong data that are complementary to the studies investigating CerS5 or CerS6 knockout mice.

Ceramides and nutrient stress

Sphingolipids have also been studied for their role in determining response to nutrient stressors including folate depletion, synthetic retinoids, vitamin E metabolites, and choline and magnesium withdrawal [7-10, 12, 208]. Short-term dietary deficiency of magnesium in mammals results in the activation of p53 in diverse cardiovascular tissues and cells along with an increase in *de novo* ceramide synthesis by activating SM synthase, SPT and CerS [7, 8]. Ceramides have also been implicated in the response to fenretinide, a synthetic retinoid that inhibits obesity and development of IR in HFD-fed mice [9]. 3T3-L1 adipocytes that were treated with fenretinide had significantly elevated concentrations of several dhCer species as well as dhCer-containing SM species. Although this was an *in vitro* study investigating a synthetic retinoid, the results still suggest a possible connection between sphingolipids and vitamin A. Additionally, γ-tocotrienol, a member of the vitamin E family, caused an increase of C_{16}-, $C_{24:0}$-, and $C_{24:1}$-Cer and dhCer species as well as increased expression of SPT and CerS6 genes in pancreatic cancer cells. While these results should be evaluated in other cell types and rodent models, there was a clear effect of this vitamin E metabolite in pancreatic cancer cells furthering the evidence that ceramides are involved in the response to nutrient stress, both withdrawal and high-dose treatments.

Ceramides respond to folate withdrawal

Previous work from our laboratory has investigated the role of folate stress in several cancer cell lines through the manipulation of aldehyde hydrogenase 1 family member L1 (ALDH1L1), an enzyme involved in the regulation of folate metabolism [12]. Over-expression of ALDH1L1 induces folate stress and has been found to increase apoptosis and other metabolic

28

alterations, specifically, increasing ceramides. C_{16}, C_{24}, $C_{24:1}$-Cer and C_{16}-dhCer were the species

increased under ALDH1L1 induction and were also the only species significantly elevated upon

withdrawal of folate from the media indicating a similar folate-stress response. CerS4 and CerS6

mRNA were transiently upregulated in cells transfected with ALDH1L1 and there was a

persistent increase in CerS6 protein expression. When *de novo* ceramide generation was

inhibited via myriocin, an inhibitor of SPT, or fumonisin B1, a CerS inhibitor, total ceramide

elevation was prevented and the ALDH1L1-expressing cells were protected from apoptosis [12].

This indicates that ALDH1L1-induced apoptosis requires *de novo* ceramide generation.

Additionally, knocking down CerS6 rescued cells from ALDH1L1-induced apoptosis and

increased the viable cell number at 48 hours post-ALDH1L1 induction [12]. These experiments

provide compelling data for the role of CerS6 and C_{16}-Cer in mediating the cellular response to

ALDH1L1, which is further enhanced by the finding that knockdown of CerS2 (the only source

of other ceramide species that were increased in these cells) via siRNA did not rescue cells from

ALDH1L1-induced apoptosis and therefore it is unlikely to play a significant role in ALDH1L1

stress response. While informative, cell culture studies are difficult to translate to humans. We

therefore sought to investigate the relationship between folate and ceramide metabolism in an

animal model.

Rationale

There is now clear evidence that ceramides orchestrate the response to cellular stress, and

additionally, a growing body of evidence implicates ceramides in the response to nutritional

stress such as HFD and alterations in micronutrient levels. We seek to better understand how

ceramides respond to dietary changes of both macro- and micronutrients (fat and folic acid) in an

animal model in order to develop approaches that could mitigate effects of this stress. Our

laboratory has demonstrated *in vitro* that folate depletion evokes a cellular response mediated by

ceramides. Here we seek to test the <u>hypothesis</u> that *alterations of dietary folic acid will induce a CerS6-dependent sphingolipid response in mice and knocking out the enzyme will mitigate this response.* We will investigate both effects of folic acid deficiency and over-supplementation as both ends of the spectrum have adverse consequences in humans. Furthermore, we will challenge the mice with a high fat diet which is deficient in or over-supplemented with FA to assess combinatorial effects of high fat and FA in modulating sphingolipid metabolism and the resulting phenotypic changes in mice. The standard Western diet is high in fat and the fortification of refined foods provides most of the population with more than sufficient folic acid. However, intake of both fat and folic acid still varies widely. We propose to investigate two different levels of fat and three levels of FA to gain a better understanding of the consequences across a range of intakes.

It should be noted that currently there are no studies investigating the interaction of folate and ceramide metabolism in the context of high fat intake. There is sufficient data indicating that folate affects lipid metabolism, but no information on sphingolipids. Therefore, our results will bridge a knowledge gap regarding the function of ceramide under different levels of dietary folate in conjunction with a standard lower-fat diet or HFD. We expect that our data will inform the future approaches to counteract ceramide elevation and metabolic stress responses by adjusting folic acid supplementation.

These studies will also provide more data to delineate the distinct roles of CerS5 and CerS6. As mentioned previously, both have been studied in response to HFD feeding. Interestingly, CerS5 and CerS6 seem to have different biological functions [209, 210] and possibly even differential expression in particular cell types [122], despite similar tissue expression pattern and substrate specificity. We will specifically focus on CerS6 based on our

findings from cell culture experiments. However, this data could be extremely useful in guiding future studies and assessing the differential responses of CerS5 and CerS6 to nutrient stress.

Public Health Relevance

Plasma ceramides may be important markers of health

Plasma ceramides have been suggested as potential biomarkers or predictive measures for several disease states. A study investigating two large cohorts in Singapore and New Zealand found 11 distinct plasma Cer and 1 plasma dhCer that were predictive of major adverse cardiovascular events in patients with previous myocardial infarction [211]. Discovery of a dihydroceramide, specifically C_{16}-dhCer in this group adds to growing literature suggesting that dihydroceramides are not simply transient species in ceramide biosynthesis but rather may serve important signaling roles [212]. Similarly, patients with stage 4 colorectal cancer were found to have altered levels of Cer and SM, but not HexCer species [3]. Specifically, the levels of C_{16}-, C_{18}-, $C_{18:1}$- and $C_{24:1}$-Cer as well as Sph were significantly higher in patients than control subjects whereas the levels of C_{24}-SM were significantly lower than those of controls.

As new technology has been developed that allows precise quantitation of individual sphingolipid species, the role of plasma ceramides can now be more appreciated. Several laboratories have been working to create plasma ceramide scores, based on measurements of individual ceramides in plasma, as a predictive tool for future events or disease risk. Most of these studies investigate aspects of cardiovascular disease, due to its strong link to ceramide. Atherosclerotic plaques have been found to be enriched with certain ceramides by as much as 50-fold [213] and pro-inflammatory cytokines including interferon-gamma (IFNγ), TNFα, and IL-1β stimulate ceramide synthesis [214]. Several groups have developed a ceramide risk score for cardiovascular events by combining the values of C_{16}-Cer, C_{18}-Cer, $C_{24:0}$-Cer and $C_{24:1}$-Cer into a single score [215-219]. Meeusen et al. found that C_{16}-, C_{18}-, and $C_{24:1}$-Cer were predictive

for a combined outcome of myocardial infarction, stroke, revascularization and death from any cause at 4 years follow up [2]. Moreover, these ceramide scores remained significantly predictive even after adjusting for common risk factors including BMI, age, sex and smoking history. Interestingly, Kaplan-Meir survival analysis demonstrated that the risk of a major adverse event at any time during 18 years of follow up was significantly greater in individuals with an increased ceramide risk score [2]. Additionally, C_{16}- and $C_{24:1}$-Cer were significantly predictive for all-cause mortality at 18 years [2], a discovery that warrants more in-depth studies to examine the mechanism and strength of association. The authors appropriately noted that useful biomarkers are those that respond to change and that give the patient ability to monitor them over time in response to lifestyle changes. It has been found that gastric bypass surgery [220], aerobic exercise [221] and statin use [217, 222] can modulate ceramides levels but more work is necessary to understand how sensitive and responsive plasma ceramides are to dietary changes.

Genetic variation in sphingolipid metabolism

While more studies are needed to investigate the response of sphingolipids to dietary intake, an additional aspect deserves special attention: the individual genetic variability underlying sphingolipid metabolism and regulation. A study identifying genetic mutations in several genes involved in ceramide synthesis and degradation found that up to 12.7% of the variation in sphingolipid species can be explained by a single genetic mutation [223]. A functional single nucleotide polymorphism (SNP) in ATPase Phospholipid Transporting 10D (Putative) (ATP10D) was significantly associated with GlucCer levels, providing evidence for the involvement of APT10D in intracellular transport of specific ceramides [223]. It was postulated that impaired function of ATP10D may impair transport of ceramides, leading to enhanced exposure to glucosyltransferases. This would allow higher concentrations of glucosylceramides to form and be released into the plasma compartment. Alternatively,

impairment of APT10D may impair transport of glucosylceramide to the trans-Golgi network. Interestingly, none of the genes involved in ceramide degradation or ceramide-related signaling were significantly associated with the analyzed traits leading the authors to conclude that genetic control of ceramide levels is primarily due to ceramide production as opposed to degradation [223]. In a mouse model of APT10D mutations, the animals demonstrated lower high-density lipoprotein concentrations and developed severe obesity, hyperglycemia and hyperinsulinemia when fed HFD [224]. Furthermore, 4 SNPs significantly associated with type 2 diabetes, fasting plasma, glucose and waist circumference were identified in the CerS6 gene in an indigenous Australian population [225]. As studies reveal more information about the genetic control underlying variation in sphingolipid concentrations and response, more work needs to be done to address mechanisms of diet effects on sphingolipid metabolism given their profound connection to several disease states.

CHAPTER 3: CERAMIDE SYNTHASE 6 MEDIATES SEX-SPECIFIC METABOLIC RESPONSE TO DIETARY FOLIC ACID SUPPLEMENTATION

Introduction

Sphingolipids, the second largest class of lipids in biological membranes, share a common structural element (the sphingoid base), comprise 10-20% of membrane lipids [226] and define the unique biophysical properties of these membranes [227, 228]. Sphingolipids are, also, involved in the regulation of fundamental cellular processes such as proliferation, differentiation, migration, survival and senescence, as well as response to stress [159, 226, 229]. Therefore it is not surprising that sphingolipids have been implicated in the development and progression of diseases including cancer, type 2 diabetes, cardiovascular and Alzheimer's diseases [83, 230-234]. Ceramides, sphingosine and sphingosine-1-phosphate are often investigated as regulatory or signaling lipids [235], however recently such roles have also been proposed for complex sphingolipids [226].

Often viewed as central players in sphingolipid metabolism, ceramides can be synthetized *de novo*, starting from the condensation of serine and palmitoyl-CoA followed by reduction to dihydrosphingosine, N-acylation to dihydroceramide by ceramide synthases, with final conversion to ceramide by dihydroceramide desaturase [233]. Ceramides can be also formed via degradation of pre-formed complex sphingolipids in the endolysosomal pathway by acid SMase and glycosidases (GCase) and by CerS utilizing free sphingosine generated via the salvage pathway [233]. Six isoforms of the ceramide synthase family (CerS1-6) have been identified [77, 236], which carry out the same chemical reaction but differ in their affinity for the specific acyl-

34

CoA used, allowing for unique regulation of the balance of different ceramides in cells and tissues. The function and distribution of these six isoforms has been reviewed extensively [77, 233, 236, 237]. An increasing number of studies have demonstrated that cellular effects of ceramides and sphingolipids depend on their specific structural characteristics, including acyl chain length [1, 237]. This makes CerS an attractive target both in biomedical research and in development of novel therapeutic approaches for treatment of diseases [237-239].

CerS6, similar to another family member CerS5, preferentially produces C_{14}- and C_{16}-ceramides. It is expressed in many tissues, but generally at low levels, and can be upregulated by various types of stress resulting in increased production of C_{16}-ceramide and an anti-proliferative/apoptotic response [111, 240-242]. CerS6 is expressed in the liver tissue which is also the primary site of folate metabolism [43, 243]. Folate is a B-vitamin that is involved in the synthesis of nucleotides, metabolism of amino acids and methylation reactions [14, 17, 244]. Inadequate intake of folate in humans contributes to folate deficiency which has widespread effects due to the role of folate in many cellular processes [245-247]. Folate cannot be synthesized by cells of higher animals but must be obtained from diet [244, 248]. However excess folate in the diet or dietary supplements in the form of FA can have negative effects [37, 43]. Recent studies from our lab have demonstrated that metabolic stress induced by disruption of folate metabolism via folate withdrawal, impairment of folate enzymes, or by antifolate drugs, results in upregulation of CerS6 and elevation of C_{16}-Cer in cultured cells [12, 249]. Because the liver is the primary site of folate metabolism and also expresses CerS6, among other CerS, we focused specifically on changes in the sphingolipid profile and metabolome of liver tissue.

In this regard, it is worth noting that the link between folate metabolism and ceramide signaling is still not clear. Here, we examined the effects of dietary folate alteration on the liver

metabolome and sphingolipids in WT and CerS6 KO mice to determine broad effects of folate deficiency and over-supplementation on liver metabolism and evaluate the role of CerS6 and ceramide in maintaining tissue homeostasis. We <u>hypothesized</u> that there would be significant increases in many ceramide species in order to compensate for the lack of CerS6 and its products C_{14}- and C_{16}-Cer and keep total ceramide concentrations constant. We did not expect to see changes in sphingomyelin concentrations as they are mostly considered to play structural roles. Additionally, we hypothesized that alterations of ceramide pools would cause changes in other lipid pools in the liver.

Materials and Methods

Animals and husbandry

All animal experiments were approved by the Institutional Animal Care and Use Committee (IACUC) at the North Carolina Research Campus (NCRC). CerS6 KO mice were generated in Dr. Ogretmen's lab and we bred them back 5-6 generations to the C57BL/6NHsd mice purchased from Envigo (Indianapolis, IN). Confirmation of protein knockout via Western Blot is shown in Figure S3.1. Animals for dietary experiments were generated by breeding heterozygous (CerS6$^{+/-}$) males and females. Wild type (CerS6$^{+/+}$) and knockout (CerS6$^{-/-}$) littermates were randomized to dietary groups. Both male and female mice were used in these experiments. Mice were group housed in microisolator cages under standard conditions (12h light/dark cycle, temperature- and humidity-control) with *ad lib* access to water and one of the three purified synthetic diets containing 14.4% kcal from fat, 66.5% kcal from carbohydrate, and 19.1% kcal from protein, and differing only in the amount of folic acid. All diets were purchased from Envigo: 1) folic acid deficient diet (FD, catalog number TD.95247) with no added FA and containing only residual 0.01ppm FA coming with added protein; 2) control diet (Ctrl) with 2ppm FA added (TD.160824) and 3) folic acid over-supplemented diet (FS) containing 12ppm

FA (TD.160825). The amino acid sources (casein and L-cystine) were consistent across diets, as were sources of carbohydrate (corn starch, sucrose, maltodextrin) and fat (soybean oil). All animals were placed on respective diets at 10 weeks of age, maintained on the diets for 4 weeks, and euthanized at 14 weeks of age. Earlier studies have shown that folate-deficient diet significantly reduces both blood and tissue folate concentrations over a period of 2 weeks [250, 251]. Blood and tissues were collected, sections of liver, brain and testes were fixed in formalin and the remaining tissues were snap-frozen in liquid nitrogen for further analysis. Body composition (lean and fat mass) was assessed before mice were placed on diet and before necropsy using the EchoMRI-130 Body Composition Analyzer. Mice were fasted 4 hours before blood draw via retro-orbital bleed.

Western blot assays

Fragments of frozen liver (~30 mg) were homogenized using Dounce homogenizer in 750 µl of RIPA buffer containing phosphatase and protease inhibitor cocktail (1:100, Sigma-Aldrich, St. Louis, MO), sonicated and centrifuged (20,000 x g, 5 min, 4°C). The supernatant was stored at -80°C. Aliquots of 20 µg of total protein were subjected to SDS-PAGE followed by immunoblot with corresponding antibodies. All antibodies were diluted in 3% BSA blocking buffer. Membranes were washed 4 times with 2% TWEEN-20 in TBS. Blots were developed with SuperSignal West Pico Chemiluminescent substrate and analyzed using the Odyssey Fc infrared scanner from LI-COR.

LC-MS/MS analysis of sphingolipids

Aliquots of frozen tissues were homogenized in PBS using Dounce homogenizer. Homogenate volumes containing 1 mg of total protein were immediately frozen and stored at -80° C. Sphingolipid concentrations were measured by High-performance liquid chromatography-

tandem mass spectrometry (HPLC-MS/MS) methodology as previously described by the MUSC

Lipidomics Shared Resource [252]. Data are presented as mean $\pm$ SEM as pmol/mg total protein.

Additionally, measurements of hexosyl-ceramides include glucosyl- and galactosyl-ceramides

but not lactosyl-ceramide species.

Plasma markers

Blood was collected into EDTA-containing tubes and plasma was separated via

centrifugation at 6,000 x g for 10 minutes at 4°C. Plasma triacylglycerol, cholesterol and glucose

were measured using Thermo Fisher Scientific Infinity colorimetric assays with appropriate

standards (Stanbio glucose standard (100mg/dl), Pointe Scientific TG standard (200mg/dl), and

Pointe Scientific Cholesterol standard (200mg/dl)). All samples were run in triplicate with n=5

per group. Plates were read using the BioTek Synergy HT plate reader and validated with

internal controls of pooled plasma.

Histology

Liver, brain, and testes fixed in 10% formalin were embedded in paraffin blocks and 5

μm sections from the blocks were placed on slides, deparaffinized, re-hydrated and stained with

hematoxylin and eosin according to standard protocol. Images were taken on Keyence BZ-X710

All-in-one fluorescence microscope at 2X, 10X, and 20X magnification.

Metabolomic analysis

Untargeted metabolomic analysis was performed by the commercial service provider

Metabolon® (Durham, NC). Snap-frozen liver, brain and testes tissue samples were subjected to

extraction with methanol and divided into aliquots for further analysis by ultrahigh performance

liquid chromatography/mass spectrometry (UHPLC/MS). The global biochemical profiling

consisted of four unique arms covering identification of both hydrophilic and hydrophobic

compounds under both positive and negative ionization conditions [253]. Metabolites were

identified by automated comparison of the ion features in the samples to a reference library of chemical standards characteristics which included retention time, m/z (mass/charge) ratio, predominant adducts and in-source fragmentation and associated spectra.

Statistical analysis

For statistical analysis of differences between two groups Student's t-test was performed using GraphPad software. For the statistical analysis of differences between three or more groups, one-way ANOVA was used with Sidak's multiple comparisons test to determine differences between specific groups. Results were determined to be statistically significantly different at $p<0.05$. Data are presented as mean $\pm$ standard error of measurement (SEM). Metabolomic data were analyzed using Qlucore Omics Explorer v.3.4 software (Qlucore, Lund, Sweden).

Results

CerS6 knockout prevents fat mass accumulation in male mice, independent of FA supplementation

We evaluated body mass and body composition in WT and CerS6 KO mice before and after dietary treatment of folate-deficient (FD), control folate (Ctrl) or folate-supplemented (FS) diet. Despite the random assignment of littermates to dietary treatment groups, the average weight of males in the KO-Ctrl group was slightly higher than in the KO-FS group, and this difference remained after the dietary treatment, resulting in the absence of significant differences in the change of body weight between the groups (Fig 3.1).
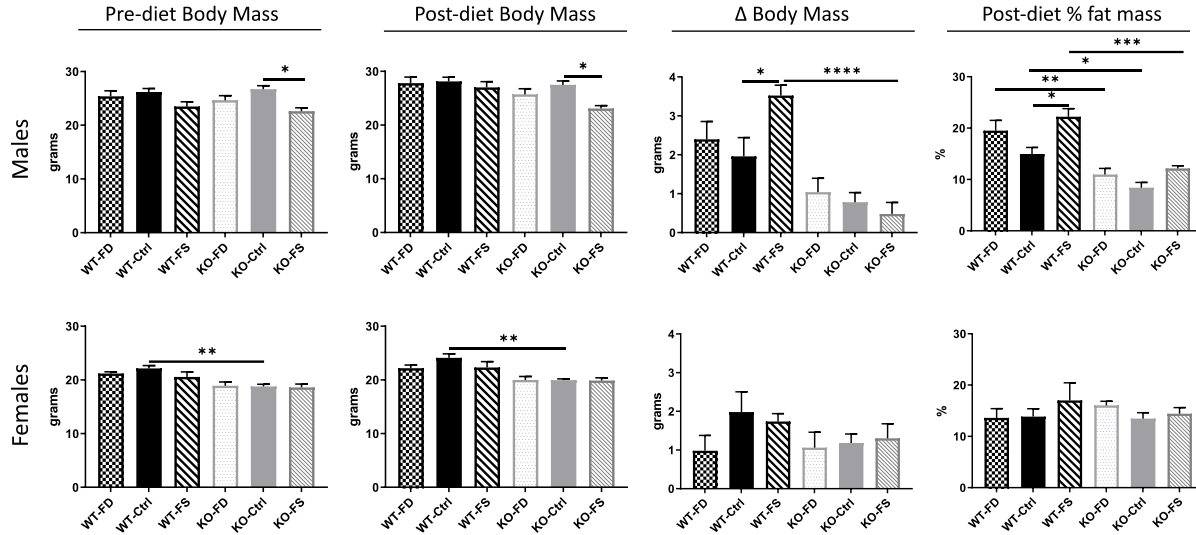
Figure 3.1 Protection of CerS6 KO male but not female mice from weight gain and fat mass accumulation. Body mass and composition were measured before and after dietary intervention. Change in body mass was calculated by subtracting pre-diet animal body mass from the post-diet mass. Fat mass was measured by Body Composition Analyzer. Data represent mean $\pm$ SEM, n=5. Checkered bars - FD diet; solid bars - Control diet; striped bars - FS diet. WT shown in black and KO shown in grey. *, p<0.05; **, p<0.01; ***, p<0.001; ****, p<0.0001, determined by One-way ANOVA with Sidak's multiple comparisons test

At the end of dietary treatment all WT male mice gained more weight and showed higher percent of fat mass than their KO counterparts on all diets. Additionally, WT-FS males gained more weight and had significantly higher fat mass than WT-Ctrl group.

Compared to male mice, WT females gained less weight and were overall leaner than males on all diets, but KO females had overall higher fat mass than KO males independent of diet. Additionally, there were no differences between WT and KO females in the gain of body mass, or in percent of fat mass (Fig 3.1), indicating that CerS6 knockout does not protect females from weight gain and fat mass increase on these diets.

Measurements of plasma glucose and cholesterol as well as evaluation of liver: body weight ratio did not show significant differences between genotypes or dietary treatments for both sexes (Fig S3.2). Histological examination of livers from WT and KO animals on different

diets did not show obvious differences between genotypes or any dietary treatments (Fig S3.3 and S3.4).

Both CerS6 knockout and folate deficiency affect ceramide profiles of liver

We next assessed sphingolipid concentrations in the liver of WT and CerS6 KO mice to evaluate changes due to knocking out CerS6 or from dietary treatment. As expected, C_{14}- and C_{16}-Cer were significantly lower (2-3-fold) in livers of CerS6 KO mice, both male and female (Fig 3.2). However, only C_{14}-Cer was significantly increased in folate deficient livers of both WT and KO mice. Levels of C_{16}-Cer in folate-deficient livers did not differ significantly from control livers in both sexes (Fig 3.2). Of note, both C_{14}- and C_{16}-Cer were higher in WT females than in WT males, while in KO mice only C_{14}-Cer was higher in females than males (Fig 3.2).
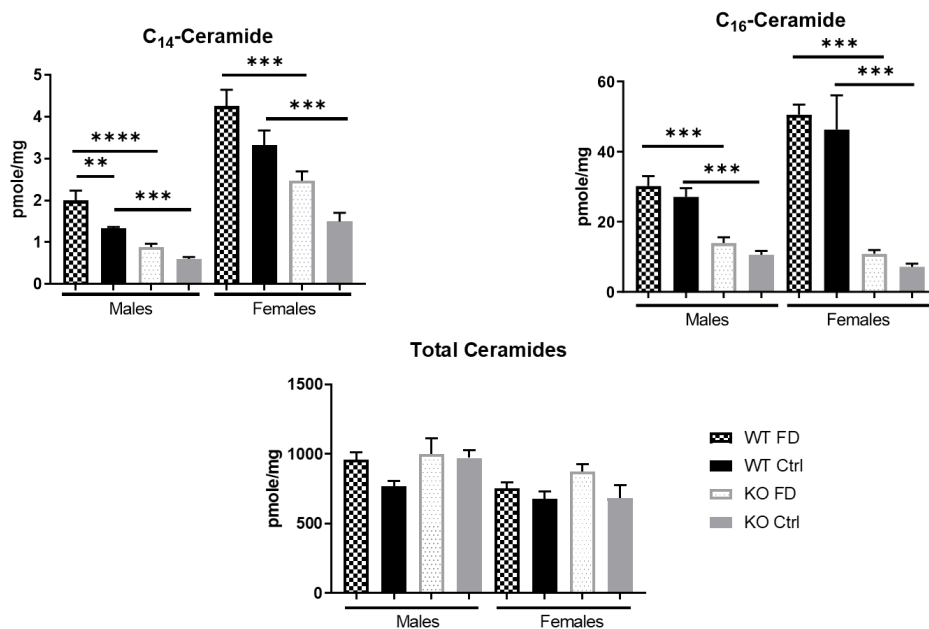
Figure 3.2 Effect of folate deficient diet on C_{14}-, C_{16}- and total ceramide levels in male and female WT and CerS6 KO mice. Data are shown as mean $\pm$ SEM, n=5. Checkered bars, FD diet; solid bars, Control diet. WT shown in black and KO shown in grey. *, $p<0.05$; **, $p<0.01$; ***, $p<0.001$; ****, $p<0.0001$, determined by One-way ANOVA with Sidak's multiple comparisons test

Among the other ceramide species, $C_{18:1}$- and $C_{20:1}$-Cer were significantly elevated in folate deficient male WT livers and showed similar trend but did not reach statistical significance

41

in KO (Fig S3.5). Additionally, very-long ceramides (C_{24}-, C_{26}- and $C_{26:1}$) were increased in

male KO livers compared to WT on control diet, but not on folate deficient diet (Fig S3.5). No

such elevation was observed in females (Fig S3.6). Overall, the Total Cer levels were not

significantly different between different genotypes and different diets, both in males and females

(Fig 3.2).

Dietary folate supplementation significantly affects sphingomyelin levels while CerS6 KO has no effect on sphingomyelins

The folate over-supplemented diet elevated multiple sphingomyelin species in WT and

KO mice: C_{20}-, $C_{20:1}$-, C_{22}-, $C_{22:1}$- and $C_{24:1}$-SM in both sexes (Fig 3.3), as well as $C_{18:1}$ in males

and C_{24} and $C_{26:1}$ in females (Fig S3.7). Total SM levels were also significantly elevated in both

sexes by folate over-supplementation (Fig 3.3).
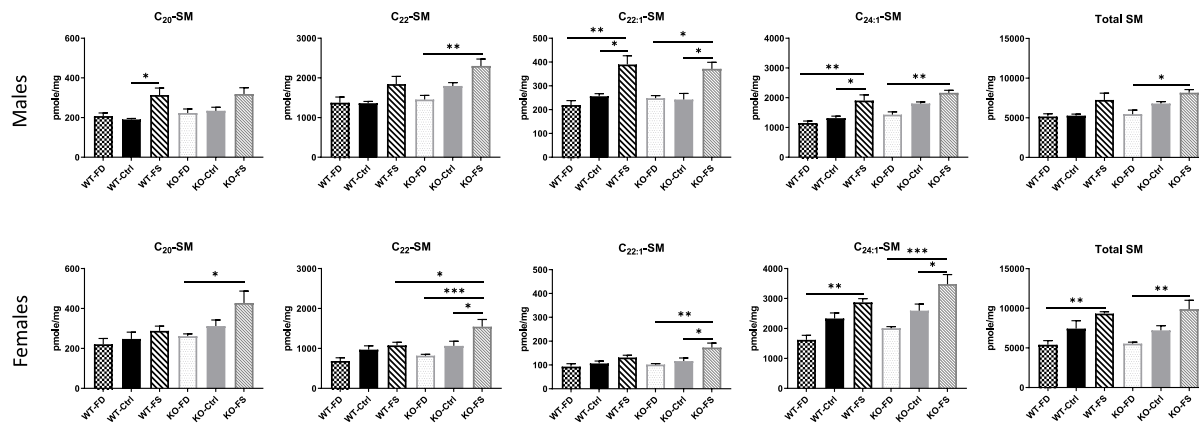
Figure 3.3 FA over-supplementation increased very-long-chain sphingomyelin levels in WT and CerS6 KO mice of both sexes. Data presented as mean $\pm$ SEM, n=5. Checkered bars, FD diet; solid bars, Control diet. WT shown in black and KO shown in grey. *, $p<0.05$; **, $p<0.01$; ***, $p<0.001$; ****, $p<0.0001$, determined by One-way ANOVA with Sidak's multiple comparisons test

However, no significant differences in C_{14}- and C_{16}-SM at different dietary folate levels

were found in either WT or KO males (Fig S3.7). Wild-type females demonstrated significantly

elevated C_{14}- and C_{16}-SM on FS diet only (Fig S3.7), and similar increase of C_{18}- and $C_{18:1}$-SM

was found in males but not in females (Fig S3.7).

Hexosyl-ceramides are modulated by dietary folate

Similar to C_{14}- and C_{16}-Cer and SM, hexosyl-ceramides with C_{14}- and C_{16}-acyl chains were significantly higher in female livers than in male (Fig 3.4a). Interestingly, levels of C_{16}-HexCer in WT females were 2 times higher than in WT males and FD diet elevated this difference to 3-fold. C_{14}-HexCer showed even greater differences between sexes and also increased in response to FD. Other HexCer species were not different in males of different genotype or on different diets. Interestingly, in females almost all HexCer species demonstrated significant increase in response to the FD diet, but only in the knockout and not WT animals (Fig 3.4b). Total HexCer levels were not different in WT on either diet but were elevated in the KO-FD group. (Fig 3.4a).
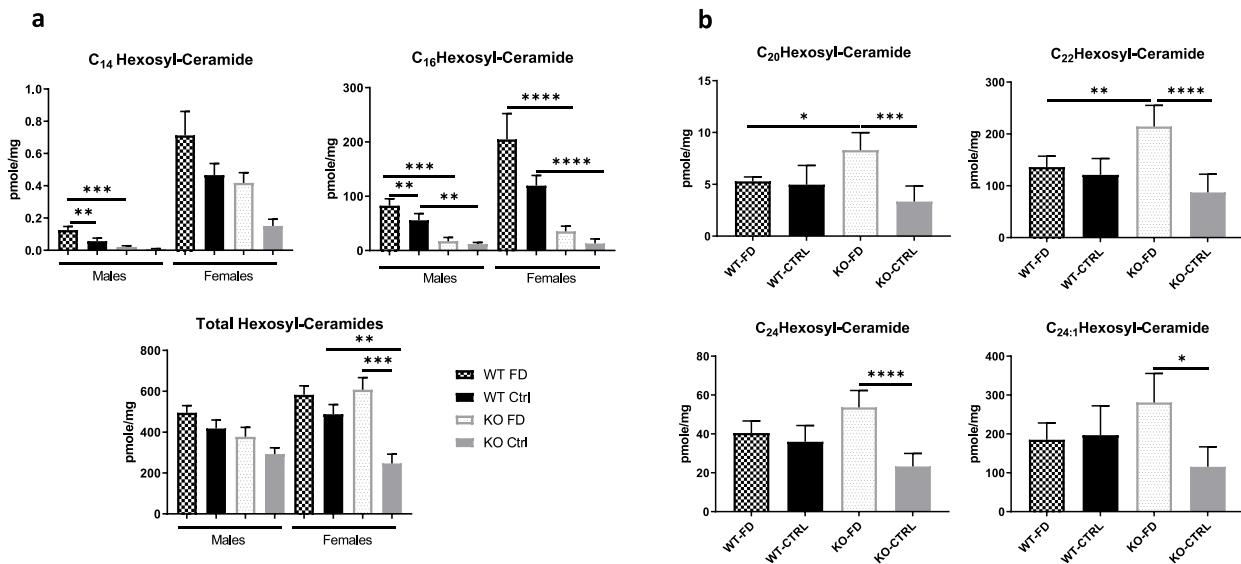
Figure 3.4 Effects of FD diet on C_{14}-, C_{16}- and total hexosyl-ceramides in males and females and on very-long-chain hexosyl-ceramides in females. (a) WT Female mice show significantly higher levels of C_{14}- and C_{16}-ceramide than males but in KO females this difference is present only for C_{14}-ceramide. (b) Female KO mice show elevated very-long-chain hexosyl-ceramides in response to FD diet. Data are shown as mean $\pm$ SEM, n=5. Checkered bars, FD diet; solid bars, Control diet. WT shown in black and KO shown in grey. *, $p<0.05$; **, $p<0.01$; ***, $p<0.001$; ****, $p<0.0001$ determined by Student's t-test between genotypes and diets

Mouse liver metabotypes show significant differences based on sex, genotype and diet, with diet effects being weaker

Additionally, we submitted liver samples for untargeted metabolomic analysis in order to evaluate changes in metabolic pathways due to dietary treatment and genotype. Untargeted metabolomic analysis provided measurements of 736 named biochemicals in mouse liver tissues. Statistical comparisons of the measured metabolites using principal component analysis and hierarchical clustering demonstrated the strongest separation of the metabotypes by sex (Fig 3.5a) and genotype (Fig 3.5b), with separation by diet being also discernible (Figure 3.5c). To that end, 550 metabolites were statistically significantly ($p \leq 0.05$) different between male and female mice regardless of diet and genotype whereas 298 and 273 metabolites differed significantly between dietary intervention and genotype, respectively (Fig S3.8a). Heat map analysis demonstrates clear separation of metabotypes by sex (Fig 3.5a), by genotype (Fig 3.5b) and by diet (Fig 3.5c).
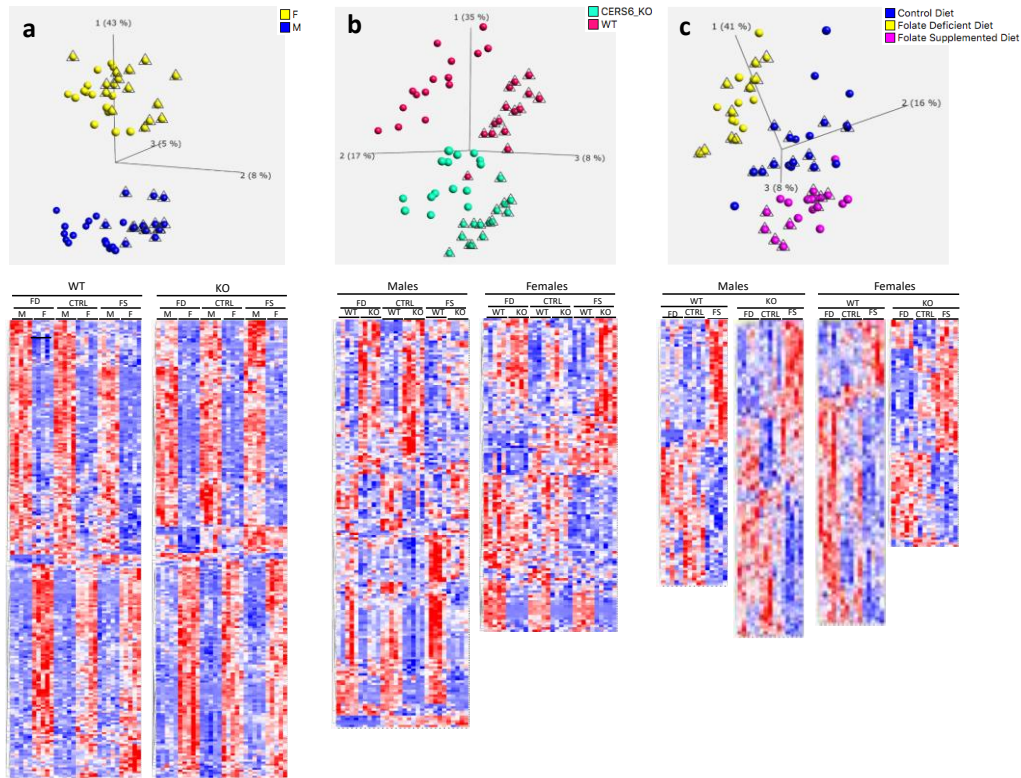
Figure 3.5 Principal component analysis and heat map analyses of liver metabolites. PCA of measured metabolites demonstrates segregation of liver samples by (a) sex, (b) genotype and (c) diet. HM analysis confirms separation of metabotypes. Analysis was performed using Qlucore Omics Explorer v.3.4 software

Random forest analysis, an unbiased supervised classification approach which splits the samples into groups based on the biochemicals providing the best separation between groups, showed a predictive accuracy of 64% compared to 8.3% due to random chance alone, when all 12 groups were included in the analysis (Fig S3.8b). The biochemical importance plot (Fig S3.9) demonstrates that the metabolites with the highest contribution to the separation of the group's metabotypes are ceramides and sphingomyelins with C_{16} acyl chain, folate derivatives and formiminoglutamate (FIGLU), as well as several phosphatidylethanolamines, which is consistent with experimental design.

Not only ceramide and ceramide-based lipids, but also free fatty acids, diglycerides and phosphatidylethanolamines are altered in CerS6 KO mice

Similar to our targeted measurements of Cer, SM, and HexCer, untargeted metabolomics demonstrated significant decreases in C_{16}-acyl chain containing sphingolipids in the CerS6 KO mouse livers (Fig S3.10). Decreases of 30 – 50 % were observed for most of these sphingolipids (C_{16} and C_{18}), while N-palmitoyl-heptadecasphingosine decreased over 90% and glycosyl-N-palmitoyl-sphingosine dropped more than 75%, in both males and females (Fig S3.10a). Slight changes (<30%) in a few longer-chain ceramides were noted (C_{22} and C_{24}), but most of these did not reach significance. At the same time longer chain sphingomyelins (C_{18}, C_{22}, C_{24}) demonstrated statistically significant increases of up to 70% with elevation in females seen more often (Fig S3.10b).

Importantly, knockout of CerS6 induced changes in other lipid classes, besides sphingolipids. Elevation of phosphatidylethanolamines (C_{16}-C_{24}) was found both in males and females, with more abundant changes in males (Fig 3.6a). On the contrary, long-chain and polyunsaturated fatty acids, as well as diacylglycerols were significantly reduced, also more frequently in males than females (Fig 3.6b and 3.6c).

<table>
<tr><th rowspan="3">a</th><th></th><th colspan="3">Female</th><th colspan="3">Male</th></tr>
<tr><th></th><th colspan="3">KO/WT</th><th colspan="3">KO/WT</th></tr>
<tr><th>Sub Pathway</th><th>Biochemical Name</th><th>CTRL</th><th>FD</th><th>FS</th><th>CTRL</th><th>FD</th><th>FS</th></tr>
</table>

Sub Pathway	Biochemical Name	CTRL	FD	FS	CTRL	FD	FS
Phosphatidylethanolamine (PE)	1,2-dipalmitoyl-GPE (16:0/16:0)*	1.17	1.37	1.54	1.09	1.45	1.12
	1-palmitoyl-2-stearoyl-GPE (16:0/18:0)*	0.76	1.58	1.38	0.76	1.99	0.63
	1-palmitoyl-2-oleoyl-GPE (16:0/18:1)	1.15	1.29	1.56	1.32	1.51	1.22
	1-palmitoyl-2-linoleoyl-GPE (16:0/18:2)	1.62	1.19	1.67	1.80	1.53	1.66
	1-palmitoyl-2-arachidonoyl-GPE (16:0/20:4)*	1.11	1.03	1.17	1.14	1.12	1.12
	1-palmitoyl-2-docosahexaenoyl-GPE (16:0/22:6)*	1.07	1.00	1.05	1.14	1.08	0.96
	1-stearoyl-2-oleoyl-GPE (18:0/18:1)	1.00	1.19	1.32	1.17	1.37	1.08
	1-stearoyl-2-linoleoyl-GPE (18:0/18:2)*	1.17	1.04	1.42	1.55	1.32	1.40
	1-stearoyl-2-arachidonoyl-GPE (18:0/20:4)	0.98	0.98	1.08	1.09	1.07	1.02
	1-stearoyl-2-docosahexaenoyl-GPE (18:0/22:6)*	1.08	0.96	1.04	1.36	1.18	0.98
	1-oleoyl-2-linoleoyl-GPE (18:1/18:2)*	1.30	1.22	1.57	1.38	1.39	1.53
	1-oleoyl-2-arachidonoyl-GPE (18:1/20:4)*	0.99	1.08	1.10	1.01	1.14	0.99
	1-oleoyl-2-docosahexaenoyl-GPE (18:1/22:6)*	0.96	1.04	0.98	1.02	1.07	0.87
	1,2-dilinoleoyl-GPE (18:2/18:2)*	1.29	0.98	1.63	2.25	1.63	2.20
	1-linoleoyl-2-arachidonoyl-GPE (18:2/20:4)*	1.00	1.02	1.27	1.39	1.27	1.37

<table>
<tr><th rowspan="3">b</th><th></th><th colspan="3">Female</th><th colspan="3">Male</th></tr>
<tr><th></th><th colspan="3">KO/WT</th><th colspan="3">KO/WT</th></tr>
<tr><th>Sub Pathway</th><th>Biochemical Name</th><th>CTRL</th><th>FD</th><th>FS</th><th>CTRL</th><th>FD</th><th>FS</th></tr>
</table>

Sub Pathway	Biochemical Name	CTRL	FD	FS	CTRL	FD	FS
Long Chain Fatty Acid	myristate (14:0)	0.88	1.04	0.93	0.65	0.71	0.61
	myristoleate (14:1n5)	0.95	0.98	0.68	0.89	0.94	0.63
	palmitate (16:0)	0.93	0.99	0.94	0.77	0.75	0.78
	palmitoleate (16:1n7)	0.76	1.07	0.78	0.44	0.56	0.47
	margarate (17:0)	0.97	1.09	0.97	0.99	0.82	0.81
	10-heptadecenoate (17:1n7)	0.78	1.13	0.93	0.64	0.65	0.68
	stearate (18:0)	0.95	0.97	1.05	1.00	0.86	0.91
	oleate/vaccenate (18:1)	0.91	1.01	0.87	0.57	0.66	0.68
	10-nonadecenoate (19:1n9)	0.90	1.19	0.88	0.63	0.66	0.79
	arachidate (20:0)	0.98	1.05	1.13	0.78	0.69	0.98
	eicosenoate (20:1)	0.82	1.14	0.72	0.45	0.55	0.73
	erucate (22:1n9)	0.92	1.11	1.04	0.57	0.69	1.05
	nervonate (24:1n9)*	0.92	1.05	1.19	0.96	0.86	1.10
Polyunsaturated Fatty Acid (n3 and n6)	heneicosapentaenoate (21:5n3)	1.27	1.04	1.30	0.91	0.58	0.75
	hexadecadienoate (16:2n6)	0.94	0.83	0.65	0.97	0.90	0.87
	stearidonate (18:4n3)	0.99	0.90	0.78	1.32	1.08	0.90
	eicosapentaenoate (EPA; 20:5n3)	0.75	0.83	0.99	1.12	0.84	0.77
	docosapentaenoate (n3 DPA; 22:5n3)	0.80	0.81	0.99	1.25	0.88	0.92
	docosahexaenoate (DHA; 22:6n3)	0.77	0.88	1.09	1.02	0.86	0.87
	nisinate (24:6n3)	0.80	0.66	0.99	0.78	0.81	1.15
	linoleate (18:2n6)	0.96	0.93	0.98	0.89	0.83	0.93
	linolenate [alpha or gamma; (18:3n3 or 6)]	0.92	0.96	0.90	0.80	0.74	0.80
	dihomo-linolenate (20:3n3 or n6)	0.81	0.79	0.95	0.82	0.75	0.96
	arachidonate (20:4n6)	0.78	0.88	1.19	0.93	0.85	0.93
	adrenate (22:4n6)	0.78	0.86	0.83	0.99	0.88	1.21
	docosapentaenoate (n6 DPA; 22:5n6)	0.55	0.69	1.09	0.90	0.75	1.08
	docosadienoate (22:2n6)	0.84	0.90	0.97	0.74	0.66	1.31
	dihomo-linoleate (20:2n6)	0.87	0.89	0.81	0.63	0.67	0.87

		Female			Male		
C			KO/WT			KO/WT	
Sub Pathway	Biochemical Name	CTRL	FD	FS	CTRL	FD	FS
	diacylglycerol (12:0/18:1, 14:0/16:1, 16:0/14:1) [1]*	0.73	2.50	0.85	0.26	0.55	0.23
	diacylglycerol (12:0/18:1, 14:0/16:1, 16:0/14:1) [2]*	0.76	1.23	0.71	0.39	0.61	0.39
	diacylglycerol (14:0/18:1, 16:0/16:1) [1]*	0.87	1.28	0.78	0.37	0.62	0.45
	diacylglycerol (14:0/18:1, 16:0/16:1) [2]*	0.86	1.19	0.86	0.47	0.69	0.51
	diacylglycerol (16:1/18:2 [2], 16:0/18:3 [1])*	0.91	1.13	0.69	0.48	0.80	0.62
	palmitoyl-myristoyl-glycerol (16:0/14:0) [1]*	0.98	1.47	0.83	0.35	0.58	0.45
	palmitoyl-myristoyl-glycerol (16:0/14:0) [2]	1.01	1.16	0.92	0.64	0.77	0.53
	palmitoyl-palmitoyl-glycerol (16:0/16:0) [2]*	1.02	1.03	0.91	0.77	0.82	0.78
	palmitoyl-oleoyl-glycerol (16:0/18:1) [1]*	0.92	1.18	0.78	0.45	0.74	0.60
	palmitoyl-oleoyl-glycerol (16:0/18:1) [2]*	0.92	1.12	0.83	0.56	0.78	0.67
	palmitoyl-linoleoyl-glycerol (16:0/18:2) [1]*	1.00	1.08	0.89	0.78	0.97	0.77
	palmitoyl-linoleoyl-glycerol (16:0/18:2) [2]*	1.01	0.99	0.89	0.86	0.97	0.89
	palmitoyl-linolenoyl-glycerol (16:0/18:3) [2]*	0.96	1.36	0.96	0.55	0.86	0.77
	palmitoleoyl-oleoyl-glycerol (16:1/18:1) [2]*	0.71	1.33	0.70	0.32	0.58	0.44
	palmitoleoyl-linoleoyl-glycerol (16:1/18:2) [1]*	0.88	1.03	0.63	0.59	0.84	0.64
	palmitoyl-arachidonoyl-glycerol (16:0/20:4) [2]*	0.84	1.13	0.90	1.08	1.08	0.95
	palmitoleoyl-arachidonoyl-glycerol (16:1/20:4) [2]*	0.83	1.23	0.78	1.51	1.29	0.98
Diacylglycerol	palmitoyl-docosahexaenoyl-glycerol (16:0/22:6) [1]*	0.84	0.97	0.87	0.95	1.01	0.86
	palmitoyl-docosahexaenoyl-glycerol (16:0/22:6) [2]*	0.63	1.41	0.88	0.77	1.18	0.78
	stearoyl-linoleoyl-glycerol (18:0/18:2) [2]*	0.88	1.13	0.75	0.83	0.88	0.92
	oleoyl-oleoyl-glycerol (18:1/18:1) [1]*	0.85	1.17	0.63	0.40	0.76	0.62
	oleoyl-oleoyl-glycerol (18:1/18:1) [2]*	0.85	1.13	0.74	0.46	0.76	0.64
	oleoyl-linoleoyl-glycerol (18:1/18:2) [1]	1.00	1.05	0.71	0.74	0.99	0.91
	oleoyl-linoleoyl-glycerol (18:1/18:2) [2]	0.95	1.05	0.78	0.64	0.96	0.93
	linoleoyl-linoleoyl-glycerol (18:2/18:2) [1]*	1.24	0.90	0.69	1.24	1.17	1.23
	linoleoyl-linoleoyl-glycerol (18:2/18:2) [2]*	0.96	1.20	0.77	0.96	1.48	1.34
	linoleoyl-linolenoyl-glycerol (18:2/18:3) [2]*	1.17	1.13	0.85	0.93	0.98	0.98
	stearoyl-arachidonoyl-glycerol (18:0/20:4) [1]*	0.78	1.02	0.75	0.90	1.18	0.79
	stearoyl-arachidonoyl-glycerol (18:0/20:4) [2]*	0.81	1.03	0.96	0.98	1.21	1.06
	oleoyl-arachidonoyl-glycerol (18:1/20:4) [1]*	0.87	0.91	0.44	0.54	0.64	0.73
	oleoyl-arachidonoyl-glycerol (18:1/20:4) [2]*	0.79	0.94	0.62	0.72	0.97	0.81
	linoleoyl-arachidonoyl-glycerol (18:2/20:4) [1]*	0.99	0.85	0.68	1.15	0.65	0.94
	linoleoyl-arachidonoyl-glycerol (18:2/20:4) [2]*	0.82	0.91	0.71	1.11	1.39	1.14
	stearoyl-docosahexaenoyl-glycerol (18:0/22:6) [2]*	0.71	1.06	0.94	1.20	1.15	0.89
	linoleoyl-docosahexaenoyl-glycerol (18:2/22:6) [2]*	0.84	0.76	0.78	1.43	1.29	1.12

Figure 3.6 CerS6 KO resulted in alterations of multiple lipid classes in livers. Significant increase of phosphatidylethanolamines (a), and significant decrease of long-chain and polyunsaturated fatty acids (b), as well as diacylglycerols (c), were observed

Alterations of dietary folate result in significant changes of liver folates, with 5-methyltetrahydrofolate showing unpredicted dynamics in liver only

As expected, untargeted metabolomics analysis revealed that higher FA in the animals' diets resulted in increased FA levels in both male and female livers (Fig 3.7a). Levels of 7,8-dihydrofolate (7,8-DHF) reached a plateau at supplementation level of 2 ppm in WT males only,

but progressively increased in KO males and both WT and KO females (Fig 3.7b). However,

response of 5-methyltetrahydrofolate (5-MTHF), the major supplier of methyl groups from folate

cycle and a storage form of the vitamin, did not show dose-dependent increase. Liver 5-

methyltetrahydrofolate did not show significant change with increase of dietary FA from 0 to 2

ppm, either in males or females (Fig 3.7c). Even more surprisingly, further increase of FA

supplementation to 12 ppm reduced the 5-MTHF levels in male and female livers of both

genotypes. At the same time, 5-MTHF levels in one of the peripheral tissues (testes), were

progressively increasing with the increase of dietary levels of FA (Fig 3.7c).
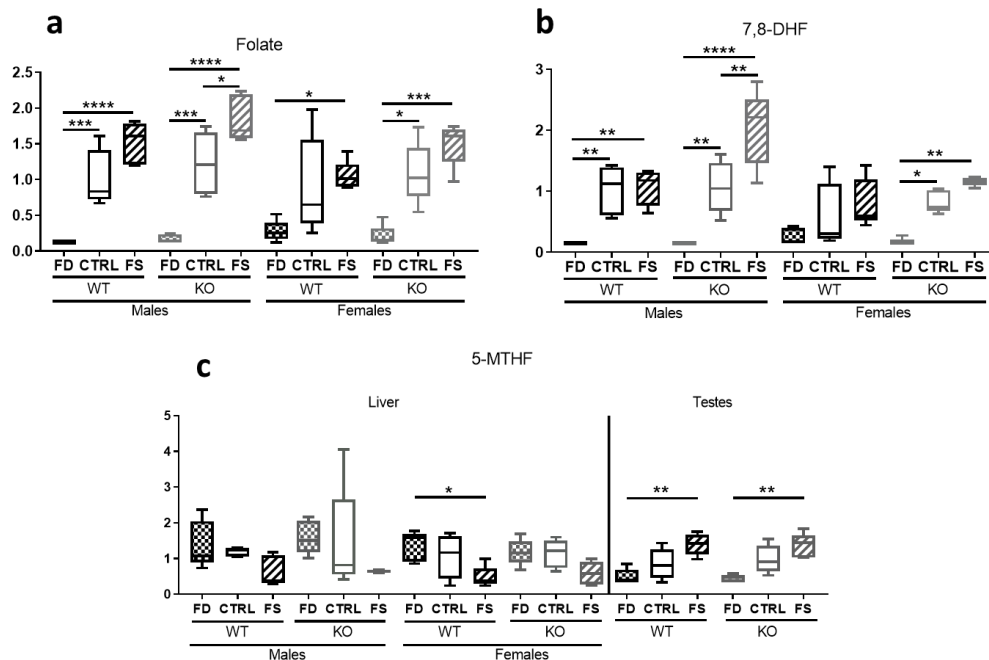
Figure 3.7 Changes of liver folate pools by different levels of dietary FA. Tissue folic acid (a)
and 7,8-dihydrofolic acid (b) demonstrated a dose-dependent response. 5-methyltetrahydrofolic acid
levels (c) were lower in the FS groups in the liver but not in testes. Metabolon ® measurements presented
as box plots showing minimum and maximum values were plotted using Prism software. Checkered bars,
FD diet; solid bars, Control diet; striped bars, FS diet. WT shown in black and KO shown in grey. *,
$p<0.05$; **, $p<0.01$; ***, $p<0.001$; ****, $p<0.0001$, determined by One-way ANOVA with Sidak's
multiple comparisons test

The folate-deficient diet did not affect 5-MTHF levels compared to control diet.

However, the levels of 7,8-DHF and FA were lowered by 54% and 69% correspondingly in WT

females and by 80% for both folate forms in KO females (data not shown). In male mice, reductions of FA and 7,8-DHF on FD were even stronger, by 88 and 86%, correspondingly, in both genotypes, confirming the reduction of liver folate pools on FD diet in our experiments. Folate-over-supplemented diet resulted in 3.8- and 3.2-fold elevations of FA and 7,8-DHF respectively in WT females, and 7.3- and 6.8-fold elevations in KO females (data not shown). As in response to FD diet, response to FS diet in males was stronger than in females, and elevation in WT livers was 12- and 7.4-fold for FA and 7,8-DHF, respectively, while in KO livers 10.7- and 14.2-fold increases were seen (data not shown). Levels of FIGLU, a product of histidine catabolism, were elevated in the folate-deficient livers and reduced in folate over-supplemented tissues, consistent with the role of tetrahydrofolate as the acceptor of the formimino group from FIGLU (data not shown).

Genotype-sex interactions are apparent from metabolomic data

Overall, our metabolomic data frequently show different metabolite levels in different sexes. We therefore examined the genotype: sex interaction, i.e. whether the genotype of the animals had impact on the metabolite levels assessed in male versus female livers, regardless of the diet. All together 143 biochemicals exhibited significant genotype: sex interactions. Among these, metabolites displaying highest statistical significance ($p \leq 0.005$) belong to the groups of ceramides and ceramide-derived sphingolipids, diacylglycerols, as well as some pentose metabolites, purine and TCA cycle metabolites (Fig S3.11a). Additionally, sex: diet interaction analysis which examined whether dietary FA levels affected metabolite differences in males compared to females, irrespective of genotype, identified 109 metabolites showing significant interactions (Fig S3.11b). This interaction was highly statistically significant ($p \leq 0.01$) for metabolites of lipid pathways, such as polyunsaturated and monohydroxy fatty acids,

lysophospholipids, ceramides, sphingomyelins, and several phospholipids. Additionally, metabolites from glycolysis, pentose pathway, and glycogen metabolism, glutathione, methionine and lysine metabolism, as well as several essential vitamin's intermediates displayed significant interactions.

Folic acid supplementation modulated liver levels of vitamin A and multiple B vitamins

Despite the fact that diets with different folate supplementation contained exactly the same levels of all other vitamins and microelements, metabolomic data show that liver levels of these other vitamins or derived cofactors were different between mouse groups depending on different folate supplementation, animal sex and genotypes (Fig 3.8). While liver levels of B_1 (thiamin) were not significantly different among all experimental groups (Fig 3.8a), the thiamin diphosphate levels (active cofactor) were higher in female than in male livers (by a factor of 2 or more in the KO mice, and by a factor of $1.3 - 2$ in the WT). Moreover, the thiamin diphosphate levels showed modest increase with the increase of FA in the diet in WT males only, though the changes did not reach statistical significance (Fig 3.8b). No significant changes depending on FA supplementation were seen in WT males, while KO males demonstrated a trend for cofactor reduction.

With regard to B_6, the vitamin forms pyridoxamine, pyridoxamine phosphate and pyridoxal phosphate were significantly lower in male versus female livers and female livers showed a trend for these forms to inversely associate with the folate supplementation (Fig 3.8c, 3.8d, 3.8e). At the same time, the levels of the cofactor pyridoxal phosphate, were not significantly different between males and females or between genotypes but demonstrated a trend to be lower at highest levels of FA (Fig 3.8f).

Pantothenate (B_5) differed significantly between male and female WT mice (Fig 3.8h), while liver CoA showed direct association with the dietary folate in females (WT and KO) and

51

KO males (Fig 3.8g). In WT males the levels of the CoA showed trend for negative association with dietary FA (Fig 3.8g).

Vitamin B_2, riboflavin, showed statistically significant negative association with dietary FA levels in females (WT and KO) and in KO males. Interestingly, no differences in liver levels of riboflavin were found in WT males at any level of folate supplementation (Fig 3.8i).

Finally, retinol (vitamin A) levels in male livers were significantly decreased at highest FA supplementation for both genotypes (Fig 3.8j). In general, retinol levels were significantly higher in males than in females and female livers did not show response of retinol levels to different FA supplementation in WT animals, but vitamin levels were significantly reduced in FS-KO group.

53
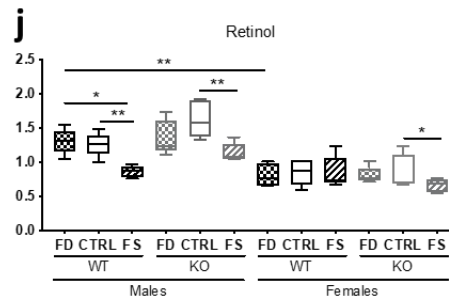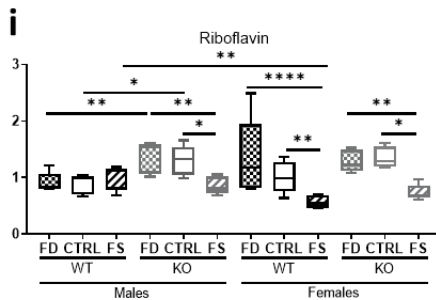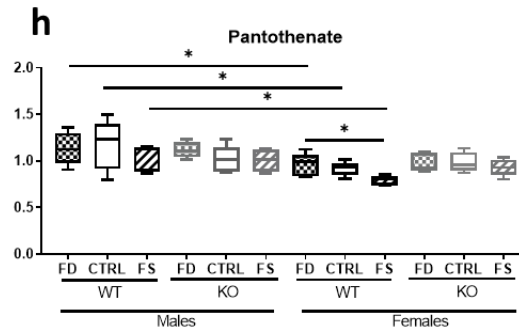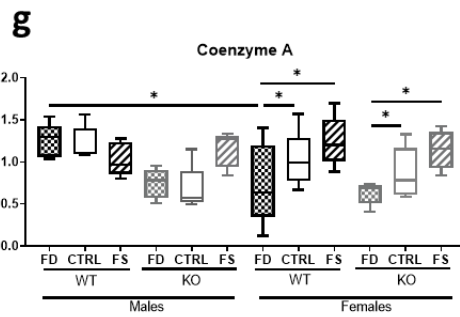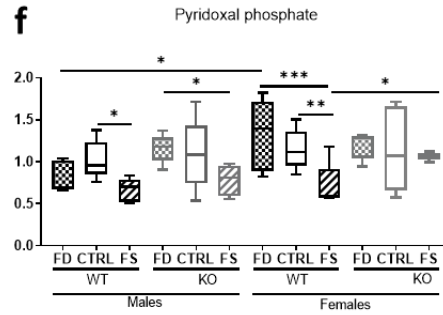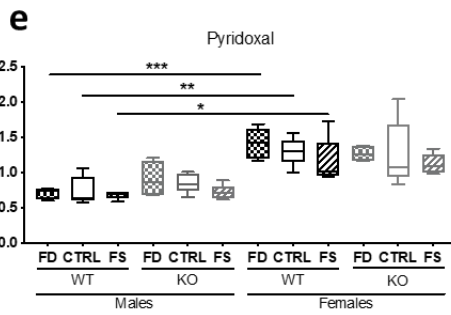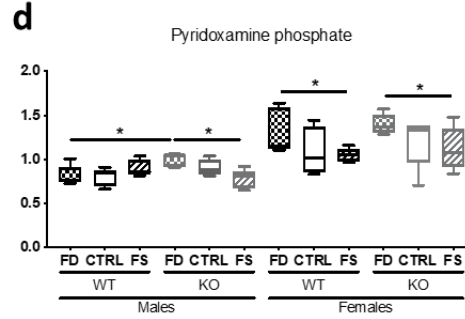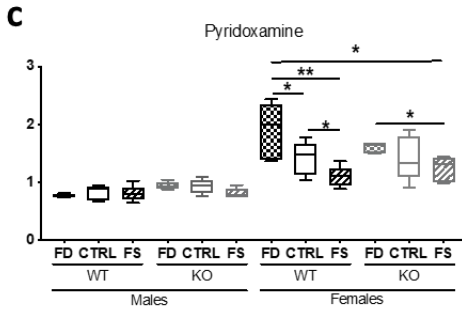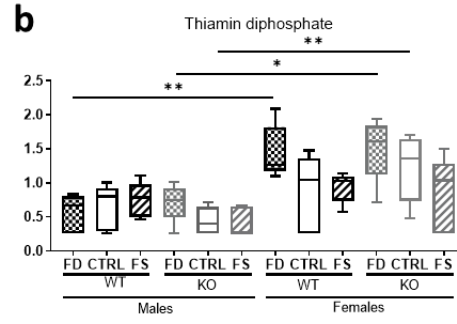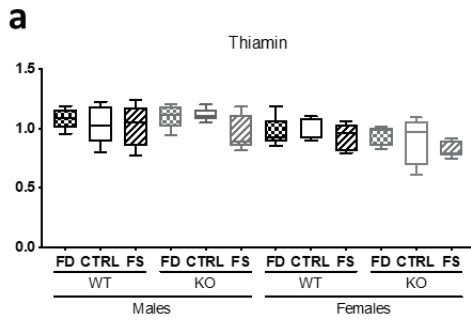
Figure 3.8 CerS6 knockout and alterations of dietary FA resulted in unexpected changes in metabolism of multiple vitamins and derived cofactors. Metabolon ® measurements presented as box plots showing minimum and maximum values were plotted using Prism software. Checkered bars, FD diet; solid bars, Control diet; striped bars, FS diet. WT shown in black and KO shown in grey. *, $p<0.05$; **, $p<0.01$; ***, $p<0.001$; ****, $p<0.0001$, determined by One-way ANOVA with Sidak's multiple comparisons test

Discussion

Our previous studies in A549 and HCT116 cultured cells revealed that perturbations in folate metabolism induced by either vitamin depletion, disruption of enzymes in the folate pathway, or by pharmacological inhibition of the enzymes result in activation of ceramide pathways [12, 249]. Specifically, CerS6 and C_{16}-Cer mediated folate stress response in cultured cells [12]. To investigate the folate–ceramide link in a whole animal model we used CerS6 KO and WT mice. Folate stress was induced in the animals by feeding purified Envigo diets that contained no FA added for folate-deficient diet, or 12ppm FA for folate over-supplemented diet, and compared their effects to control diet with 2ppm FA (average rodent chows contain 2-3ppm FA). Since we are interested in the animal response to physiological folate restriction and not to severe vitamin deficiency, we abstained from the use of antibiotic in the FD diet. Our previous work has demonstrated that after two weeks on the FD diet, total blood folate was reduced 2.2-fold, liver folate was lower by 18% and lung folates dropped by 2.7 fold [254]. Thus, the dietary exposure was chosen to be 4 weeks in order to detect early responses in liver.

Untargeted metabolomic analysis of the liver tissues has demonstrated that, over the course of 4 weeks, selected diets were able to alter liver folate pools in all mice. We observed both sex- and genotype-dependent differences in response to alterations of dietary FA. Tissue levels of folate coenzymes are defined by the vitamin transport as well as by folate enzymes and binding proteins (the cell concentration of these are higher than the total folate concentration [15]). Folates and FA are transported into the cells via two major facilitative transporters, the

ubiquitously expressed RFC and by proton-coupled folate transporter (PCFT), which has more limited tissue expression profile [255]. While for RFC a rather complex transcriptional and post-transcriptional regulation of protein levels has been established [256], no information on sex differences in expression or regulation is available. Proton-coupled folate transporter, discovered just over a decade ago, is less studied, and likewise, its regulation in different genders has not been investigated. In this regard, the folate metabolism enzymes sex-related differences at the mRNA and/or protein levels were found for the *Shmt, Mthfd1, Hprt1, Bhmt, Ppat* and *Mtr* [31]. Additionally, sex-specific dysregulation of cysteine oxidation as well as methionine and folate cycles have been found in *Cgl$^{-/-}$* mice [257]. The exact mechanisms of these sex-specific effects are still not established. Complex formation between FA receptor, progesterone receptor, estradiol receptor and cSrc was proposed recently as a mechanism for prevention of FA effects on proliferation and migration [258]. However, it is not clear, what authors meant under the term "FA receptor", which type of the folate receptor they investigated, α, β, or γ (if it was the folate receptor), and whether this mechanism could affect the vitamin delivery to the cells. Thus, the understanding of how exactly folate metabolism is regulated in different sexes is still missing, but the fact that CerS6 knockout changed the 7,8-DHF response in male mice and 5-MTHF response in female mice, indicates that ceramides might be involved.

Contrary to what could be expected, levels of 5-MTHF in livers did not follow the trend of FA and 7,8-DHF. The FS groups of both genotypes and both sexes showed reduced levels of this cofactor (Fig 3.7). Our data agree with the observations published for WT and MTHFR-deficient mice (MTHFR$^{+/-}$) fed diets over-supplemented with FA (20 ppm FA) for 6 months [37]. In that study, FA over-supplemented male mice had liver levels of folic acid elevated by 60%, and the fraction of 5-MTHF levels in total folate pool was reduced by nearly 40% in WT

animals. In MTHFR$^{+/-}$ mice 5-MTHF levels were lower on control diet and were reduced further by FA over-supplementation to the same levels as in WT animals. Overall reduction of SAM both due to diet and genotype was noted, with more pronounced effect on SAM/SAH ratio [37]. Our metabolomic data also show reduction of SAM in both sexes, but this reduction was statistically significant in WT males only, and the increase of SAH levels reached significance only in KO males and females (data not shown). This difference could be attributed to the shorter dietary exposure (4 weeks versus 6 months in the earlier study). The previous study also has provided an explanation of over-supplementation effect on 5-MTHF. It demonstrated that FA over-supplementation was able to inhibit MTHFR activity *in vitro*, reduced overall MTHFR levels in over-supplemented animals, and also increased phosphorylation of the enzyme, which reduced its activity [37]. All of these mechanisms reduced liver methylation capacity on the high FA diet, mobilized the use of methyl groups from choline and betaine, altered gene expression of one-carbon and lipid metabolism genes and led to hepatocyte degeneration, raising concerns about clinical effects of consumption of high-dose FA supplements [37]. Our experiments, in this regard, demonstrate that metabolic perturbations in the methyl group metabolism become noticeable much earlier, within four weeks of FA over-supplementation, thus, arguing for caution with regard to high-dose supplements even when used for a limited time.

Our metabolomic analysis also included one peripheral tissue, in addition to liver. Previous work from our laboratory has found significant histological changes in testes of CerS6 KO mice which prompted us to include this tissue into analysis. However, there were no changes in FA metabolites between WT and CerS6 KO mice testes. Interestingly, 5-MTHF in the testes was increased dose-dependently with FA supplementation. This could be explained, by the fact, that liver is the main organ of folate metabolism and a major depot of the vitamin [243, 259]. All

peripheral tissues are exposed to blood folate only, where 83 - 95% is represented by 5-MTHF [254, 260-262]. Thus, peripheral tissues should be less affected by the inhibitory effects of high dietary FA on MTHFR.

The relatively short duration of our study is a probable reason for the lack of major histopathological changes which could be related to specific diet or genotype in our animals (Fig S3.3, S3.4). Indeed, while the above referenced study have shown increase of liver and spleen weights in animals after six month on folate over-supplemented compared to control diet [37], in our experiment, organ weights were not different and no significant differences in plasma glucose and cholesterol levels were observed (Fig S3.2). While involvement of CerS6 in lipid droplet biology has been shown previously [165], in our study occasional lipid droplets formation could be seen on any of the three diets, though more often in livers of folate-deficient mice, while livers of the KO folate supplemented animals of both sexes were protected from steatosis.

Despite the fact that at the end of dietary treatment the animals body weights were not different between different dietary groups, the KO males on all diets gained significantly less weight than WT males and had significantly lower fat mass. This protection of the KO males from weight gain is in agreement with the results obtained in a different CerS6 KO model, where protection from obesity and improvement of glucose tolerance were found [205], thus, spurring the interest in pharmacological inhibition of CerS6 for development of therapeutic approaches to combat obesity and type 2 diabetes. It should be noted that this previous study used only male mice, and the concept of "protection by CerS6 inhibition" requires further investigation of the CerS6 function, since our results demonstrate that over the period of 4 weeks, CerS6 KO showed no protection in females. Conversely, the use of CerS6 antisense oligonucleotides to knockdown

CerS6 in male and female obese mice (either due to HFD feeding or the use of *ob/ob* mice) demonstrated differences between sexes in ceramide levels, specifically hepatic $C_{16:0}$-Cer [4], further underscoring sex differences in responding to dietary intervention.

Our results are in agreement with conclusions from a study of the relationship between hepatic ceramides and insulin resistance in the Hybrid Mouse Diversity Panel [263]. This work has found large differences in genetic, hormonal, and dietary regulation of liver C_{16}-, C_{18}- and C_{20}-Cer indicating that different ceramides have different effects in males and females. It was also demonstrated that part of the sex differences could be explained by inhibitory effect of testosterone on the expression of sphingolipid biosynthesis enzymes, such as *Sptlc1*, *CerS6*, *Degs1*, *Asah1*, *Cerk* and *Kdsr* [263]. Additionally, associations of several genomic loci with C_{16}-, C_{18}-, and C_{20}-Cer were sex-specific. Sex-specific differences in sphingolipid metabolism in the aging human brains [264] and sex-specific regulation of CerS6 in a study of experimental autoimmune encephalomyelitis [265] have also been reported. It should be noted that evidence for sex-specific regulation and function of sphingolipids has been accumulating since 1985 [266], however the information regarding sex-dependent activity and regulation of sphingolipids (as well as their mechanisms) is still scarce. Thus, investigation of sphingolipid effects, as well as approaches to target them, need to be evaluated mechanistically in each sex.

The data generated in this study confirmed our hypothesis that in the whole animal, similar to the cultured cells, ceramides respond to alterations of dietary folate. Thus, folate depletion in WT livers caused significant increase in C_{14}-Cer levels, however C_{16}-Cer levels were not significantly different between control and FD livers in WT animals of both sexes. The lack of C_{16}-Cer elevation could be explained by the tight control of this sphingolipid mediator due to its role in lipotoxicity [267]. On the other hand, increase of ceramides with longer acyl

chains in KO males on the control diet could be explained by the compensatory mechanisms induced upon knockout, similar to those observed in cultured cells upon individual CerS knockdown [268]. In cultured cells, CerS6 knockdown was accompanied by upregulation of CerS1, CerS4 and CerS5 producing C_{18}-Cer; C_{18}-C_{20}-Cer and C_{14}-C_{16}-Cer correspondingly. Such up-regulation could explain medium-long-chain ceramide elevation. At the same time, increase in expression of CerS5 in the knock-out could also favor heterodimerization of CerS5 and CerS2 (shown in cultured cells), which had increased activity of CerS5 by a fraction, and activity of CerS2 three-fold in CerS6$^{-/-}$ cells [133]. Thus, this mechanism could also account for the increase in very-long-chain ceramides in the KO males. Interestingly, no significant changes in the C_{18}- and C_{26}-Cer were noted for females, further underscoring sex-specific regulation of ceramides. Overall, due to such compensatory changes of ceramide levels in males and rather limited ceramide responses in females, no significant changes in total ceramide levels were observed in either males or females due to diet alteration or due to genotype.

In addition to compensatory changes in CerS activity, the homeostatic levels of ceramides could be maintained via their conversion to complex sphingolipids, such as SM and/or HexCer. Since we did not observe significant changes in C_{14}- and C_{16}- SM in male livers (Fig S3.7), SM biosynthesis is likely not the mechanism for stabilization of ceramide concentrations. Observed increase of multiple SM species on FS diet was sex-specific for long-chain SM but showed no sex difference for very-long-chain SM. This increase in SMs on folate over-supplemented diets could be related to the function of folate metabolism as a supplier of methyl groups for the metabolic processes, including the formation of phosphatidylcholine from phosphatidylethanolamine via PEMT pathway [269, 270], with phosphatidylcholine donating the phosphocholine group for biosynthesis of SM.

Hexosyl-ceramides, another group of complex sphingolipids, also showed sensitivity to dietary folate. Both C_{14}- and C_{16}-HexCer were elevated in livers on FD diet in WT and in CerS6 KO mice, with the changes in males being statistically significant, and in females following the trend, but not reaching significance. These sphingolipids are generated by glycosylation of corresponding ceramides; thus, their elevation masks the increase in production of ceramide by CerS6. Ceramides are important regulatory molecules and their levels must be tightly regulated [271, 272]. Conversion of Cer to SM or HexCer could function as a safety mechanism protecting from damaging effect of response to dietary alterations [273, 274]. C_{14}-HexCer is significantly higher in females than in males for both genotypes, while C_{16}-HexCer is higher in females than in males for WT mice, and shows no significant difference in KO mice, pointing to sex-specific regulation of liver C_{16}-Cer by CerS6. Interestingly, very-long-chain Cer were insensitive to folate depletion in males but responded to folate depletion in females. Total HexCer also showed statistically significant response to folate depletion only in female KO, with similar trends for WT females and both WT and KO males. The consequences of this response are unclear. Hexosyl-ceramides represent the simplest members and precursors for a whole class of membrane lipids, the glycosphingolipids [275]. Only glucose or galactose can be added to ceramide head group in mammalian cells [276] and 85% of complex sphingolipids have glucose as a first sugar [277]. Apart from serving as basic substrates for building complex sphingolipids, hexosyl-ceramides have their own biochemical functions. Glucosylceramide is required for intracellular membrane transport, is involved in control of cell proliferation and survival, multidrug resistance, natural killer T-cell functions, while galactosyl-ceramide plays major role in myelin formation, promotes immunotolerance and induction of cytokines [276].

Unfortunately, our analysis was not able to differentiate between glucosyl- and galactosyl-ceramide.

Overall, our study has shown that dietary folate affects ceramides as well as complex sphingolipids in both sex and genotype-dependent manners. Sphingolipids, and ceramides in particular, are established regulators of proliferation, differentiation, senescence and apoptosis. Thus, it is easy to conclude that alteration of dietary folate could have an effect on these important cellular processes. One limitation to the current study is that hepatic sphingolipid pools were measured but none of the other tissues were analyzed to understand how other tissues may have been affected by dietary FA intervention or by knockout of CerS6. We also did not investigate effects of FA on lipoprotein particles composition or FA effects on lipids delivery from the liver to other tissues.

We employed the untargeted metabolomics to investigate how broadly the response to dietary FA affects liver metabolism and found that sex was the strongest factor separating the liver metabolomes while genotype and diet were weaker discriminators. The random forest analysis, an unbiased and supervised classification technique splitting data into groups based on the biochemicals providing best separation between groups, resulted in predictive accuracy of 64% when all 12 groups were included, compared to 8.3% by random chance alone (Fig S3.8b). The top 30 biochemicals ranked on their importance in separating metabotypes of the groups included C_{16}-acyl chain containing Cer, SM, and GlucCer, folate coenzymes, FIGLU and gamma-glutamyl-peptides, all of which are linked to the effect of genotype and dietary FA (Fig S3.9). Several phosphatidylethanolamines were also among the top metabolites (Fig 3.6a) indicating broader effect of the diet and genotype in our experiment. On the contrary, levels of multiple long-chain fatty acids as well as diacylglycerols were reduced, especially in male KO

mice (Fig 3.6b, 3.6c). Apparently, changes in sphingolipid biosynthesis due to absence of CerS6 altered free fatty acid utilization as well as phospholipid homeostasis.

Additionally, we evaluated whether the genotype of the animals had an impact on metabolite levels assessed in the male compared to female samples, irrespective of the diet fed (genotype: sex interaction, Fig S3.11a). Out of total 143 biochemicals displaying significant genotype: sex interaction, the top 46 metabolites are sphingolipids, phosphatidylethanolamines, diacylglycerols, long-chain fatty acids, as well as guanosine, TCA cycle, glycolysis, pentose and fructose, mannose and galactose metabolic pathways. The sex: diet interaction evaluated the diet effect on the differences in metabolites assessed in males and females, irrespective of genotype. Out of 86 metabolites demonstrating genotype: diet interactions (Fig S3.11b), the top 46 metabolites (with p-value ≤ 0.01) represented a more versatile group: polyunsaturated fatty acids, monohydroxy fatty acids, long-chain fatty acids, ceramide, sphingomyelin, phosphatidylcholines, phosphatidylethanolamines, phosphatidylserine, lysophospholipids, branched chain fatty acid metabolism, glycolysis, glycogen, pentose and fructose, mannose and galactose metabolism, glutamate, methionine, lysine and glutathione metabolism. Importantly, sex: diet interaction was also found for multiple vitamin metabolites, such as folate, pantothenate, and vitamin B_6.

Closer examination of vitamin levels revealed previously unknown responses of multiple vitamins levels to changes of dietary FA. The initial expectation was that since all vitamins' supplementation levels (excluding FA) were absolutely identical in all diets and these vitamins do not use the FA transporters, the vitamins and their metabolite/cofactor forms will be at the same levels in mouse tissues from different groups. However, liver metabolomic analysis

revealed unexpected differences in the multiple vitamin cofactors levels between the groups that have identical supplementation levels.

For example, thiamin (B_1) liver levels were not significantly different between the groups (Fig 3.8a), indicating that cellular vitamin transport was not affected by FA. However, the active coenzyme form thiamine diphosphate levels were changed depending on dietary FA and animal sex (Fig 3.8b). Sex difference in the levels of this cofactor could be linked to the differences in the levels of enzymes utilizing it, and while there is no data on male/female enzyme expression, a higher level of pyruvate dehydrogenase complex activity was found in brain mitochondria of young adult female mice compared to young adult males [278], which could be a reflection of higher expression levels. While male WT mice did not show changes in thiamin diphosphate levels, the KO males had decreased levels with increase of dietary FA, similar to females. It is not clear why the active coenzyme levels would be reduced as dietary FA increased, but one of the explanations could be the reduced tissue adenosine triphosphate (ATP) levels, which is required to phosphorylate the imported vitamin in the cells. At present, there is no information regarding the FA over-supplementation effects on hepatocyte ATP levels, however, our metabolomic data show significant accumulation of succinyl-carnitine in over-supplemented males and females as well as reduced isocitrate levels in over-supplemented groups, with the exception of WT females. These changes in TCA cycle metabolites could indicate the impairment in the cellular ATP production. However, this needs to be confirmed experimentally.

Another vitamin demonstrating response to dietary FA is B_6. Specifically, the vitamin forms pyridoxamine, pyridoxamine phosphate, and pyridoxal were higher in females and were reduced with increase of FA in females and KO males, although not always reaching statistical significance (Fig 3.8c, 3.8d, 3.8e). Wild-type males did not show such reduction for any of the

forms. The active coenzyme form pyridoxal phosphate did not show sex-related difference and demonstrated reduced coenzyme levels with increase of FA only in KO males and WT females (Fig 3.8f). WT males and KO females did not show such trend. Pyridoxal phosphate is involved in folate metabolism serving as a cofactor for enzyme serine hydroxymethyltransferase (SHMT), which brings one-carbon groups to folate cycle [279]. However, it is still not clear how FA could affect this cofactor levels. Similar to thiamin diphosphate the modulation of ATP levels could be responsible for the coenzyme decrease.

Vitamin B_5 (pantothenate) differed between male and female WT mice and between WT female mice between low and high FA diets. Additionally, the concentration of cofactor CoA, showed dependence on FA dietary supplementation. In this case, the cofactor concentrations increased with the increase of the FA in females of both genotypes, and in male KO mice (Fig 3.8g). Wild-type males rather showed tendency to decrease CoA concentrations with FA increase (Fig 3.8g) but this trend did not reach statistical significance. Correlation of CoA changes with FA levels could be linked to the CoA biosynthetic pathway. Indeed, elevated cysteine concentrations in female FS groups of both genotypes and male KO FS mice could drive increase in formation of 4-phospho-pantetheine and the coenzyme production.

Riboflavin, vitamin B_2, was also augmented by FA supplementation, with increase in FA causing reduction of tissue vitamin levels in females of both genotypes and in KO males (Fig 3.8i). WT males did not show changes of B_2 cofactor dependent on FA. Riboflavin is involved in the folate cycle by being a co-factor of MTHFR and methionine synthase, and thus its reduction upon FA supplementation could affect the one-carbon groups flow to the methylation processes. Interestingly, an intervention study of the folate and riboflavin supplementation effects on lowering plasma homocysteine in humans also noted that supplementation with FA (400μg/day)

decreased the riboflavin status in humans [280]. The vitamin status in the study was evaluated by measurements of plasma riboflavin levels and by erythrocyte glutathione reductase activation values as a surrogate of the cellular vitamin status. No information on tissue vitamin levels was obtained in that study. While increased rate of B_2 turnover or increased binding of FAD to MTHFR were proposed as possible mechanisms [280] there is a lack of studies on riboflavin interacting with or being regulated by FA.

Another vitamin that displayed response to FA levels was a fat-soluble vitamin retinol (vitamin A). Retinol levels were higher in males than in females, and in WT and KO males and KO females they were significantly reduced with increase of FA in the diet (Fig 3.8j). As in the case of pyridoxal and riboflavin, it is not clear how water-soluble FA could affect tissue levels of vitamin A. Potentially changes in sphingolipids could affect liver stores of retinol.

Thus, our metabolomic data show perturbations in multiple vitamins metabolism upon FA over-supplementation, which could affect numerous metabolic pathways. Significant differences were observed for several vitamins between males and females, pointing to sex differences in vitamins metabolism. Importantly, knockout of CerS6 resulted in shift from the WT vitamin-FA relationship pattern to the relationship pattern of the opposite sex. For example, for thiamin diphosphate, pyridoxamine phosphate, pyridoxal, CoA, and riboflavin, the pattern of response to FA in male KO livers was similar to a female response pattern and not to WT male response. At the same time, for pyridoxal phosphate and retinol, the pattern of response to FA in KO females was similar to male response patterns and not to a WT female response. While multiple signaling and regulatory roles for C_{16}-Cer have been established, current knowledge of its effects on vitamin metabolism is lacking.

Conclusion

In conclusion, our study determined that dietary folic acid depletion or over-supplementation affect levels of ceramides and complex sphingolipids in mouse livers and that CerS6 plays a central role in this adaptation. Sphingolipid response to dietary folate in our study depended on sex and CerS6 genotype, and sphingolipids with C_{14}- and C_{16}-acyl chains were significantly higher in females than in males. This underscores the need for establishing sex-specific reference values for sphingolipid biomarkers and for the investigation of sex-specific mechanisms of their regulation. Additionally, CerS6 and CerS5 have been investigated for their role in disease states including obesity and metabolic syndrome [4, 173, 205] but there is little data about how short- and long-term dietary changes affect sphingolipid levels. While knockout or knockdown of these CerS has been found to be protective, it is necessary to understand how sphingolipids respond to diet in order to translate these findings to humans. Despite being required in relatively small quantities in the diet, folate is clearly important for liver metabolism including metabolism of sphingolipids.

Metabolomic analysis indicates that both dietary folic acid and CerS6 knockout have pleiotropic effects on liver metabolome, and some of these effects, such as alterations in tissue levels of other vitamins or their cofactor forms, cannot be linked directly to folate metabolism but may be mediated by additional regulators. Further studies of the mechanisms connecting folate and sphingolipid metabolism as well as characterization of the FA effects on liver metabolic pathways will help to avoid unwanted side-effects of over-supplementation.
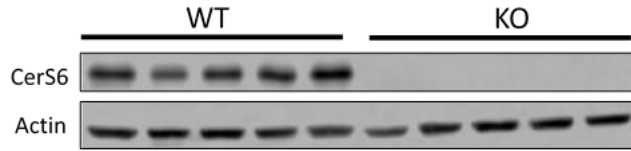
Figure S3.1 CerS6 protein is not detected in livers of CerS6 KO mice by Western blotting
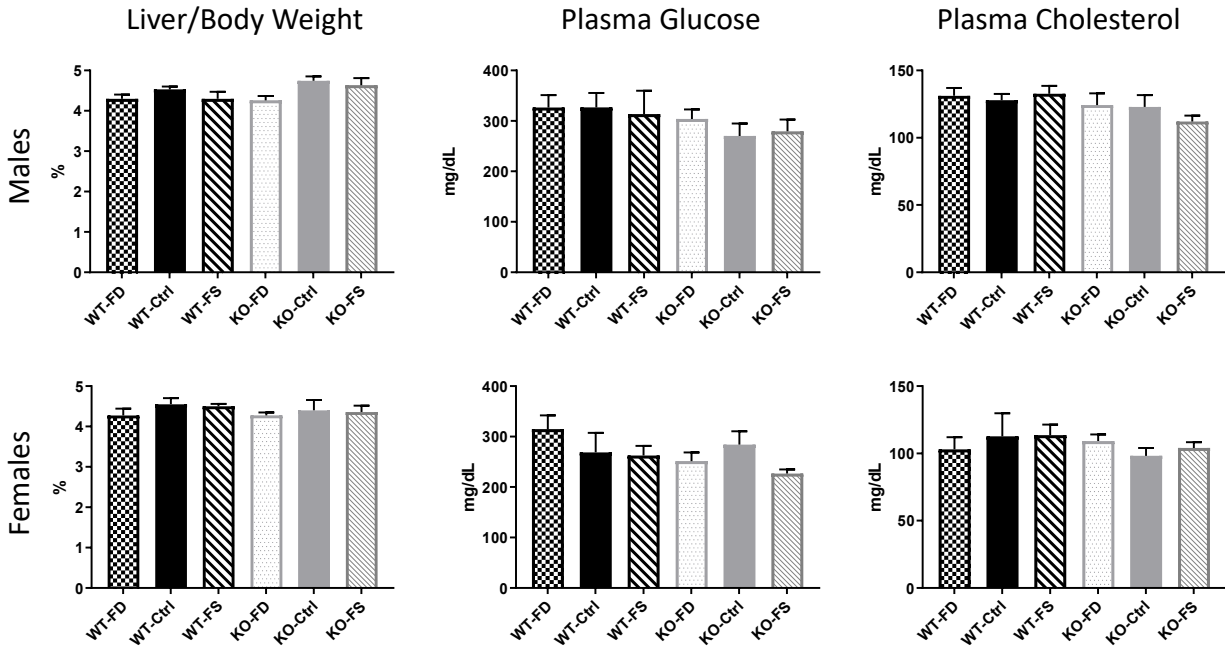
Figure S3.2 Knockout of CerS6 did not change liver weight, nor plasma glucose, nor cholesterol. Data are shown as mean $\pm$ SEM, n=5. Checkered bars, FD diet; solid bars, Control diet; striped bars, FS diet. WT shown in black and KO shown in grey. *, $p<0.05$; **, $p<0.01$; ***, $p<0.001$; ****, $p<0.0001$ determined by One-way ANOVA with Sidak's multiple comparisons test
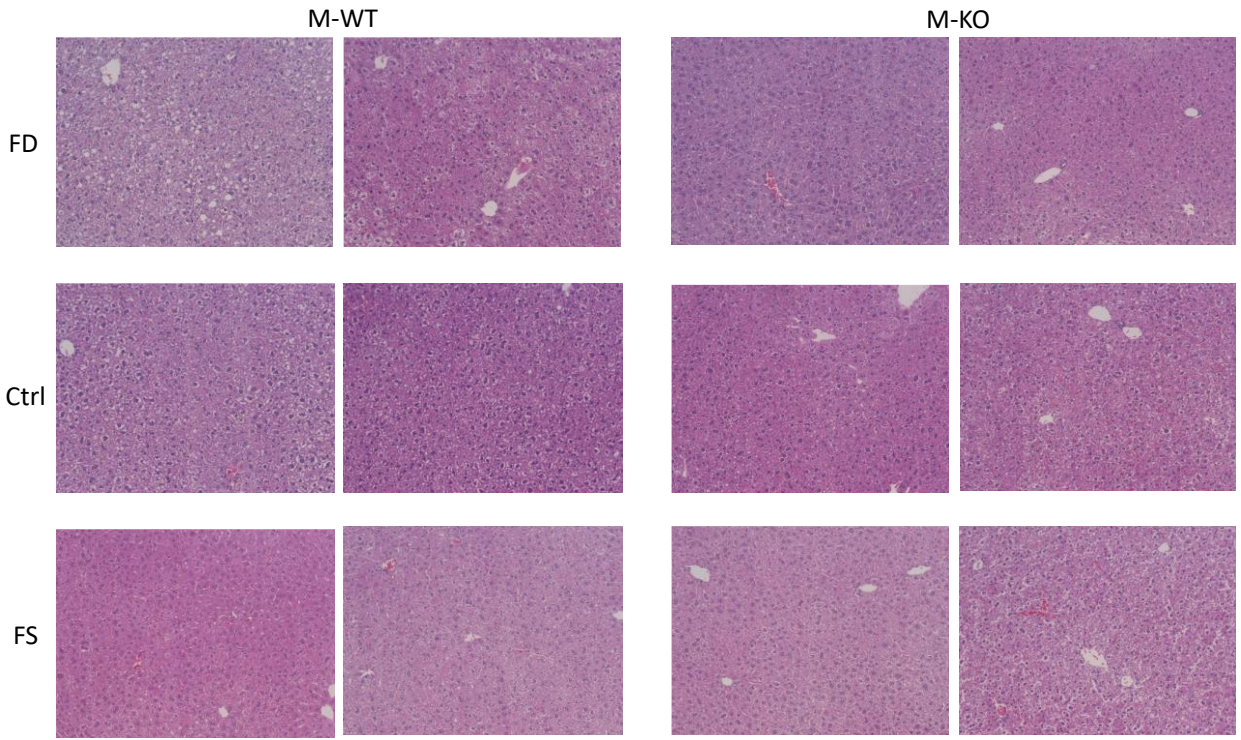
Figure S3.3 Liver sections stained with H&E revealed no significant differences between male WT and KO mice on any diet
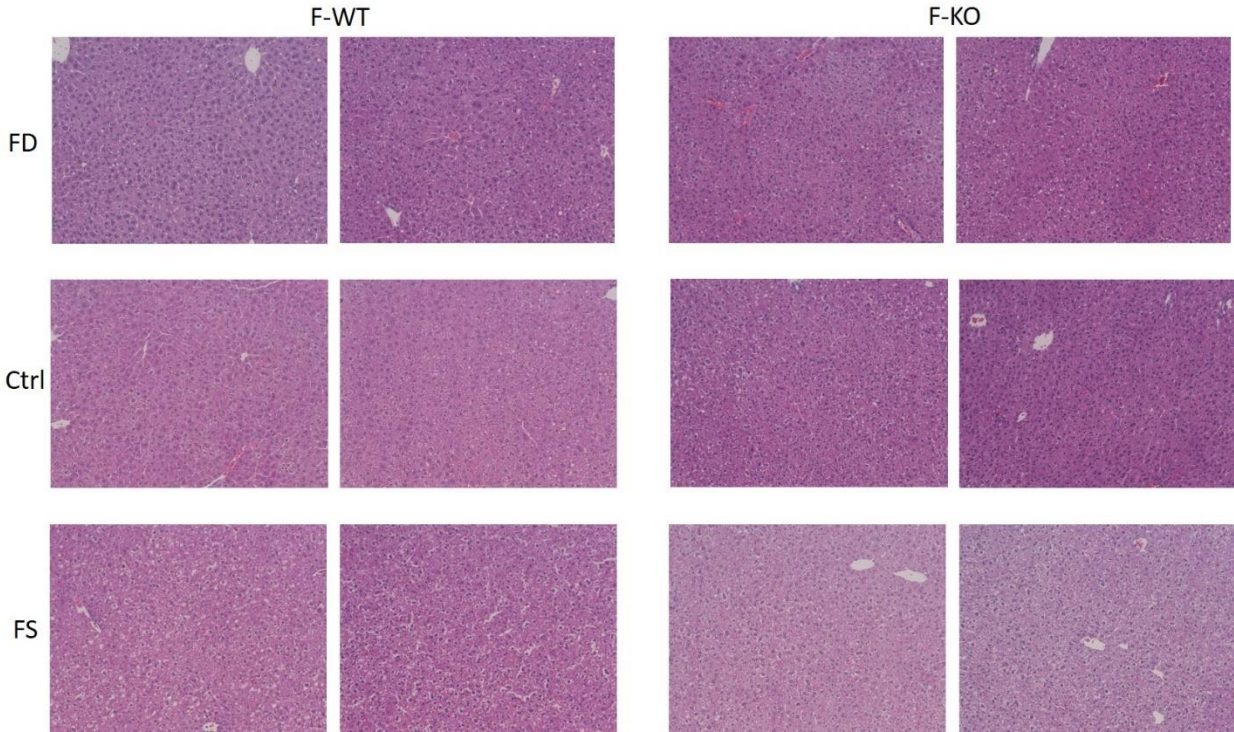
Figure S3.4 Liver sections stained with H&E revealed no significant differences between female WT and KO mice on any diet
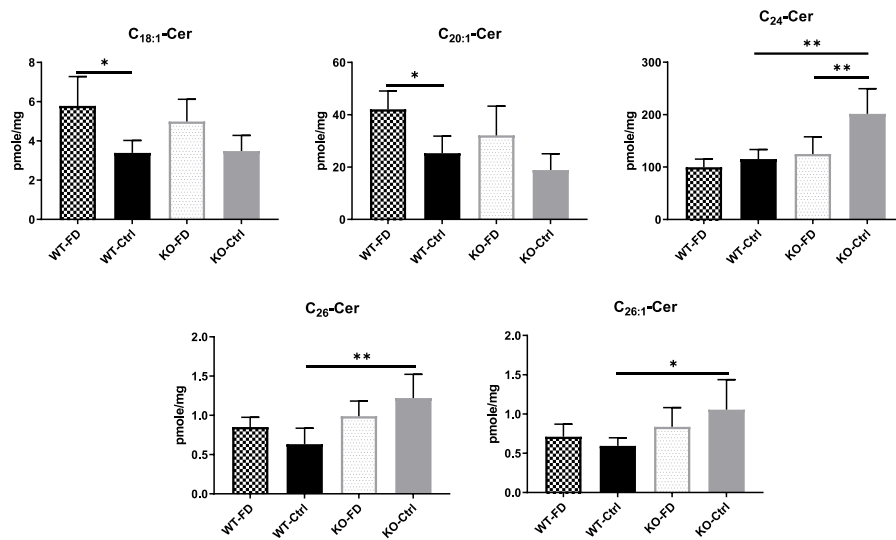
Figure S3.5 Folate deficient diet elevated long-chain ceramides while CerS6 KO elevated very-long-chain ceramides in male mice. Data presented as mean $\pm$ SEM, n=5. Checkered bars, FD diet; solid bars, Control diet. WT shown in black and KO shown in grey. *, $p<0.05$; **, $p<0.01$; ***, $p<0.001$; ****, $p<0.0001$, determined by Student's t-test between genotypes and diets
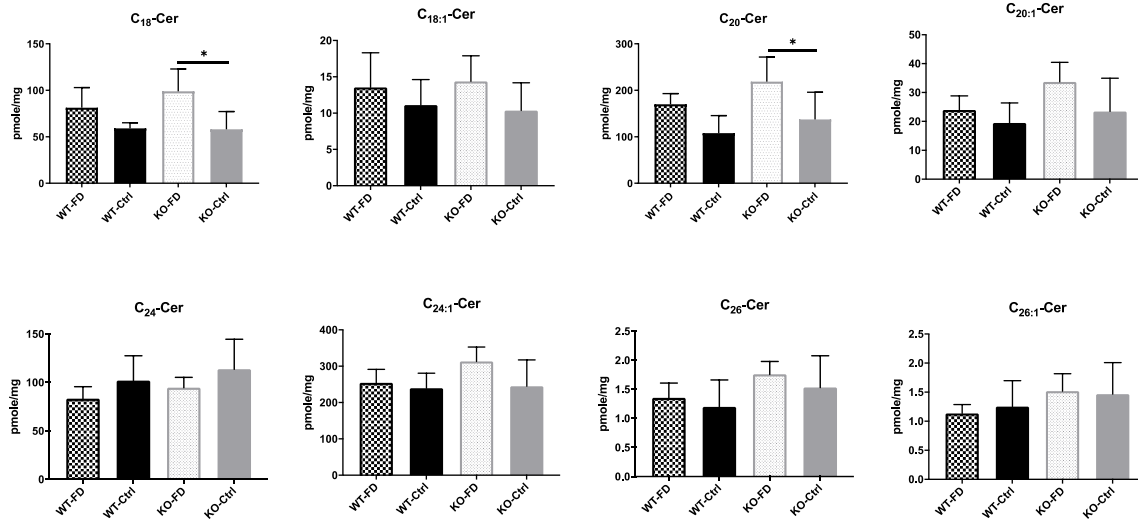
Figure S3.6 Ceramides levels are mostly unchanged in female mice. C_{18}- and C_{20}-ceramides in CerS6 KO mice were the only species responding to FD diet. Data represent mean $\pm$ SEM. Checkered bars, FD diet; solid bars, Control diet. WT shown in black and KO shown in grey. *, $p<0.05$; **, $p<0.01$; ***, $p<0.001$; ****, $p<0.0001$ determined by Student's t-test between genotypes and diets
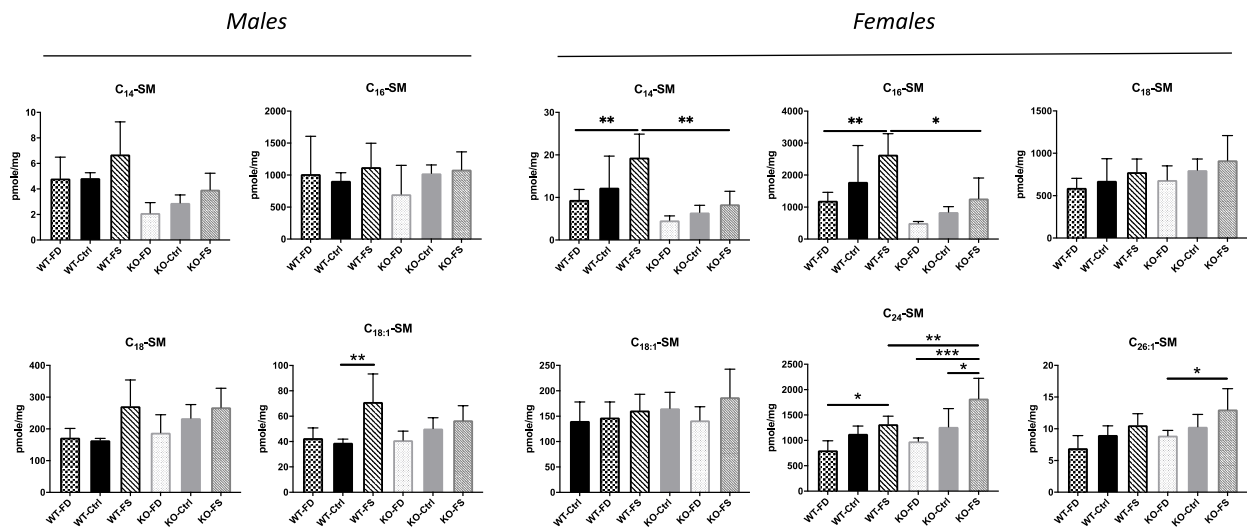
Figure S3.7 Sphingomyelins are elevated in response to FA over-supplementation. Male mice did not show significant changes on FS diet changes in sphingomyelin levels when placed a folic acid over-supplemented diet for both WT and KO mice but there were more changes in females than males. Data are shown as mean values $\pm$ SEM. Checkered bars: FD diet, Solid bars: Control diet, Striped bars: FS diet. WT shown in black and KO shown in grey. *, $p<0.05$; **, $p<0.01$; ***, $p<0.001$, ****, $p<0.0001$ according to One-way ANOVA with Sidak's multiple comparisons test

70

a

Statistically Significant Biochemicals	ANOVA Main Effects						
	Genotype Main Effect	Sex Main Effect	Diet Main Effect	Genotype: Sex Interaction	Genotype: Diet Interaction	Sex: Diet Interaction	Genotype: Sex: Diet Interaction
Total biochemicals p≤0.05	273	550	298	143	86	112	44
Total biochemicals 0.05<p<0.10	47	35	68	57	44	70	49

b

<div align="center">Predicted group</div>

Actual group	CerS6 KO Ctrl F	CersS6 KO FD F	CerS6Ko FS F	WT Ctrl F	WT FD F	WT FS F	CerS6 KO Ctrl M	CersS6 KO FD M	CerS6Ko FS M	WT Ctrl M	WT FD M	WT FS M	Class Error
CerS6 KO Ctrl F	1	1	2	0	0	1	0	0	0	0	0	0	80%
CersS6 KO FD F	0	5	0	0	0	0	0	0	0	0	0	0	0%
CerS6Ko FS F	0	0	5	0	0	0	0	0	0	0	0	0	0%
WT Ctrl F	0	0	0	1	2	2	0	0	0	0	0	0	80%
WT FD F	0	2	0	1	2	0	0	0	0	0	0	0	60%
WT FS F	0	0	0	0	0	5	0	0	0	0	0	0	0%
CerS6 KO Ctrl M	0	0	0	0	0	0	3	1	1	0	0	0	40%
CersS6 KO FD M	0	0	0	0	0	0	2	2	0	1	0	0	60%
CerS6Ko FS M	0	0	0	0	0	0	0	1	4	0	0	0	20%
WT Ctrl M	0	0	0	0	0	0	0	0	0	4	1	0	20%
WT FD M	0	0	0	0	0	0	0	1	0	1	2	1	60%
WT FS M	0	0	0	0	0	0	0	0	1	0	0	4	20%
Predictive accuracy = 64%													

Figure S3.8 Metabolomics data summary. (a) Numbers of biochemicals out of total 736 measured metabolites that show differences between genotypes, gender and diets, as well as interactions between genotype and gender, genotype and diet, gender and diet. (b) Random forest analysis of the metabolomic data based on the biochemicals that provide best separation between the groups gives predicted accuracy of 64% when 12 experimental groups were compared. Predictive accuracy when separation into groups is done by random chance alone is 8.3%
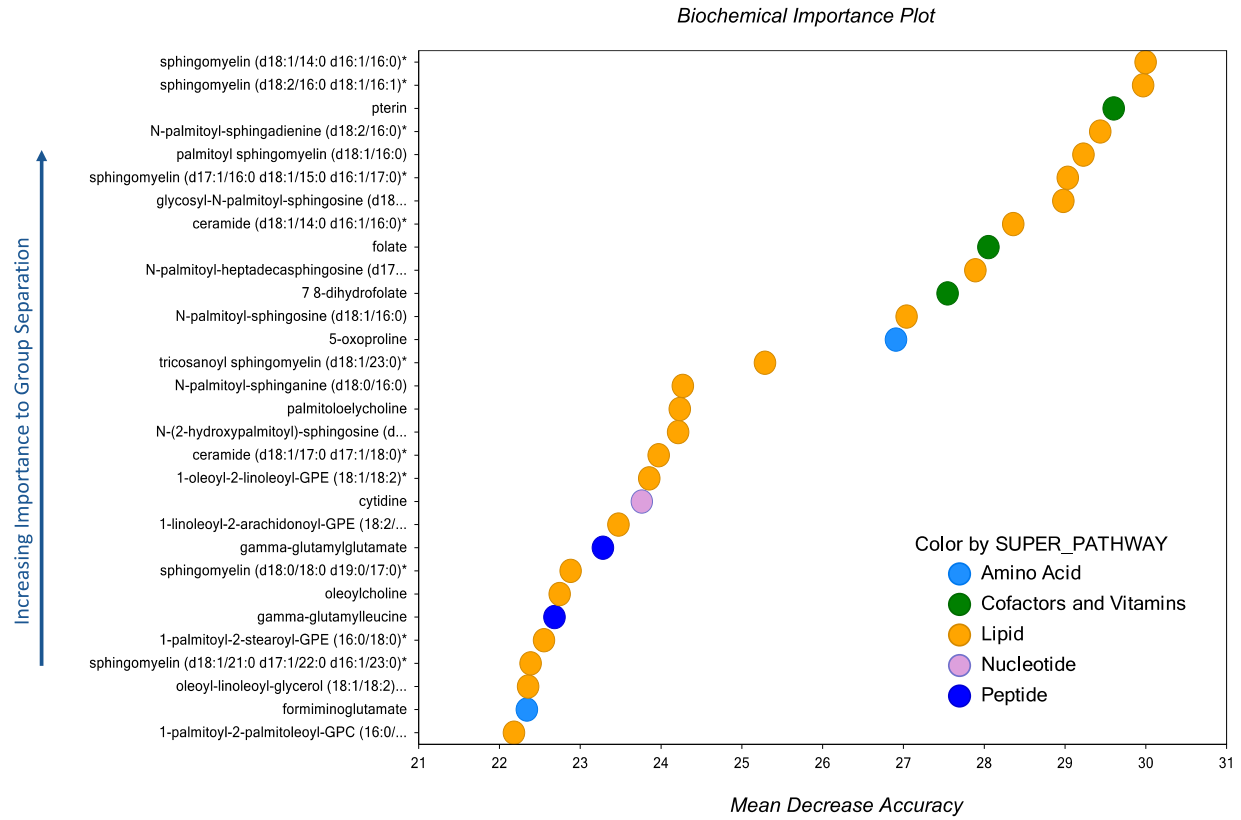
Figure S3.9 Top 30 biochemicals ranked by their importance in separating metabolic profiles of 12 groups

a

Sub Pathway	Biochemical Name	Fold Change					
		KO CTRL F WT CTRL F	KO FD F WT FD F	KO FS F WT FS F	KO CTRL M WT CTRL M	KO FD M WT FD M	KO FS M WT FS M
Dihydroceramides	N-palmitoyl-sphinganine (d18:0/16:0)	0.75	0.63	0.62	1.05	1.00	0.75
Ceramides	N-palmitoyl-sphingosine (d18:1/16:0)	0.37	0.35	0.39	0.74	0.74	0.48
	N-stearoyl-sphingosine (d18:1/18:0)*	1.08	0.90	1.00	1.20	1.31	0.89
	ceramide (d18:1/14:0, d16:1/16:0)*	0.47	0.47	0.40	0.29	0.39	0.27
	ceramide (d18:1/17:0, d17:1/18:0)*	0.77	0.60	0.77	1.00	0.94	0.70
	ceramide (d18:1/20:0, d16:1/22:0, d20:1/18:0)*	1.10	1.10	1.20	1.08	1.17	0.96
	ceramide (d18:2/24:1, d18:1/24:2)*	1.08	1.03	1.17	1.06	1.24	0.97
	N-(2-hydroxypalmitoyl)-sphingosine (d18:1/16:0(2OH))	0.53	0.49	0.71	0.69	0.85	0.49
	N-erucoyl-sphingosine (d18:1/22:1)*	1.06	1.03	1.09	0.86	1.15	0.78
	N-palmitoyl-sphingadienine (d18:2/16:0)*	0.43	0.36	0.44	0.59	0.61	0.50
	N-behenoyl-sphingadienine (d18:2/22:0)*	0.92	0.94	1.22	0.96	0.92	1.03
	N-palmitoyl-heptadecasphingosine (d17:1/16:0)*	0.07	0.07	0.07	0.09	0.12	0.08
Hexosylceramides	glycosyl-N-palmitoyl-sphingosine (d18:1/16:0)	0.15	0.13	0.15	0.27	0.23	0.22
	glycosyl-N-stearoyl-sphingosine (d18:1/18:0)	0.90	0.75	0.69	1.02	1.09	0.74
	glycosyl-N-arachidoyl-sphingosine (d18:1/20:0)*	1.02	1.03	0.97	0.81	0.93	0.86
	glycosyl-N-erucoyl-sphingosine (d18:1/22:1)*	0.88	0.91	0.85	0.50	0.81	0.65
	glycosyl ceramide (d18:1/23:1, d17:1/24:1)*	0.86	0.82	0.89	0.65	0.82	0.82
	glycosyl-N-nervonoyl-sphingosine (d18:1/24:1)*	0.93	1.00	0.94	0.92	1.14	0.94
	glycosyl ceramide (d18:2/24:1, d18:1/24:2)*	1.12	0.99	1.11	1.03	1.28	1.07
Lactosylceramides	lactosyl-N-palmitoyl-sphingosine (d18:1/16:0)	0.52	0.35	0.43	0.36	0.45	0.52
	lactosyl-N-nervonoyl-sphingosine (d18:1/24:1)*	1.06	1.06	0.98	1.14	1.27	1.10

b

Sub Pathway	Biochemical Name	Fold Change					
		KO CTRL F WT CTRL F	KO FD F WT FD F	KO FS F WT FS F	KO CTRL M WT CTRL M	KO FD M WT FD M	KO FS M WT FS M
Sphingolipid Metabolism	sphinganine	1.22	1.09	0.94	1.30	1.28	0.97
	palmitoyl dihydrosphingomyelin (d18:0/16:0)*	0.92	0.79	0.91	0.96	1.04	0.93
	behenoyl dihydrosphingomyelin (d18:0/22:0)*	1.12	1.48	1.58	1.41	1.43	1.19
	palmitoyl sphingomyelin (d18:1/16:0)	0.56	0.46	0.53	0.70	0.71	0.64
	stearoyl sphingomyelin (d18:1/18:0)	1.17	1.04	1.28	1.01	1.14	1.05
	behenoyl sphingomyelin (d18:1/22:0)*	1.16	1.20	1.59	1.15	1.32	1.33
	tricosanoyl sphingomyelin (d18:1/23:0)*	1.25	1.46	1.65	1.09	1.34	1.33
	lignoceroyl sphingomyelin (d18:1/24:0)	1.01	1.33	1.49	1.10	1.46	1.56
	sphingomyelin (d18:1/14:0, d16:1/16:0)*	0.63	0.55	0.48	0.30	0.38	0.35
	sphingomyelin (d17:1/16:0, d18:1/15:0, d16:1/17:0)*	0.08	0.07	0.08	0.10	0.10	0.11
	sphingomyelin (d18:2/16:0, d18:1/16:1)*	0.50	0.43	0.47	0.51	0.53	0.55
	sphingomyelin (d18:1/17:0, d17:1/18:0, d19:1/16:0)	0.86	0.77	0.87	0.93	0.85	0.85
	sphingomyelin (d18:1/18:1, d18:2/18:0)	1.13	1.01	1.17	0.83	1.01	0.95
	sphingomyelin (d18:1/20:0, d16:1/22:0)*	1.28	1.14	1.52	1.09	1.21	1.05
	sphingomyelin (d18:1/20:1, d18:2/20:0)*	1.21	1.19	1.48	0.67	0.96	0.83
	sphingomyelin (d18:1/21:0, d17:1/22:0, d16:1/23:0)*	1.10	1.11	1.64	0.88	0.89	0.96
	sphingomyelin (d18:1/22:1, d18:2/22:0, d16:1/24:1)*	1.16	1.05	1.33	0.86	1.13	0.90
	sphingomyelin (d18:2/23:0, d18:1/23:1, d17:1/24:1)*	1.08	1.05	1.11	0.86	1.04	0.92
	sphingomyelin (d18:1/24:1, d18:2/24:0)*	1.19	1.23	1.44	1.22	1.53	1.16
	sphingomyelin (d18:2/24:1, d18:1/24:2)*	1.34	1.14	1.42	1.04	1.28	1.10
	sphingosine	1.07	1.02	0.95	1.07	1.14	0.86
	phytosphingosine	1.04	1.04	1.00	0.94	1.02	1.00
	sphingomyelin (d18:2/23:1)*	1.08	0.95	1.27	0.68	0.89	0.86
	sphingomyelin (d18:2/24:2)*	0.96	1.43	0.84	1.09	1.03	1.48
	sphingomyelin (d18:1/25:0, d19:0/24:1, d20:1/23:0, d19:1/24:0)*	1.28	1.06	1.39	1.27	1.49	1.63
	sphingomyelin (d18:1/22:2, d18:2/22:1, d16:1/24:2)*	1.25	1.13	1.35	0.59	0.95	0.87
	sphingomyelin (d18:0/20:0, d16:0/22:0)*	1.69	1.44	2.31	1.25	1.73	1.24
	sphingomyelin (d18:0/18:0, d19:0/17:0)*	1.46	1.38	1.62	1.15	1.40	1.17
	sphingomyelin (d18:1/19:0, d19:1/18:0)*	1.29	1.02	1.39	0.91	0.89	0.88
	heptadecasphingosine (d17:1)	0.70	0.67	0.61	0.57	0.61	0.58
	hexadecasphingosine (d16:1)*	0.77	0.82	0.83	0.73	0.83	0.79
	sphingadienine	1.02	0.95	0.89	0.77	0.88	0.79

Figure S3.10 CerS6 KO livers have significantly lower levels of C$_{16}$-acyl chain-based ceramide (a) and sphingomyelin (b) species and significantly higher levels of very-long-chain sphingomyelins in both male and female mice

a

Sub-pathway	Metabolite	Genotype/Sex p-value
Ceramides	N-palmitoyl-sphingosine (d18:1/16:0)	0.00000001
Sphingolipid Metabolism	palmitoyl sphingomyelin (d18:1/16:0)	0.00000015
Chemical	S-(3-hydroxypropyl)mercapturic acid (HPMA)	0.00000365
Sphingolipid Metabolism	sphingomyelin (d18:1/22:2, d18:2/22:1, d16:1/24:2)*	0.00000719
Phosphatidylcholine (PC)	1-palmitoyl-2-gamma-linolenoyl-GPC (16:0/18:3n6)*	0.00001063
Hexosylceramides (HCER)	glycosyl-N-palmitoyl-sphingosine (d18:1/16:0)	0.00001356
Diacylglycerol	diacylglycerol (12:0/18:1, 14:0/16:1, 16:0/14:1) [1]*	0.00001418
Ceramides	N-palmitoyl-sphingadienine (d18:2/16:0)*	0.00001431
Dihydroceramides	N-palmitoyl-sphinganine (d18:0/16:0)	0.00001801
Diacylglycerol	diacylglycerol (14:0/18:1, 16:0/16:1) [2]*	0.00006077
Sphingolipid Metabolism	sphingomyelin (d18:1/14:0, d16:1/16:0)*	0.00006145
Diacylglycerol	diacylglycerol (14:0/18:1, 16:0/16:1) [1]*	0.00006517
Sphingolipid Metabolism	sphingomyelin (d18:1/20:1, d18:2/20:0)*	0.00007675
TCA Cycle	succinylcarnitine (C4-DC)	0.00010000
Diacylglycerol	diacylglycerol (12:0/18:1, 14:0/16:1, 16:0/14:1) [2]*	0.00010000
Diacylglycerol	palmitoyl-myristoyl-glycerol (16:0/14:0) [2]	0.00010000
Diacylglycerol	palmitoyl-oleoyl-glycerol (16:0/18:1) [2]*	0.00010000
Sphingolipid Metabolism	sphingomyelin (d18:1/21:0, d17:1/22:0, d16:1/23:0)*	0.00010000
Diacylglycerol	palmitoyl-myristoyl-glycerol (16:0/14:0) [1]*	0.00020000
Diacylglycerol	palmitoyl-oleoyl-glycerol (16:0/18:1) [1]*	0.00020000
Diacylglycerol	oleoyl-oleoyl-glycerol (18:1/18:1) [2]*	0.00030000
Phosphatidylethanolamine (PE)	1,2-dilinoleoyl-GPE (18:2/18:2)*	0.00040000
Diacylglycerol	palmitoleoyl-oleoyl-glycerol (16:1/18:1) [2]*	0.00040000
Long Chain Fatty Acid	oleate/vaccenate (18:1)	0.00050000
Purine Metabolism, Guanine containing	guanosine	0.00050000
Pentose Metabolism	ribulose/xylulose	0.00060000
Phosphatidylethanolamine (PE)	1-linoleoyl-2-arachidonoyl-GPE (18:2/20:4)*	0.00060000
Sphingolipid Metabolism	sphingomyelin (d18:1/19:0, d19:1/18:0)*	0.00070000
Pyrimidine Metabolism, Thymine containing	3-aminoisobutyrate	0.00100000
Glutathione Metabolism	ophthalmate	0.00120000
Long Chain Fatty Acid	palmitoleate (16:1n7)	0.00130000
Guanidino and Acetamido Metabolism	guanidinosuccinate	0.00140000
Phosphatidylcholine (PC)	1-myristoyl-2-palmitoyl-GPC (14:0/16:0)	0.00150000
Chemical	O-sulfo-L-tyrosine	0.00160000
Glycolysis, Gluconeogenesis, and Pyruvate Metabolism	pyruvate	0.00170000
Fructose, Mannose and Galactose Metabolism	galactonate	0.00180000
Fatty Acid, Monohydroxy	16-hydroxypalmitate	0.00180000
Plasmalogen	1-(1-enyl-palmitoyl)-2-oleoyl-GPE (P-16:0/18:1)*	0.00190000
Sterol	4-cholesten-3-one	0.00230000
Diacylglycerol	diacylglycerol (16:1/18:2 [2], 16:0/18:3 [1])*	0.00240000
Phosphatidylcholine (PC)	1-palmitoyl-2-dihomo-linolenoyl-GPC (16:0/20:3n3 or 6)*	0.00260000
Long Chain Fatty Acid	myristate (14:0)	0.00330000
Diacylglycerol	linoleoyl-docosahexaenoyl-glycerol (18:2/22:6) [2]*	0.00340000
Ceramides	ceramide (d18:1/14:0, d16:1/16:0)*	0.00340000
Diacylglycerol	oleoyl-oleoyl-glycerol (18:1/18:1) [1]*	0.00350000
Long Chain Fatty Acid	eicosenoate (20:1)	0.00380000

b

Sub-pathway	Biochemical	Sex/Diet p-value
Fatty Acid, Monohydroxy	3-hydroxylaurate	0.0001
Chemical	S-(3-hydroxypropyl)mercapturic acid (HPMA)	0.0002
Polyunsaturated Fatty Acid (n3 and n6)	docosahexaenoate (DHA; 22:6n3)	0.0003
Glycolysis, Gluconeogenesis, and Pyruvate Metabolism	dihydroxyacetone phosphate (DHAP)	0.0005
Phosphatidylethanolamine (PE)	1-stearoyl-2-oleoyl-GPE (18:0/18:1)	0.0006
Methionine, Cysteine, SAM and Taurine Metabolism	N-acetyltaurine	0.0008
Polyunsaturated Fatty Acid (n3 and n6)	linoleate (18:2n6)	0.0008
Polyunsaturated Fatty Acid (n3 and n6)	linolenate [alpha or gamma; (18:3n3 or 6)]	0.0009
Fatty Acid, Monohydroxy	16-hydroxypalmitate	0.0009
Sphingolipid Metabolism	sphingomyelin (d18:1/18:1, d18:2/18:0)	0.0012
Polyunsaturated Fatty Acid (n3 and n6)	docosapentaenoate (n3 DPA; 22:5n3)	0.0013
Polyunsaturated Fatty Acid (n3 and n6)	arachidonate (20:4n6)	0.0014
Lysophospholipid	1-oleoyl-GPE (18:1)	0.0014
Polyunsaturated Fatty Acid (n3 and n6)	heneicosapentaenoate (21:5n3)	0.0016
Glycogen Metabolism	maltopentaose	0.0018
Pyrimidine Metabolism, Thymine containing	thymine	0.0018
Pantothenate and CoA Metabolism	3'-dephosphocoenzyme A	0.0023
Phosphatidylethanolamine (PE)	1-linoleoyl-2-arachidonoyl-GPE (18:2/20:4)*	0.0026
Glutamate Metabolism	glutamate, gamma-methyl ester	0.0029
Long Chain Fatty Acid	palmitate (16:0)	0.0029
Phosphatidylcholine (PC)	1,2-dilinoleoyl-GPC (18:2/18:2)	0.0031
Methionine, Cysteine, SAM and Taurine Metabolism	N-formylmethionine	0.0033
Lysophospholipid	1-arachidonoyl-GPI (20:4)*	0.0033
Lysine Metabolism	N-trimethyl 5-aminovalerate	0.0034
Phosphatidylcholine (PC)	1-linoleoyl-2-arachidonoyl-GPC (18:2/20:4n6)*	0.0035
Ceramides	N-(2-hydroxypalmitoyl)-sphingosine (d18:1/16:0(2OH))	0.0035
Endocannabinoid	N-oleoyltaurine	0.0036
Lysophospholipid	1-palmitoyl-GPE (16:0)	0.0036
Fatty Acid Metabolism (also BCAA Metabolism)	methylmalonate (MMA)	0.0039
Pantothenate and CoA Metabolism	pantetheine	0.0039
Secondary Bile Acid Metabolism	taurolithocholate	0.0044
Long Chain Fatty Acid	stearate (18:0)	0.0045
Glycogen Metabolism	maltohexaose	0.0054
Folate Metabolism	7,8-dihydrofolate	0.0054
Lysophospholipid	1-arachidonoyl-GPE (20:4n6)*	0.0057
Long Chain Fatty Acid	oleate/vaccenate (18:1)	0.0058
Pentose Metabolism	ribulose/xylulose	0.0061
Glycogen Metabolism	maltotetraose	0.0066
Phosphatidylethanolamine (PE)	1-oleoyl-2-linoleoyl-GPE (18:1/18:2)*	0.0066
Glycolysis, Gluconeogenesis, and Pyruvate Metabolism	glucose	0.0067
Glutathione Metabolism	cysteinylglycine	0.0070
Polyunsaturated Fatty Acid (n3 and n6)	dihomo-linolenate (20:3n3 or n6)	0.0071
Fructose, Mannose and Galactose Metabolism	mannitol/sorbitol	0.0073
Fatty Acid, Monohydroxy	3-hydroxylaurate	0.0079
Phosphatidylserine (PS)	1-stearoyl-2-oleoyl-GPS (18:0/18:1)	0.0101
Vitamin B6 Metabolism	pyridoxamine	0.0101

Figure S3.11 Metabolites exhibiting the most significant genotype: sex interactions (a) and sex: diet interactions (b). Metabolites are listed with sub-pathway to which they belong

CHAPTER 4: CERAMIDE SYNTHASE 6 CONTROLS MOUSE RESPONSE TO HIGH-FAT DIET: METABOLOMICS STUDY

Introduction

Ceramides are bioactive lipids that play important roles in cell signaling and regulation of cellular processes [80, 82, 116, 273, 281-283]. Additionally, their role in the initiation and progression of several diseases including Alzheimer's disease, type 2 diabetes, and obesity have been recognized [83, 109, 136, 169, 177, 284]. Ceramides are formed from a sphingoid base and Acyl-CoA by CerS, of which there are 6 isoforms having unique specificities with regard to the acyl group chain length that is attached to the sphingoid base. CerS5 and CerS6 produce C_{14}- and C_{16}-Cer and exhibit distinct tissue distribution in both mice and humans [77, 99, 122]. C_{16}-Cer has gained attention from researchers as an important cellular lipid due to its roles in cellular processes including apoptosis and response to cellular stressors. Recent evidence suggests that it plays a role in inflammatory pathways as well (reviewed in [79]). Ceramides represent a hub of sphingolipid metabolism: they can be converted to sphingomyelins and hexosyl-ceramides by the attachment of a phosphocholine or sugar headgroup, respectively, as well as generated from complex sphingolipids by the action of SMase and glycohydrolases. Because of their diverse functions in cellular signaling, production of ceramides and their derivatives are highly regulated [80, 82, 99, 129].

Alterations in ceramide metabolism are thought to be closely connected to the development of type 2 diabetes and obesity. Several studies have suggested that sphingolipids act as metabolites promoting obesity, IR and inflammation [173] and changes in the lipid profiles of

mice fed a HFD have been documented [136, 169, 172-174]. Additionally, ceramide and its

metabolites are now considered to be important in the development of IR, as well as in obesity-

induced alterations to cellular metabolism, thus contributing to onset of metabolic disease [175].

Specifically, human studies have found that CerS6 expression positively correlated with BMI,

body fat content and hyperglycemia [169]. Moreover, ceramide levels are often found to be

elevated in skeletal muscle and plasma, among other tissues, in obese humans [109, 170, 171].

There are few animal studies examining the relationship between ceramide metabolism

and the development of obesity and diabetes. When CerS5 KO mice were fed a HFD, there were

changes in energy homeostasis and insulin sensitivity [173]. The KO mice showed a reduction of

C_{16}-Cer and of sphingolipids derived from it, without alterations in other ceramide species.

CerS6 which also generates C_{16}-Cer was unable to compensate for the loss of CerS5. In a

different approach involving the whole-body and tissue-specific CerS6 knockout models,

investigators found reduced C_{16}-Cer levels in white and brown adipose tissues and liver in KO

compared to WT mice after animals were challenged with a high fat diet [169]. CerS6 KO mice

were also protected from DIO which the authors suggested could be due to increased energy

expenditure and lipid utilization in BAT and liver of the KO mice. However, this hypothesis was

not investigated in detail.

Our previous studies in cultured cells have demonstrated that CerS6 mediates cellular

response to metabolic stress [12, 285, 286] and we hypothesized that this enzyme will also

mediate metabolic stress response in the whole animal. We further proposed that animals

deficient in CerS6 will have different response to metabolic stress induced by HFD and will be

protected from weight gain. We expected to see significant reductions of CerS6-produced

sphingolipids in the plasma of mice fed either a control or HFD and this is <u>expected</u> to confer a protective effect in terms of weight gain and body composition.

Materials and Methods

Animals and husbandry

All animal experiments were approved by the Institutional Animal Care and Use Committee (IACUC) at the North Carolina Research Campus (NCRC). CerS6 KO mice were generated in Dr. Ogretmen's lab and were backcrossed for at least 11 generations to C57BL/6NHsd mice from Envigo (Indianapolis, IN). Absence of CerS6 protein was confirmed through western blot protein analysis (Fig S4.1). Male CerS6$^{+/-}$ mice were bred to obtain CerS6 KO and CerS6 WT littermates that were randomized to dietary groups at weaning. Mice were group housed in microisolator cages under standard conditions (12h light: dark, temperature- and humidity-controlled conditions), and received *ad lib* access to water and one of two purified synthetic diets purchased from Envigo. The protein sources (casein and L-cystine) were consistent across diets, as were sources of carbohydrate (corn starch, sucrose, maltodextrin) and fat (soybean oil). The additional fat in the high fat (HF) diet came from lard (See Table S4.1 for diet composition). Mice were placed on respective diets at weaning and maintained on the diets for 16 weeks, with body weight recorded weekly. After 14 weeks on the diet, mice underwent metabolic phenotyping which included MRI, followed by 48 hours in calorimetry cages. Data were normalized to lean body mass. At 16 weeks on the diet, all mice were fasted for 4 hours and body composition was assessed prior to euthanasia.

Calorimetry cages measurements

Energy expenditure, heat production, locomotor activity, food and water intake were assessed by the NORC Animal Metabolism Phenotyping Core using indirectly calorimetry cages (TSE systems). The respiratory exchange ratio (RER) was calculated as the ratio of CO_2

production to O_2 consumption (VCO_2/VO_2). The light cycle began at 7:00am and ended at 7:00pm in the climate-controlled facility.

Body composition

Body composition (lean and fat mass) was assessed before mice were placed on diet and before necropsy using the EchoMRI-130 Body Composition Analyzer.

Western Blot analysis

Fragments of snap-frozen liver tissue (~30mg) was homogenized using Dounce homogenizer in 750µl RIPA buffer containing protease and phosphatase inhibitor cocktail, incubated on ice for 30 minutes, sonicated and centrifuged at (20,000 x g, 5 min, 4°C). The supernatant was stored at -80°C. 5X dissociation buffer was added to tissue lysates (1:4 v/v) and incubated at room temperature for 30 minutes to allow proteins to dissociate and denature. Aliquots of 20 µg of total protein were subjected to SDS-PAGE followed by immunoblot with corresponding antibodies. All antibodies were diluted in 5% BSA blocking buffer. Membranes were washed 4 times with 2% TWEEN-20 in TBS. Blots were developed with PicoWest Super Signal Chemiluminescent substrate and analyzed on the Odyssey Fc infrared scanner from LI-COR.

HPLC-MS/MS analysis of sphingolipids

75µL aliquots of plasma was immediately frozen and stored at -80° C until analysis. Sphingolipid levels were measured by HPLC-MS/MS the MUSC Lipidomics Shared Resource facility as previously described [252].

Gene expression

mRNA from snap frozen liver samples was isolated using the Maxwell LEV simplyRNA tissue kit from Promega (AS1280). cDNA synthesis was performed using Applied Biosystems High Capacity Reverse transcriptase kit with random primers mix from 1 µg of total RNA for a

total reaction size of 20uL. Samples were placed in thermocycler with heated lid (95°C) and

incubated at 25°C for 10 minutes, 37°C for 120 minutes, 85°C for 5 minutes and held at 4°C.

cDNA was diluted with nuclease free water (1:5) and a pooled standard was created. 3 samples

were selected from each group based on highest quality RNA (concentration >100ng/µl,

260:280~2, and 260:230~2). Expression levels of sphingolipid biosynthesis genes and β-actin

were evaluated using SYBR Green Dye (SsoAdvanced Universal SYBR Green Super Mix, Bio-

Rad) in an 8 µL reaction with 10uM enzyme-specific primers (Table S4.2) on the Roche

LightCycler 480 II. All samples were run in triplicate and normalized to β-actin before being

analyzed using the $\Delta\Delta C_T$ method.

Plasma cytokines

Plasma cytokines (IFNγ, IL-1β, IL-6, IL-10, IL-17A, and TNFα) were measured using

the Bio-Plex Pro Mouse Cytokine TH17 Panel A 6-Plex (M60000007NY). Plasma was diluted

and run in duplicate as outlined in manufacturer's protocol. MagPix Luminex was used to

measure and Bio-Plex MP software was used to assess quality. A pooled plasma sample was run

on all plates as an internal control.

Histology

Freshly isolated liver, kidney, lung, heart, white adipose tissue, brown adipose tissue,

testes/ovaries, and brain were fixed in 10% buffered formalin were embedded in paraffin blocks

and 5 µm sections from the blocks were placed on slides, deparaffinized, re-hydrated and stained

with hematoxylin and eosin according to standard protocol. Images were acquired using Keyence

BZ-X710 All-in-one fluorescence microscope at 2X, 10X, and 20X magnification.

Metabolomic analysis

Untargeted metabolomic analysis was performed by the commercial service provider

Metabolon[®] (Durham, NC). Approximately 100mg of snap-frozen liver and 100µL of plasma

were subjected to extraction with methanol and divided into aliquots for further analysis by ultrahigh performance liquid chromatography/mass spectrometry (UHPLC/MS). The global biochemical profiling consisted of four unique arms covering identification of both hydrophilic and hydrophobic compounds under both positive and negative ionization conditions [253]. Metabolites were identified by automated comparison of the ion features in the samples to a reference library of chemical standards characteristics which included retention time, m/z (mass/charge) ratio, predominant adducts and in-source fragmentation and associated spectra.

Statistical analysis

For statistical analysis of differences between two groups Student's t-test was performed using GraphPad software. For the statistical analysis of differences between three or more groups, one-way ANOVA was used with Sidak's multiple comparisons test to determine differences between specific groups. Results were determined to be statistically significantly different at $p<0.05$. Metabolomic data were analyzed using Qlucore Omics Explorer v.3.4 software (Qlucore, Lund, Sweden). Calorimetry data over 24 hours were analyzed using multiple t-tests, one per row, representing differences between 2 groups for each 30-minute increment.

Results

CerS6 KO mice gained less weight and fat mass and were protected from lipid droplet accumulation in liver.

In order to assess metabolic and phenotypic changes due to the lack of CerS6 in mice fed a high fat diet, WT and CerS6 KO mice were randomized to either the control or high fat diet upon weaning and maintained on their respective diets for 16 weeks. Body weight was assessed weekly and body composition was measured before the mice were placed on diet and at the end of dietary intervention. CerS6 KO mice on both the control (Ctrl) and HF diets gained less weight over the duration of the intervention, with a clear separation between WT and CerS6 KO

mice appearing sooner (after three weeks) on the high fat diet than on the control diet (after nine

weeks) (Fig 4.1A).
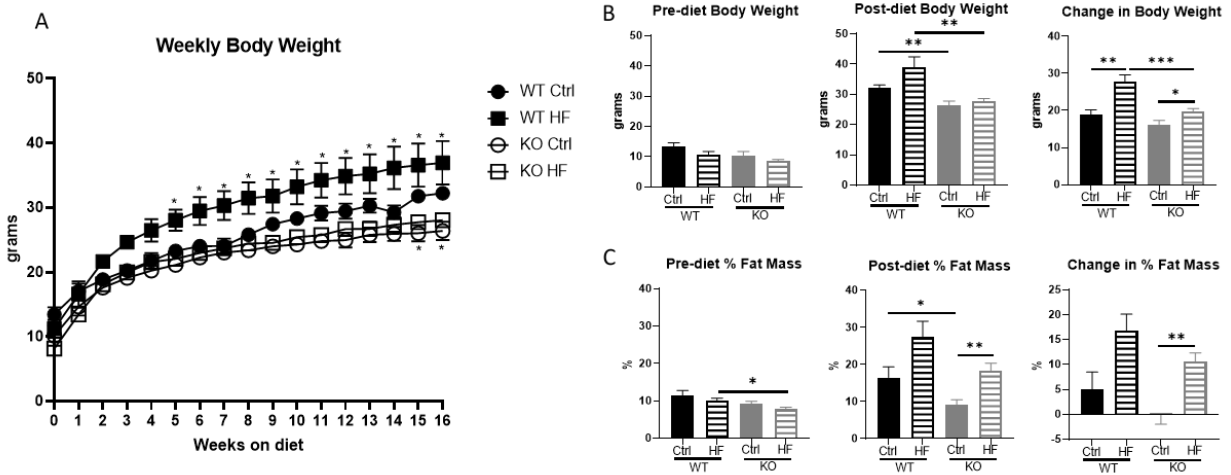
**Figure 4.1 CerS6 KO mice were protected from diet-induced weight gain and fat
accumulation.** Data are shown as mean $\pm$ SEM, n=6-8. Solid bars, control diet; striped bars, high-fat
diet. WT shown in black and KO shown in grey. *, $p<0.05$; **, $p<0.01$; ***, $p<0.001$; ****, $p<0.0001$
determined by Student's t-test between genotypes and diets. Differences in weekly body weight are
denoted with * between WT and KO for each diet

Additionally, WT mice on the HFD gained significantly more weight than the CerS6 KO

mice on HFD (Fig 4.1B). CerS6 KO mice on the HFD also gained more weight than the KO

mice on the control diet, indicating protection from diet-induced weight gain but not complete

prevention. The protection from diet-induced weight gain also manifested in body composition

(Fig 4.1C). CerS6 KO mice on the Ctrl diet had significantly lower percent fat mass at the end of

the dietary intervention compared to WT on Ctrl diet and compared to CerS6 KO mice on a HF

diet (Fig. 4.1C). CerS6 KO mice also demonstrated significantly higher percentage of lean mass

before being placed on the HFD as compared to WT mice (Fig S4.2), however this difference did

not persist. After dietary intervention, the KO-Ctrl group had significantly higher percentage of

lean body mass as compared to WT controls and the KO-HFD group (Fig S4.2) indicating that

growth was not restricted. Additionally, we found that the HFD caused significant accumulation

of lipid droplets in the livers of WT mice, but the CerS6 KO mice demonstrated no such effect (Fig 4.2).
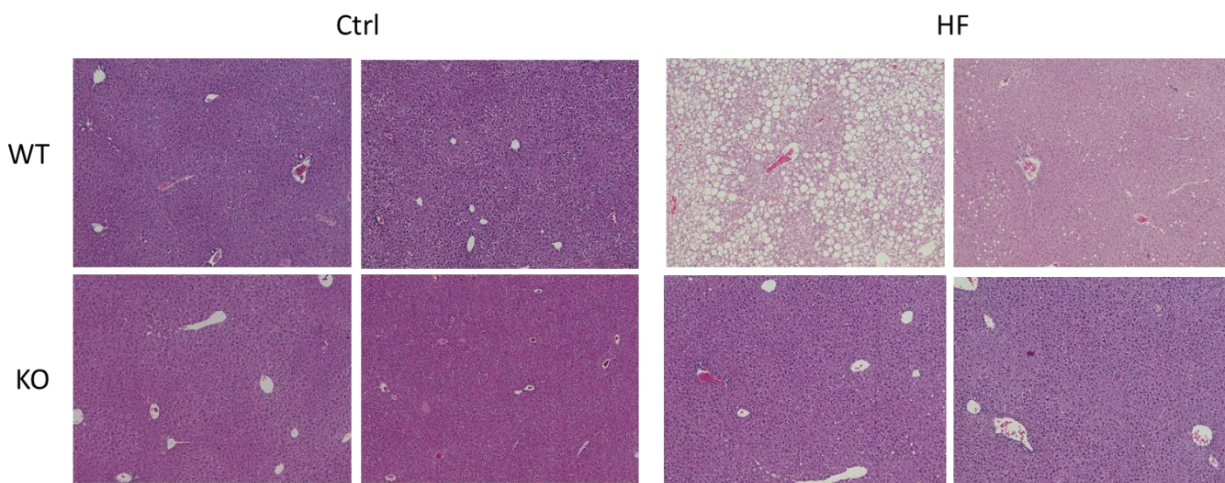
Figure 4.2 CerS6 KO prevented accumulation of hepatic lipid droplets

CerS6 KO mice were protected from lipid droplet accumulation in the liver, both on the Ctrl and on HF diet.

CerS6 KO mice compared to WT show difference in nutrients utilization as energy source on control diet and consume less food when on the high fat diet.

After 14 weeks on respective diets, food and water intake, physical activity and RER were evaluated using calorimetry cages which could provide relevant data to explain the differences in body weight gain between WT and CerS6 KO mice. Over the 24-hour period, the groups did not show significant differences in the distance travelled in the X- and Y- planes (Fig 4.3A), nor of the activity in the Z-plane (jumping) (Fig 4.3B), pointing to similar physical activity between the groups.

Further, we did not observe differences in food intake by WT mice on either diet, or by WT and CerS6 KO mice on the Ctrl diet (Fig 4.3C). However, CerS6 KO mice consumed a significantly lower amount of food per day on HFD. This resulted in higher caloric intake by WT mice on HFD than either WT or KO mice on Ctrl diets, and in the lowest caloric intake by CerS6

KO mice on HFD, than any of the other groups (Fig 4.3D). Mice on the HFD oxidized fat for energy production (RER ~0.7) regardless of genotype. However, on control diet, KO mice showed a preference for oxidizing glucose (RER ~1.0) while the WT mice utilized a combination of glucose, fat and protein (RER ~0.8-0.9) for energy production (Fig 4.3E).

Dietary fat levels did not affect plasma cytokines in WT or CerS6 KO mice.

Ceramides have been linked to cytokine signaling both as a signal to increase cytokine production [11, 287] and as a response to increases in cytokine levels [288]. So, we assessed plasma cytokines (IFNγ, IL-1β, IL-6, IL-10, IL-17A, and TNFα) and found that high fat diet increased levels of IL-6 and IL-17A in WT mice, but those changes did not reach statistical significance. In CerS6 KO mice, HFD had the opposite effect on IL-6 and IL-17A with a trend to decrease when on high fat diet (Fig S4.3). Overall, there was a trend for decreased plasma cytokine levels in CerS6 KO mice regardless of diet.

* denotes significant difference
KO Ctrl v KO HF
# denotes significant difference
WT Ctrl v KO Ctrl
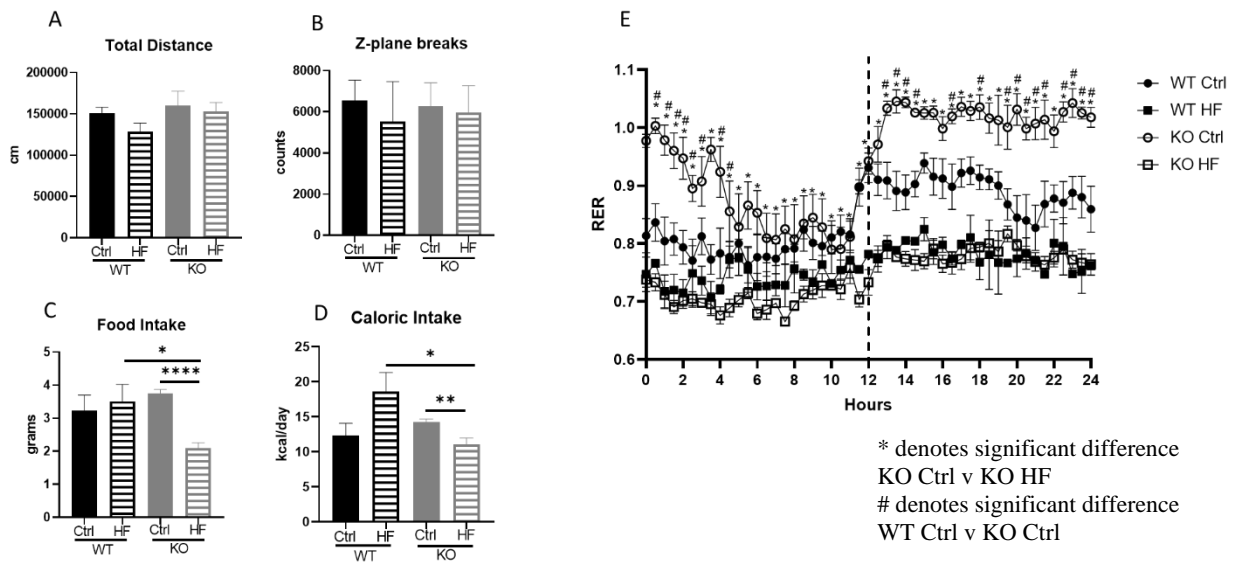
Figure 4.3 CerS6 KO mice differed from WT mice in food consumption and preferred substrate for energy production. Data are shown as mean $\pm$ SEM, n=6-8. Solid bars, control diet; striped bars, high-fat diet. WT shown in black and KO shown in grey. *, $p<0.05$; **, $p<0.01$; ***, $p<0.001$; ****, $p<0.0001$ determined by Student's t-test between genotypes and diets. RER (Panel E) analyzed with multiple t-tests over 24 hour period

Plasma sphingolipids respond to both dietary fat and to CerS6 status

To evaluate the systemic effects of CerS6 and HF diet, we measured plasma levels of ceramides and derived sphingolipids, SM and HexCer. CerS6 KO mice showed significantly lower C_{14}- and C_{16}-Cer and SM in plasma than WT mice (Fig 4.4). Both C_{14}- and C_{16}-Cer, along with C_{14}- and C_{16}-SM were significantly elevated on HFD in both WT mice and CerS6 KO mice, compared to control diet groups. However, in the KO mice, C_{14}- and C_{16}- Cer and SM levels on HFD were still similar to or below the WT control diet levels (Fig 4.4). The total plasma Cer and SM levels were significantly lower in the KO mice, but responded to HFD in both genotypes with KO mice exhibited levels on the HFD comparable to WT mice consuming the Ctrl diet.
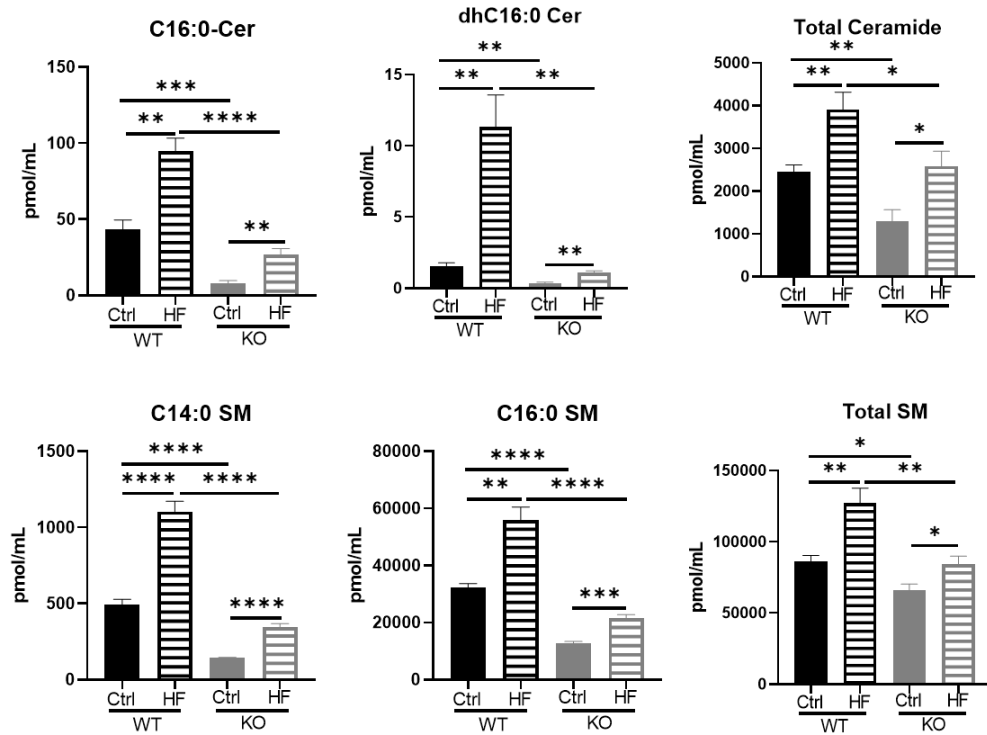
Figure 4.4 CerS6 KO significantly lowers plasma levels of C_{14} and C_{16} sphingolipids but cannot overcome effect of HFD. Data are shown as mean $\pm$ SEM, n=5. Solid bars, control diet; striped bars, high-fat diet. WT shown in black and KO shown in grey. *, p<0.05; **, p<0.01; ***, p<0.001; ****, p<0.0001 determined by Student's t-test between genotypes and diets

Other plasma sphingolipids, which are not generated by CerS6, were also affected by CerS6 knockout. Specifically, on the control diet, C_{18}-, C_{20}-, C_{22}- and $C_{22:1}$-Cer were significantly lower in plasma of CerS6 KO mice than WT mice, while C_{24}- and C_{26}-Cer showed similar trend but did not reach significance (Fig 4.5).
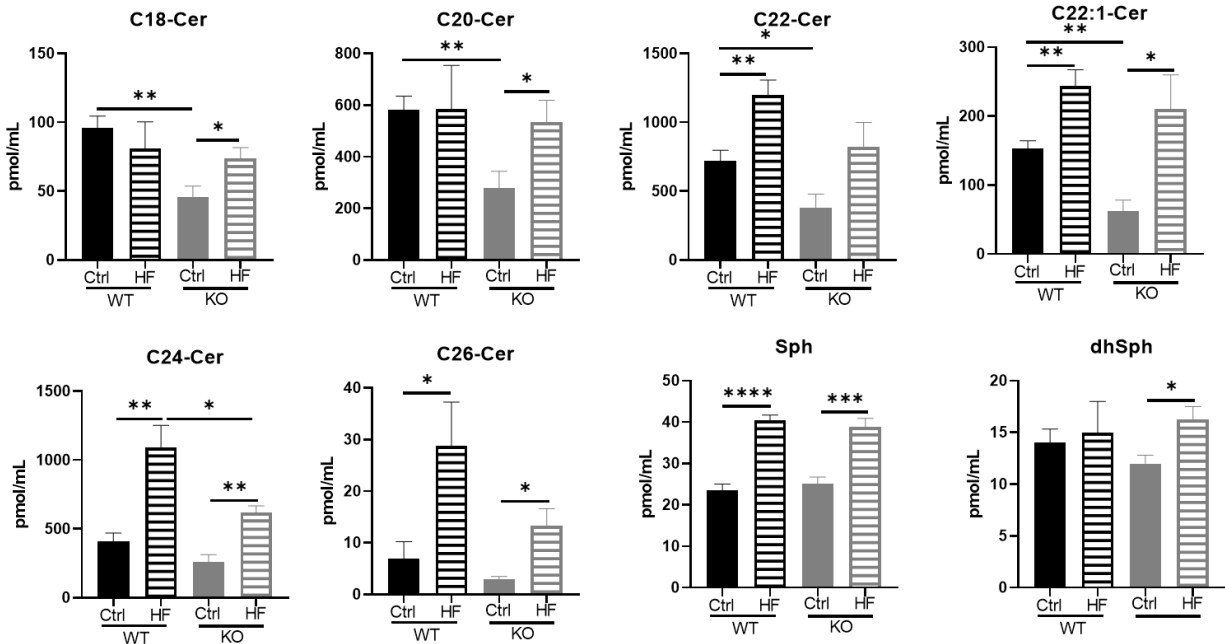
Figure 4.5 CerS6 KO mice demonstrate lower levels of several ceramide species in plasma on control diet. Data are shown as mean $\pm$ SEM, n=5. Solid bars, control diet; striped bars, high-fat diet. WT shown in black and KO shown in grey. *, $p<0.05$; **, $p<0.01$; ***, $p<0.001$; ****, $p<0.0001$ determined by Student's t-test between genotypes and diets

Interestingly, HFD elevated all of the plasma ceramides listed above in CerS6 KO animals, while plasma C_{18}- and C_{20}-Cer were not elevated in the WT mice on HFD. Plasma Sph did not differ due to genotype but was significantly increased by the HFD, whereas dihydro-Sph was significantly elevated due to HFD consumption in CerS6 KO mice only (Fig 4.5). While non-CerS6-produced ceramide species tended to be lower in CerS6 KO compared to WT plasma on control and in some cases on HFD, the corresponding SM species were not different between

genotypes on control diet, and elevated similarly in plasma of WT and CerS6 KO mice when fed

a HFD (Fig 4.6).
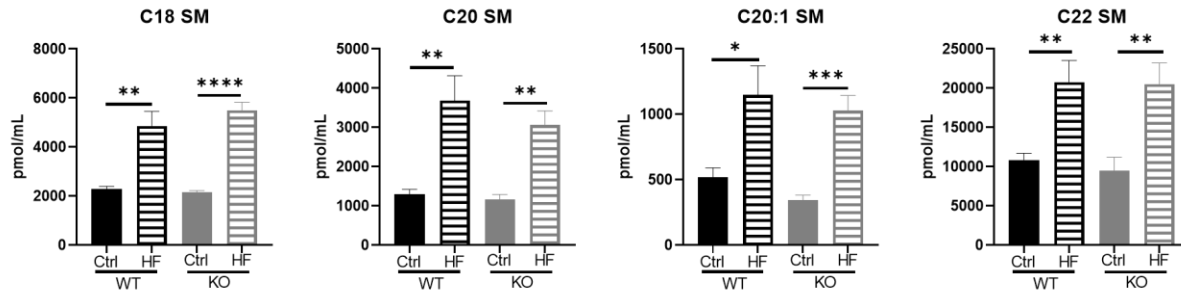
Figure 4.6 CerS6 KO does not protect from HFD-induced increase in plasma SM species.
Data are shown as mean $\pm$ SEM, n=5. Solid bars, control diet; striped bars, high-fat diet. WT shown in black and KO shown in grey. *, $p<0.05$; **, $p<0.01$; ***, $p<0.001$; ****, $p<0.0001$ determined by Student's t-test between genotypes and diets

Contrary to SM, plasma HexCer were significantly lower in CerS6 KO mice than in WT

mice on HFD, across all of the species measured, resulting in significantly lower Total HexCer

pool (Fig 4.7).
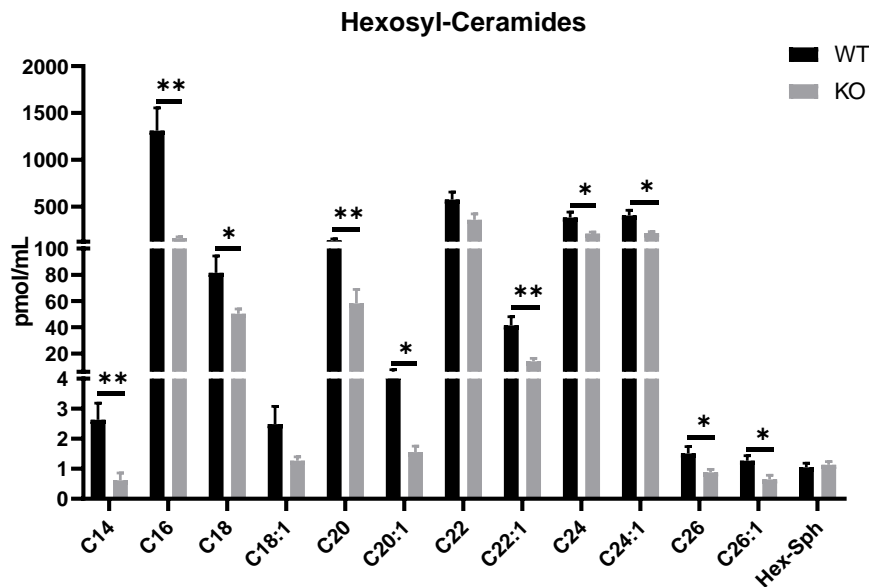
Figure 4.7 CerS6 KO decreased plasma hexosyl-ceramide levels on HF diet. Data are shown as mean $\pm$ SEM, n=5. Solid bars, control diet; striped bars, high-fat diet. WT shown in black and KO shown in grey. *, $p<0.05$; **, $p<0.01$; ***, $p<0.001$; ****, $p<0.0001$ determined by Student's t-test between genotypes and diets

CerS6 KO significantly increased mRNA levels of sphingolipid genes in the liver but HFD had no effect on gene expression

In plasma, complex lipids are transported and distributed by lipoproteins [289] and lipoproteins originate in the intestine and liver [290] So, we evaluated hepatic expression of genes involved in sphingolipid metabolism. CerS6 KO mice demonstrated significant elevation (2-6-fold) of several sphingolipid genes, including *Sptlc1*, the first and rate-limiting enzyme in *de novo* sphingolipid biosynthesis pathway, *Sgms1* and *2,* involved in sphingomyelin synthesis, *Smpd1,* acid sphingomyelinase, *Ugcg,* ceramide glucosyltransferase and *Asah2*, neutral ceramidase (Fig 4.8). However, no effect of HFD on these genes was seen in either genotype. Similarly, no significant effects of HFD on the expression of five CerS isoforms was found (Fig S4.4a), with the exception of lower CerS2 mRNA levels on HFD in WT mice. Interestingly, even in the absence of changes in mRNA levels, HFD resulted in a noticeable increase of CerS6 protein expression in WT mice (Fig S4.4B), in line with elevated C_{16}-sphingolipid species.
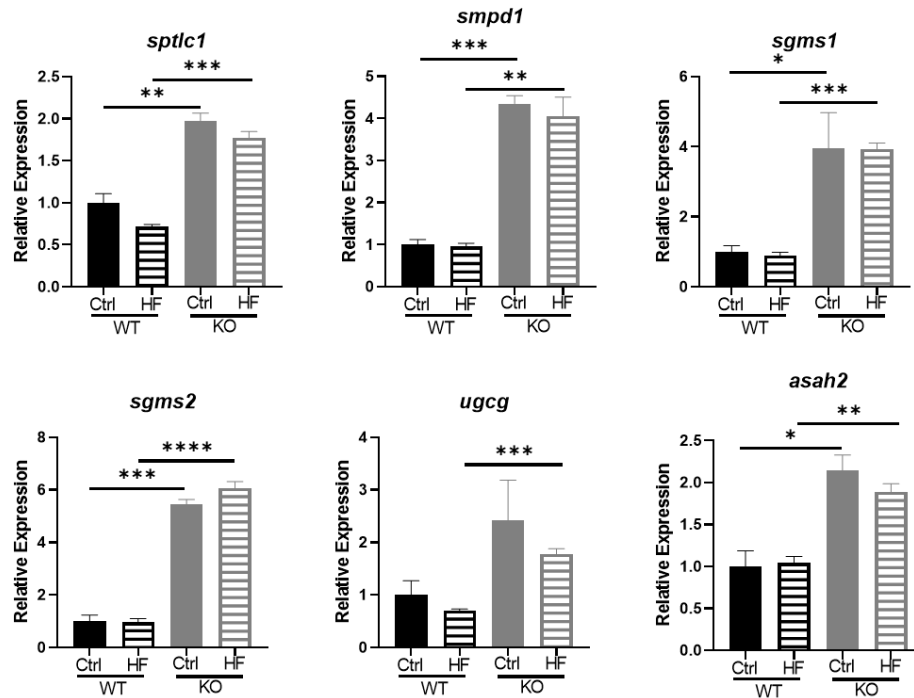
Figure 4.8 Knocking out CerS6 increased hepatic gene expression of several other genes involved in sphingolipid biosynthesis. Data are shown as mean $\pm$ SEM, n=3. Solid bars, control diet; striped bars, high-fat diet. WT shown in black and KO shown in grey. *, $p<0.05$; **, $p<0.01$; ***, $p<0.001$; ****, $p<0.0001$ determined by Student's t-test between genotypes and diets

Both liver and plasma metabolomes respond to diet and CerS6 knockout

To better understand the metabolic effects of HFD and the role of CerS6 in mediating these effects we performed untargeted metabolomic analysis of liver and plasma as liver is the central player in nutrients metabolism and plasma connects metabolites systemically. Statistical comparisons of the measured metabolites using principal components analysis showed clear separation of both liver (Fig 4.9A) and plasma (Fig 4.9B) metabotypes by genotype and by diet.
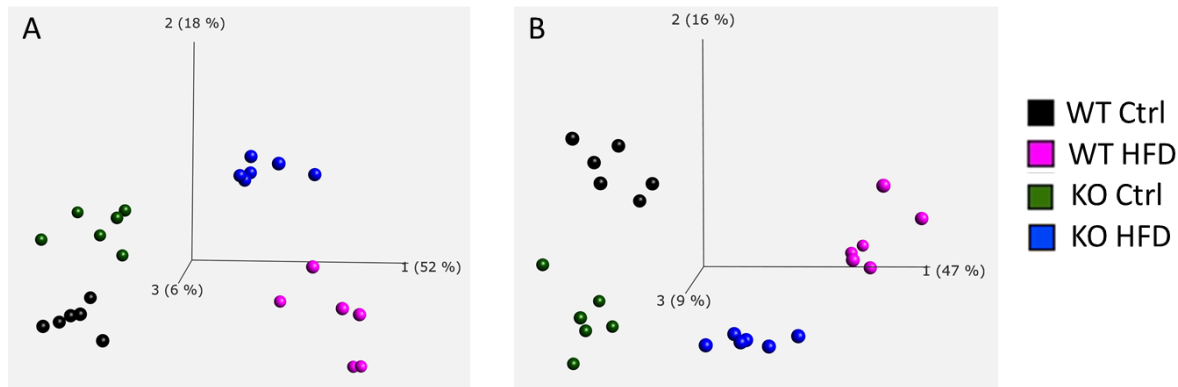
Figure 4.9 Principal components analysis of liver (A) and plasma (B) metabolites demonstrates distinct separation between both genotype and diet.

Additionally, changes of metabolites in plasma in response to genotype were not directly reflected by changes in liver. Almost twice as many significantly changed metabolites were found in CerS6 KO versus WT mice on HFD, as compared to control diet. In plasma, the number of changes in the KO mice on the HFD were only 20% higher than on control diet (Table S4.3). At the same time numbers of changed metabolites in response to HFD were 40% and 45% higher for CerS6 KO mice compared to WT in liver and plasma, correspondingly (Table S4.4). Heat Map analysis of metabolites showing differences of more than 50% with statistical significance p<0.05 confirms separation of the groups both by diet and genotype, as well as different separation patterns between liver and plasma (Fig S4.5a).

All C_{16}- acyl-chain-containing sphingolipids are lower in CerS6 KO mice, but only plasma C_{16}-ceramide was reduced 20-fold.

Untargeted metabolomic analysis demonstrated significantly lower levels of sphingolipids with C_{16} acyl chain in KO versus WT mice across all classes: Cer, HexCer, and SM, both in liver and plasma (Fig S4.5b). The differences between genotypes were similar in liver and plasma, except for N-palmitoyl-sphingosine (d18:1/16), which was reduced in KO mice by ~95% in plasma on both diets, and only by 30 and 70 % in liver on control and HF diets respectively. Sphingomyelin (d18:1/17:0, d17:1/18:0, d19:1/16:0), was reduced by 52 and 38%

(control and HF diets, respectively) in plasma, but showed no difference between KO and WT mice in liver on any diet (Fig S4.5b). Interestingly, multiple Cer species with C_{18}, C_{22}, C_{24}, and $C_{24:1}$ acyl-chains were elevated both on Ctrl and on HF diets in the liver of KO mice, but plasma levels of these species were either not changed or even reduced on both diets in KO mice. However, liver levels of Sph were slightly increased (30%) in KO versus WT mice on Ctrl diet, with no differences on HF diet, while plasma Sph level was elevated 2.2 times on Ctrl diet with no differences on HF diet (Fig S4.6)

CerS6 KO showed differential response of phospholipids and glycerolipids in liver and plasma on both diets

In addition to changes in sphingolipids, knocking out CerS6 also affected many other lipid pathways. Multiple free fatty acids as well as acyl-carnitines and acyl-cholines were elevated in KO versus WT livers on Ctrl diet, with a few of them showing higher levels in KO mice on the HF diet (Fig S4.7A). In plasma, fewer free fatty acids as well as acyl-carnitines and acyl-cholines were elevated and many were lower in KO than in WT mice (Fig S4.7B) while HF diet resulted in most of them becoming significantly lower in KO versus WT, with only dicarboxylic fatty acids and docosapentaenoate remaining significantly higher in KO mice.

Levels of phospholipids did not differ significantly in livers of KO and WT mice on the control diet but were elevated in KO versus WT mice on HFD (Fig S4.8a). Plasma phospholipids demonstrated a different effect, however. Lower levels of phosphatidylcholine in KO compared to WT animals on control diet was almost completely abrogated on the HF diet (Fig S4.8b). On the other hand, phosphatidylethanolamine levels, which did not differ between KO and WT mice on control diet, were lower in KO versus WT mice on the high fat diet and phosphatidylinositol levels increased in KO versus WT animals.

91

Liver glycerolipids were slightly elevated in KO vs WT livers on the control diet (without reaching statistical significance) but became significantly elevated (by 40-80%) on HFD (Fig S4.9). However, in plasma, glycerolipids were significantly lower in KO mice on both diets. Interestingly, eicosanoids showed exactly opposite pattern of changes in liver vs plasma. On HFD, CerS6 KO mice had significantly lower levels than WT animals, but eicosanoids were slightly elevated in KO vs WT animals on control diet. At the same time, no significant differences on any diet were seen in plasma, with the exception of 12-hydroxyheptadecanoic acid, which was elevated ~2.8 fold.

CerS6 KO mice show differential response of carbohydrate metabolites to diet in liver and plasma

Metabolomic data additionally show significant changes in carbohydrate and amino acid metabolism induced by knocking out CerS6. Almost all glycolytic metabolites, ribose-1-phosphate, and erythrose-4-phosphate were lower on KO mice than in the WT animals on control diet, with differences disappearing on the HF diet (Fig S4.10a). At the same time pentose pathway metabolites, hexoses and oligosaccharides produced by glycogen degradation, were significantly higher in KO animals than in WT on the HF diet but not on the control diet (Fig S4.10A). In plasma, glycolytic metabolites were higher in KO versus WT mice on both diets while pentose metabolism intermediates were higher on Ctrl diet only. Hexose intermediates mannitol and mannose were lower in KO compared to WT animals on Ctrl diet but either higher or similar to WT on the HF diet (Fig S4.10B). TCA cycle metabolites showed no difference between genotypes on control diet but were significantly lower in KO livers on the HF diet (Fig S4.10C). In plasma, however, TCA cycle metabolites showed no difference or were higher in KO animals than in WT on both diets (Fig S4.10D).

CerS6 KO significantly affected amino acid metabolism response to diet in liver and plasma but in a different manner

Levels of all amino acids in KO mouse livers did not differ from WT on the Ctrl diet but were significantly elevated in KO versus WT livers on the HFD (Fig S4.11). Interestingly, levels of betaine, methylhistamine, and creatine were higher in KO livers on control diet but not HFD, whereas S-methylmethionine and homocysteine were higher in KO mice on both diets. Reduced glutathione levels were lower in KO livers regardless of diet and cysteine-glutathione disulfide was higher in KO animals on both diets. However, oxidized glutathione showed no difference between KO and WT mice on Ctrl diet but was significantly higher in KO mice than in WT mice on the HF diet. Additionally, fatty acid degradation products of amino acids were higher in KO livers versus WT on the control diet but did not differ from WT on the HFD (Fig S4.11). Of note, on control diet urea cycle metabolites were similar in KO and WT livers, but on the HF diet they were significantly higher in KO versus WT animals. In plasma, most amino acids were not different between KO and WT animals on either diet (Fig S4.12, tables show only metabolites that are different between KO and WT on one or both diets), although glycine, methionine and aromatic amino acids were elevated in KO mice at least on one of the diets. Products of metabolism of most amino acids were elevated in KO versus WT plasma on both diets, however, histidine metabolites, isoleucine and valine, as well as methylated cysteine and cysteine sulfoxide, as well as sarcosine and dimethylglycine were lower in KO than in WT animals on HFD (Fig S4.12). Similarly, plasma urea cycle metabolites and polyamine metabolites were lower in KO mice on the HFD.

Bile acids are dramatically elevated in CerS6 KO mice liver and plasma but high fat diet scales down these differences

Striking differences between KO and WT livers were observed in bile acids metabolism. Four conjugated primary bile acids were increased ~20-70 times in KO mice compared to WT

mice on the control diet but differences of 2 to 3.4-fold were observed for just a few of them on the HFD diet (Fig S4.13A). Secondary bile acids were also dramatically higher in KO than in WT mice on the control diet, with taurolitho-, taurourso- and taurohyodeoxycholate reaching 10 – 86-fold increase in levels of the WT animals on the control diet, but they were only 2-4 times higher on the HFD. Plasma primary and secondary bile acids were also dramatically higher in KO versus WT samples on the control diet with fold-difference ranging from 4 to 124 for primary and from 2.5 to 52 for secondary bile acids (Fig S4.13B). On the HFD, the fold-difference between KO and WT mice was slightly lower, from 1.5- to 24-fold for primary and from 4- to 8-fold for secondary plasma bile acids.

Discussion

Our study confirms the initial hypothesis and shows that CerS6 KO mice are protected from diet-induced weight gain when fed a high fat diet (Fig 4.1A). Additionally, CerS6 KO mice on the control diet demonstrate no change in percent fat mass over the 16-week dietary intervention. We sought to examine why CerS6 KO mice remain leaner through indirect calorimetry analysis and found that none of the groups were more active than the others. Interestingly, while both genotypes consumed similar amounts of food on a control diet, on HFD the CerS6 KO mice consumed less chow than their WT littermates (Fig 4.3C). Previous studies have reported that mice over-eat when given *ad libitum* access to HFD [291] and we found that WT mice did consume significantly more food and calories than their CerS6 KO littermates. Caloric intake of CerS6 KO mice was not different from the WT mice on control diet (Fig 4.3D) despite the fact that CerS6 KO mice demonstrated significantly lower weight gain (Fig 4.1B). This effect of genotype-diet interaction on food consumption and homeostatic regulation needs to be further investigated, along with assessments of these measures at different timepoints and longer exposures to provide a clearer understanding of genotype and diet effects.

Measurements of RER demonstrate that consumption of HFD led to utilization of fat as a source of energy both by WT and CerS6 KO mice (Fig 4.3E). However, on the control diet which was significantly lower in fat content, the WT mice oxidized a mix of protein, fat and carbohydrates for energy, as expected [292]. The CerS6 KO mice preferentially used glucose for energy as can be determined from RER values near 1.0 during their waking hours. It is not quite clear why or how the absence of CerS6 and lower C_{16}- sphingolipid levels switched mouse tissues to using glucose for active part of the day cycle on control diet. Our metabolomic data indicate that while liver short-, medium- and long-chain fatty acids were mostly higher in the KO animals, the plasma levels of medium-, long- and long-chain monounsaturated fatty acids were lower in these mice (Fig S4.7). Thus, lower availability of free fatty acids from blood could give a partial explanation of the metabolic switch. However, this difference was not dramatic, from 50 to 25% and may not be the only factor in different nutrient utilization for energy production. The KO mice also remained leaner for the duration of the study, indicating that they may oxidize glucose for energy because they do not have sufficient fat stores to pull from. Of note, CerS6 has been implicated in the fatty acid storage in the lipid droplets and CerS6 knockout was shown to prevent lipid droplets formation [165, 293]. It is also possible that overall changed lipid metabolism is the driving force behind the use of carbohydrates for energy.

We examined several tissues for histological characteristics and found that CerS6 KO prevented the accumulation of lipid droplets in the livers of mice fed HFD (Fig 4.2). Non-alcoholic fatty liver disease (NAFLD) is the result of dyslipidemia and lipotoxicity due to insulin resistance, oxidative stress, fibrosis and hepatocellular death in the liver [294] and is strongly associated with obesity and type 2 diabetes [295, 296]. Published data suggest that $C_{24:0}$ and C_{16} ceramides are reciprocally regulated and contribute to insulin resistance and non-alcoholic

steatohepatitis [296]. In cell culture studies, CerS6 overexpression in isolated primary hepatocytes resulted in significant accumulation of triglycerides, inhibition of insulin signaling, and altered mitochondrial function, all of which are classical characteristics of NAFLD [130]. In rats with NAFLD, inhibition of ceramide with myriocin reduced hepatic lipid accumulation and reduced markers of hepatic steatosis [297]. Ceramides may be especially relevant to the development of NAFLD due to their combinatorial proinflammatory and cytotoxic effects. Ceramides are also particularly relevant to NAFLD because the liver is a central site of ceramide production, making it prone to sphingolipotoxicity [298-300]. Our study provides further evidence that mice lacking CerS6 and demonstrating significantly lower levels of C_{16}-Cer are protected from hepatic lipid droplet accumulation.

We expected to see significantly decreased levels of cytokines in the plasma, in line with current literature suggesting that TNFα mediates some of its effects through increased production of ceramide [301] or that ceramides can lead to an increase in cytokine production [287]. Additionally, a separate study demonstrated an association between IL-6 and insulin resistance with a probable connection through ceramides [189]. However, our data show that CerS6 KO mice did not have changes in plasma cytokines, including IL-6 and TNFα (Fig S4.3). Despite the lack of significant differences in TNFα levels, a clear trend for reduced TNFα in CerS6 KO mice was noted.

Our hypothesis predicted differential response to metabolic stress in CerS6KO mice, so as a first step, we performed targeted measurements of major sphingolipid classes in experimental groups. Our data demonstrate a strong and significant effect of CerS6 KO on the sphingolipids specifically produced by CerS6 (Fig 4.4), as expected. C_{14}-Cer, C_{16}-dhCer-, C_{16}-Cer and total Cer as well as corresponding sphingomyelins including total SM were significantly

lower in KO versus WT mice on both diets. Additionally, HFD significantly elevated these species compared to levels on control diet. Moreover, we also found that the effects of CerS6 KO extend beyond C_{14}- and C_{16}-ceramides (Fig 4.5). Interestingly, while CerS6 KO protected animals from C_{14}-, C_{16}- SM accumulation of HFD, no protection was seen for C_{18}- through C_{22}- SM (Fig 4.6) suggesting that this effect of CerS6 does not extend to all sphingomyelin species. Elevation of SMs across all chain lengths may reflect a homeostatic mechanism that controls ceramide levels. Since HFD increases supply of free fatty acids it will increase the synthesis of sphingoid bases through the first and rate-limiting reaction catalyzed by SPT [302]. *De novo* synthetized spingoid base will be acylated by the over-supplied acyl-CoAs thus increasing levels of ceramide. However, since ceramides are signaling lipids and their elevation generally has apoptotic effect, to avoid cell death signaling, ceramides are converted to SMs by hepatocytes and further released into plasma. While CerS5 is also capable of producing C_{14} and C_{16} ceramides, the dramatic lowering effect of knockout on plasma C_{14}- and C_{16}- species indicates that CerS6 is likely the primary source of these sphingolipids in the plasma. Additionally, it has been suggested that CerS5 functions more as a housekeeping gene to produce ceramides for membrane functions whereas CerS6 responds to stimuli [82]. Additionally, CerS6 KO mice were protected from accumulation of other ceramide species in plasma indicating that CerS6 has a role in regulation of the synthesis of other ceramides. It is now appreciated that CerS can heterodimerize with data indicating that CerS6 may interact with CerS2 and CerS5 [133]. This could be a possible mechanism behind the lower levels of other ceramide species as it is likely that the absence of CerS6 is affecting the expression and activity of other CerS.

A similar effect was also seen for plasma HexCer species, CerS6 KO on HFD demonstrated lowered levels of nearly every species, not just those produced by CerS6 (Fig 4.7).

It is possible that CerS6 plays a significant part in nutrient stress by modulating HexCer levels. Metabolomics confirmed that CerS6 KO mice had significantly lower HexCer on HFD but fewer differences on the Ctrl diet. Furthermore, hepatic HexCer were significantly elevated due to HFD. Glucosyl-ceramides and glycosphingolipids have gained attention recently as possessing more than a structural role. Studies have found that inhibition of glycosphingolipids lessens measures of atherosclerosis in a rabbit model of the disease [303] and may work independently of ceramide to influence insulin signaling and thus insulin resistance [304]. Accumulation of glycosphingolipids and GlucCer has been reported in disease states including Gaucher disease which is often accompanied by IR [305].

Gene expression was measured to better understand compensatory changes that may be occurring in CerS6 KO mice or due to high fat diet which could partially explain the altered sphingolipid levels. Knocking out CerS6 led to significant elevation in several genes involved in sphingolipid synthesis, including the rate-limiting step catalyzed by SPT and genes involved in modification of Cer to SM or GlucCer as well as ceramidase which is involved in the synthesis of Sph from Cer (Fig 4.8). Change of expression ranged from 2 to 8-fold for different genes in CerS6 KO mice. The increase in expression of several genes, both related to *de novo* synthesis and the salvage sphingolipid pathway indicates increased flux, possibly in an attempt to maintain proper ceramide levels. Interestingly, the mRNA levels of other CerS isoforms were largely unaltered by either CerS6 KO or dietary intervention (Fig S4.4A), except that CerS6 KO mice fed a HFD had significantly elevated expression of CerS2 in the liver compared to WT mice fed a HFD. CerS2 is the predominant CerS expressed in the liver which indicates it may be more sensitive to dietary intervention. It is also possible that changes in other CerS could be found in different tissues, depending on the specific tissue expression profile. CerS6 is expressed at low

levels in most tissues which could explain why we did not see a significant increase in liver expression when mice were fed a HFD. Importantly, we observed increase in the protein levels of CerS6 on HFD, indicating post-transcriptional regulation of the enzyme in response to HFD (Fig S4.4B).

While several studies characterizing CerS using knockout mouse models have been published, our study presents metabolomic data for both liver and plasma to explain the unique characteristics of CerS6. Untargeted metabolomics approach allows discovery of less obvious metabolic connections between different pathways, which was the rationale for using it in our investigation. Principal component analysis of metabolomics data shows distinct separation between WT and CerS6 KO mice for liver with a closer alignment due to diet, whereas the plasma samples had a clear separation between both genotype and diet (Fig 4.9). Heat map analysis of the metabolites showing at least 50% change due to diet or genotype and the p-value <0.05, confirmed separation of liver and plasma samples by both diet and genotype (Fig S4.5). Meanwhile, both liver and plasma showed significantly lower C_{16}-acyl chain containing sphingolipids showing good correlation with our targeted sphingolipid measurements. Interestingly, C_{16}-Cer levels in liver showed reduction by 32-65% by the CerS6 KO, while in plasma reduction was by 94-95%, indicating that the source of this ceramide in plasma is mostly CerS6, not CerS5. At the same time C_{16}-SM and C_{16}-GlucCer showed similar reductions in both tissues. Overall, clear group separation demonstrates that the plasma metabolome could be used for selection of biomarkers or indicators of nutrient stress due to its sensitivity in response to a high fat diet.

In addition to changes of sphingolipids, CerS6 KO also induced profound alterations in metabolite levels of other lipid classes. Increases in short and medium-chain fatty acids as well

99

as long-chain polyunsaturated fatty acids, mono-hydroxy and dicarboxylic fatty acids were seen in KO livers on the control diet (Fig S4.7A). However, some of these fatty acids were reduced in KO livers on the HFD. No differences in long-chain saturated fatty acids were found in either tissue. Additionally, acyl-carnitines and acyl-cholines were elevated in KO livers on control but were mostly unchanged in HFD diet. In plasma, however, most of the fatty acids, conjugated or not, were reduced in the KO mice on both diets with stronger effects on high fat diet (Fig S4.7B). Acyl-carnitines, being intermediates in fatty acid oxidation, were found to be associated with insulin resistance and are studied for their role in lipotoxicity, along with ceramides (reviewed by Schooneman [306]). Their lower levels in CerS6 KO mice points to a potential protective mechanism that enables CerS6 KO mice to remain insulin sensitive and maintain a healthy weight. However, plasma acyl-carnitine levels do not always correlate with tissue levels and the use of acyl-carnitines as a biomarkers for risk of IR should be used with caution [307]. These data indicate that not all fatty acids are transported from liver to plasma even if they are increased in liver.

Phospholipids also showed changes due to genotype and diet (Fig S4.8). On the control diet, mouse liver phosphatidylcholine, phosphatidylethanolamine, phosphatidylserine, and phosphatidylglycerol were not different between KO and WT animals, while phosphatidylinositol was slightly reduced (by 27%). At the same time, on HFD, all of these phospholipids were elevated in KO livers (Fig S4.8A). Quite different effects were seen in plasma (Fig S4.8B). On control diet, phosphatidylcholines were significantly lower in KO plasma while phosphatidylethanolamines and phosphatidylinositols were unchanged. However, on the HFD, phosphatidylcholines were almost unchanged, but phosphatidylethanolamines were significantly reduced and phosphatidylinositols were significantly elevated. While elevation of

liver phosphatidylcholine, phosphatidylethanolamine, glycosyl-phosphatidylethanolamine, phosphatidylserine and phosphatidylglycerol on HFD could be explained by oversupply of dietary fatty acids, it is not clear at present, why phosphatidylcholines would be reduced in KO versus WT plasma with no changes in phosphatidylethanolamines and phosphatidylinositols on control diet. While no differences were seen between KO and WT plasma in phosphatidylcholines on the HFD, phosphatidylethanolamines were significantly reduced and phosphatidylinositols are significantly increased in KO versus WT plasma samples. It is possible that reduced phosphatidylethanolamine levels play protective role in reducing fat mass accumulation in KO mice, as abnormal phosphatidylethanolamine levels has been linked to several diseases (reviewed in [308, 309]).

Hepatic glycerolipids were mostly elevated in KO versus WT on both control and HFD, excluding some C_{16} and C_{18}-glycerolipids. Plasma glycerolipids, on the contrary, were significantly reduced in KO versus WT samples on both control and HFD. Interestingly, liver eicosanoids were mostly unchanged in KO mice livers on control diet (Fig S4.9A) but were significantly lower in KO versus WT livers on HFD. As for the plasma, no significant differences in eicosanoid levels were observed between genotypes on either diet (Fig S4.9B). Ceramides and eicosanoids are both known to function in signal transduction pathways and sphingolipids may regulate inflammatory response through eicosanoids as well as cytokines [310, 311]. CerS6 KO livers could be protected from increased inflammation by having lower eicosanoid levels and possibly decreased cytokine levels.

Along with lipid metabolic pathways, which were affected by CerS6 KO and HFD, multiple metabolic pathways, which may not be directly linked to lipid metabolism were also significantly altered by genotype and diet. Reduction of glycolytic metabolites, pentose

phosphate pathway and pentose metabolites, with no changes in TCA cycle metabolites in KO versus WT livers on control diet (Fig S4.10 A,C) could be reflecting the preferential use of glucose for energy seen in the RER measurements in calorimetry cages. On the HFD, though, TCA cycle metabolites were lower in KO mice than in WT, but glucose, lactate, pentose and glycogen metabolites are significantly elevated in KO livers (Fig S4.10 A,C), reflecting the switch to oxidation of fatty acids by both KO and WT mice. Studies of HFD feeding in rats showed insulin resistance and decreased levels of TCA cycle intermediates in skeletal muscle [206], similar to our data in liver. At the same time on control diet, glycolytic and pentose metabolites were elevated in KO versus WT plasma together with TCA cycle intermediates succinate, fumarate, and malate (Fig S4.10 B, D). Upon HFD consumption, almost all of the glycolytic and TCA cycle metabolites were significantly elevated in the KO plasma compared to WT, again in agreement with the preferential fatty acid oxidation on the HFD.

Multiple changes in amino acid metabolism are notable in KO mice and also in response to consumption of HFD. On the Ctrl diet, no differences in the levels of amino acids between KO and WT livers was found. Calorimetry data indicate that on this diet, KO mice preferentially oxidize glucose, while WT use a mix of fatty acids, glucose and amino acids, and higher levels of lysine, tyrosine, tryptophan, leucine/isoleucine/valine metabolites in KO versus WT mice on control diet (Fig S4.11) support calorimetry measurements. Furthermore, on the HFD levels of all amino acids and their metabolites were significantly increased in KO, compared to WT mice (Fig S4.11). While to some extent counter-intuitive, this further increase in amino acids may result from preferential use of fatty acids for energy, and channeling TCA cycle metabolites into production of amino acids (reflected in lower TCA cycle metabolites in KO vs WT mice on HFD). Alternatively, altered ceramide levels due to CerS6 KO could potentially be affecting

amino acid transport between peripheral tissues and plasma resulting in increased accumulation of several amino acids in the plasma (Fig S4.12). It has been demonstrated that ceramides downregulate the amino acid transport system in a rat skeletal muscle cell culture model, leading to decreased amino acid abundance in those cells which could affect protein synthesis [312]. In plasma, glycine, phenylalanine and tyrosine, as well as their metabolites and leucine/isoleucine/valine metabolites were elevated in KO mice on control diet (Fig S4.12), which does not mirror the liver profile. Moreover, urea cycle metabolites were slightly higher in KO mice on control diet and slightly lower on the HFD (Fig S4.12), which is opposite to the liver profile, which showed unchanged or slightly lower urea cycle metabolites in KO versus WT mice on Ctrl diet and significantly elevated metabolites on the HFD (Fig S4.11). These differences underscore the fact that metabolomic profiles in plasma do not precisely reflect liver amino acid metabolism but represent cumulative contributions from multiple tissues of the body.

The biggest differences in the effects size for metabolites (30-120-fold) were found for bile acids, both primary and secondary (Fig S4.13), and in this case plasma profiles reflected the overall liver trends, but not necessarily for individual metabolites. Overall, both liver and plasma levels of KO mice were dramatically higher in KO than in WT livers on control diet with difference disappearing on the HFD. While higher levels of liver bile acids in KO mice could be excreted with bile, it is not clear what effects would 123-fold elevated plasma alpha-muricholate have on peripheral tissues. Of note, bile acids are important metabolic regulators acting through the PPARs and farnesoid receptors, which may be a part of the explanation of reduced fat accumulation by KO mice.

Conclusion

Several studies have demonstrated that reduction of C_{16}-Cer levels protects against diet-induced weight gain and promotes liver health. Recently, targeting CerS6 with antisense

oligonucleotides in *ob/ob* mice on HFD was shown to decrease C_{16}-Cer and restore glucose sensitivity and plasma adiponectin levels [4]. Another model unrelated to CerS6 (heterozygous CerS2 knockout) was found to increase C_{16}-Cer and showed impairment of glucose tolerance, plasma cholesterol, liver damage and other markers common to obesity [130]. Nevertheless, none of the studies have been able to provide mechanisms for such effects of CerS6 and C_{16}-Cer.

Our work confirmed our hypothesis regarding the link between CerS6, C_{16}-Cer, and overall animal metabolism and has established that reducing C_{16}-Cer by CerS6 knockout significantly changes nearly every metabolic pathway, irrespective of diet. It also demonstrated that the plasma metabolome rarely reflects changes observed in liver (and likely other tissues). This study also showed that not all metabolites are "created equal": only CerS6-produced C_{16}-Cer can be transported to plasma, as can be seen from comparison of the C_{16}-Cer levels in WT and KO mice. Thus, C_{16}-Cer concentrations in KO livers (CerS5-produced) were only 65% and 35% of the concentrations seen in WT liver on control and HFD respectively, however in the KO mice plasma C_{16}-Cer levels were only 6% and 5%, of the WT plasma levels on Ctrl and HFD, respectively). This suggests that plasma C_{16}-Cer may be a good indicator of CerS6 status. Additionally, our study indicated that both primary and secondary bile acids may mediate effects of C_{16}-ceramide in metabolic response.

It should be noted that current study has its limitations. The additional fat in the HFD comes from lard which is not typical of human consumption. Effect of different dietary fat composition (saturated versus polyunsaturated fatty acids, or combinations thereof, as well as acyl chains lengths of constituent fat) should be evaluated to give a better understanding of how CerS respond to different types of fat in the diets. Another feature of the HFD used in our experiments was 58% kcal derived from fat, which is higher than the standard Western diet

[313]. While such diets are commonly used to induce fat accumulation in animals, diets that more accurately reflect the standard Western diet (moderate fat, higher in fructose) will provide results more translatable to human physiology and disease states. The biggest limitation though, is that we still do not understand the mechanisms driving these metabolic changes. However, our metabolomics data provide directions for generation of novel hypotheses and future investigations.

Supplementary Materials
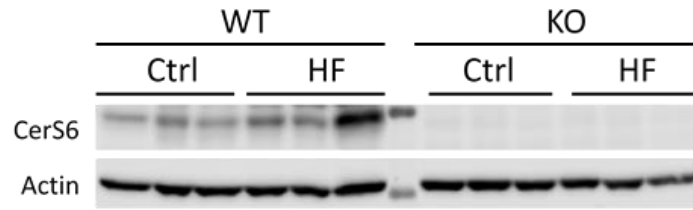
Figure S4.1 Western Blot confirming expression of CerS6 protein in WT mice only

Diet Number (Teklad)	TD.04194	TD.180093
Diet Name	Control	High Fat Diet
Ingredient (g/kg)		
Caseine, Vitamin-Free	195.0	195.0
L-Cystine	3.0	3.0
Corn Starch	314.488	34.237
Sucrose	200.0	200.251
Maltodextrin	130.0	130.0
Soybean Oil	60.0	60.0
Lard	0.0	280.0
Cellulose	50.0	50.0
Mineral Mix (AIN-93G-MX (94046))	35.0	35.0
TBHQ, antioxidant	0.012	0.012
Vitamin Mix (AIN-93-VX (94047))	10.0	10.0
Choline Bitartrate	2.5	2.5
% kcal from protein	**19.0**	**13.6**
% kcal from carbohydrate	**66.6**	**28.3**
% kcal from fat	**14.4**	**58.2**
kcal/g	**3.8**	**5.3**

Table S4.1 Diet composition including ingredients by weight and caloric content of control diet and high fat diet

Category	Gene		Sequence
CerS isoforms	CerS1	F	GGAGCTACTGCGCTTACCTG
		R	CCATGCCTGACCTCCAGT
	CerS2	F	AGAAGTGGGAAACGGAGTAGC
		R	TTCCCACCAGAAGTAGTCATACAA
	CerS3	F	GGCGATTTACATTTTACTTGCTG
		R	GGTCATATGCCCATGGTTTG
	CerS4	F	GCTGTGCGAATTGTCTTTGA
		R	AGTCTGCCGAAGCGTGAG
	CerS5	F	CGGGGAAAGGTGTCTAAGGAT
		R	GTTCATGCAGTTGGCACCATT
	CerS6	F	GATTCATAGCCAAACCATGTGCC
		R	AATGCTCCGAACATCCCAGTC
Sphingolipid metabolism	SPT (long chain base subunit 1)	F	ACGAGGCTCCAGCATACCAT
		R	TCAGAACGCTCCTGCAACTTG
	SM Synthase 1	F	TTGGCACGCTGTACCTGTATC
		R	CAGTCTCCAAAGAGCTTCGGA
	SM Synthase 2	F	GAGACAGCAAAACTTGAAGGTCA
		R	CCCGTTGGATAAGGTCTTGGG
	Acid Sphingomyelinase (1)	F	TGGCTCTATGAAGCGATGGC
		R	TTGAGAGAGATGAGGCGGAGAC
	Neutral Sphingomyelinase	F	ACACGACCCCCTTTCCTAATA
		R	GGCGCTTCTCATAGGTGGTG
	Glucosyl-CerS	F	AGGAAGGATGTGCTAGATCAGG
		R	TTTGCATGGCAACTTGAGTAGA
	Ceramidase	F	GCAAAGCGAACCTTCTCCAC
		R	ACTGGTAACAAACAAGAGGGTGA
Control	β-actin	F	ATTGGCAATGAGCGGTTCC
		R	GGTAGTTTCGTGGATGCCACA

Table S4.2 qPCR primer sequences
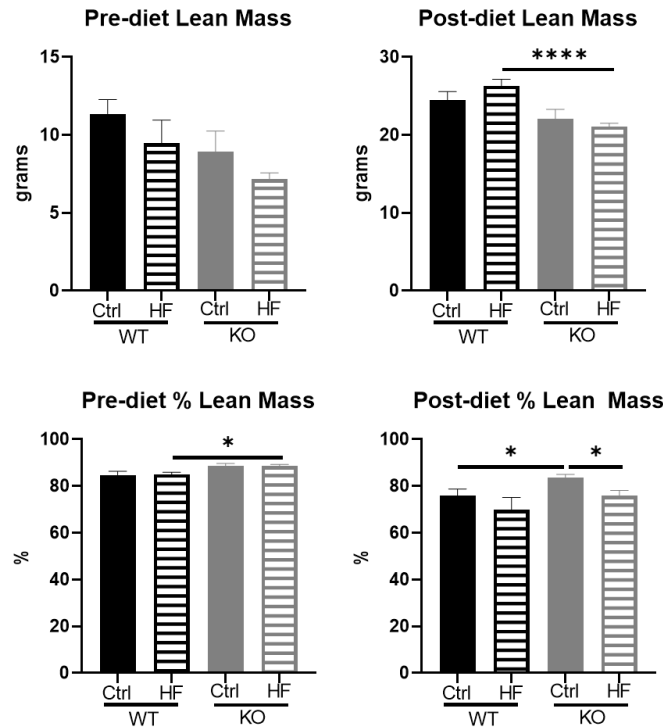
Figure S4.2 CerS6 KO mice tended to have more lean body mass before dietary intervention and those placed on the Control diet remained leaner throughout study. Data are shown as mean ± SEM, n=3-4. Solid bars, control diet; striped bars, high-fat diet. WT shown in black and KO shown in grey. *, p<0.05; **, p<0.01; ***, p<0.001; ****, p<0.0001 determined by Student's t-test between genotypes and diets
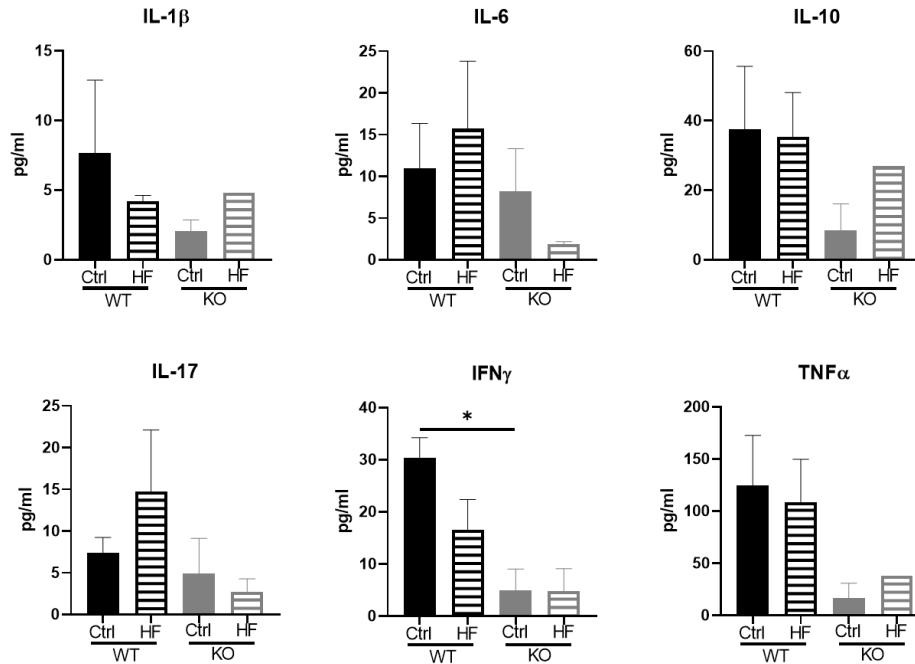
Figure S4.3 Plasma cytokines not significantly altered due to diet or knockout. Data are shown as mean $\pm$ SEM, n=3-4. Solid bars, control diet; striped bars, high-fat diet. WT shown in black and KO shown in grey. *, $p<0.05$; **, $p<0.01$; ***, $p<0.001$; ****, $p<0.0001$ determined by Student's t-test between genotypes and diets
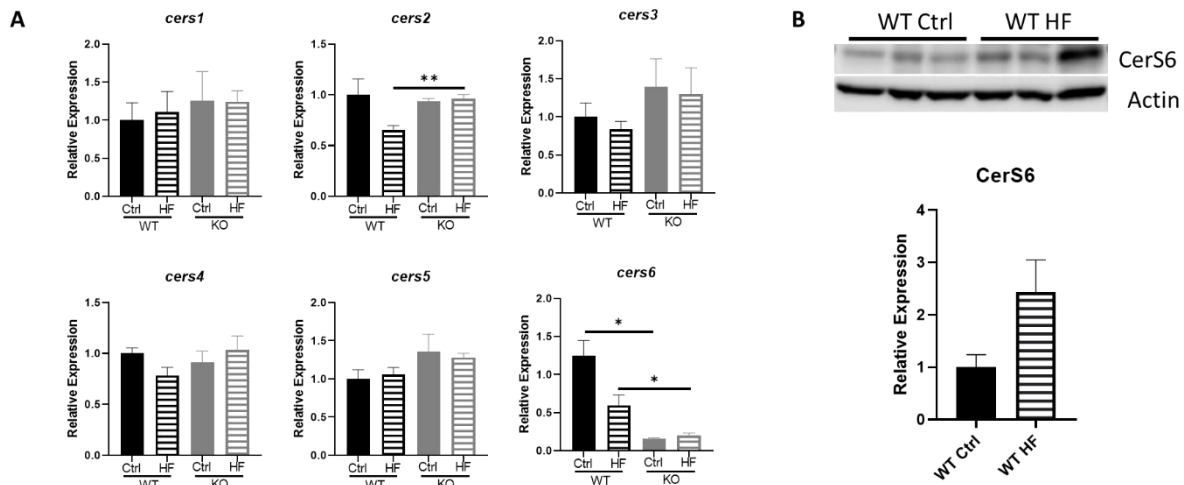
Figure S4.4 A) HFD decreased CerS2 mRNA in WT mice but had no biologically relevant effects on CerS mRNA levels in livers of either genotype. B) However, CerS6 protein was increased in WT livers by HFD. Data are shown as mean $\pm$ SEM, n=3. Solid bars, control diet; striped bars, high-fat diet. WT shown in black and KO shown in grey. *, $p<0.05$; **, $p<0.01$; ***, $p<0.001$; ****, $p<0.0001$ determined by Student's t-test between genotypes and diets

Statistically Significant Biochemicals	KO/WT Changes			
	Liver		Plasma	
	HF	CTRL	HF	CTRL
Total Biochemicals p<0.05	234	118	195	162
Biochemicals (↑/↓)	150/84	71/47	64/131	86/76
Total Biochemicals 0.05 <p <0.10	51	59	57	68
Biochemicals (↑/↓)	31/20	32/27	25/32	42/26

Table S4.3 Number of metabolites with significantly different levels in CerS6 KO versus WT mice on HFD were ~2-fold and ~1.2-fold higher in liver and plasma, respectively

Statistically Significant Biochemicals	HF/LF Changes			
	Liver		Plasma	
	WT	KO	WT	KO
Total Biochemicals p<0.05	206	289	288	189
Biochemicals (↑/↓)	125/81	150/139	146/142	66/123
Total Biochemicals 0.05 <p <0.10	70	67	49	64
Biochemicals (↑/↓)	38/32	37/30	24/25	13/51

Table S4.4 Number of metabolites changed by high fat diet compared to low fat is 40% higher in KO than in WT livers but 45% higher in WT plasma compared to KO
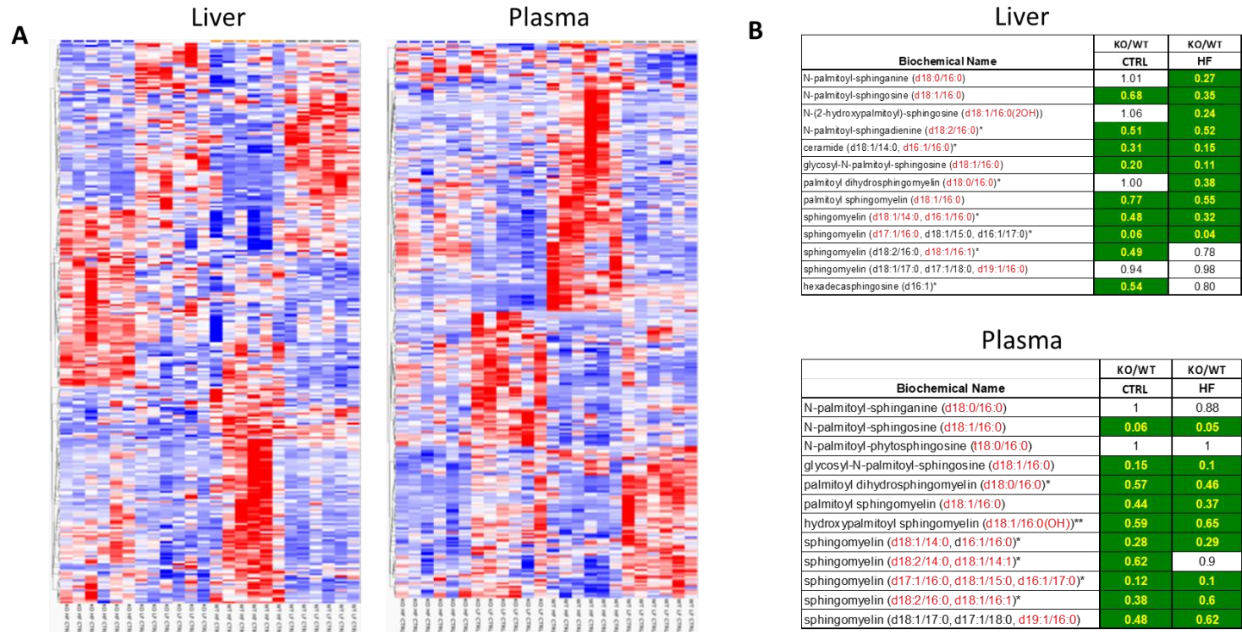
Figure S4.5 Heat map analysis(A) confirms separation of metabotypes both by diet and by genotype in liver and plasma, with patterns of separation being different between plasma and tissue. C_{16}-sphigolipids are lower in KO animals on both diets (B)

Liver

Biochemical Name	KO/WT CTRL	KO/WT HF
N-palmitoyl-sphinganine (d18:0/16:0)	1.01	0.27
N-palmitoyl-sphingosine (d18:1/16:0)	0.68	0.35
N-(2-hydroxypalmitoyl)-sphingosine (d18:1/16:0(2OH))	1.06	0.24
N-palmitoyl-sphingadienine (d18:2/16:0)*	0.51	0.52
ceramide (d18:1/14:0, d16:1/16:0)*	0.31	0.15
glycosyl-N-palmitoyl-sphingosine (d18:1/16:0)	0.20	0.11
palmitoyl dihydrosphingomyelin (d18:0/16:0)*	1.00	0.38
palmitoyl sphingomyelin (d18:1/16:0)	0.77	0.55
sphingomyelin (d18:1/14:0, d16:1/16:0)*	0.48	0.32
sphingomyelin (d17:1/16:0, d18:1/15:0, d16:1/17:0)*	0.06	0.04
sphingomyelin (d18:2/16:0, d18:1/16:1)*	0.49	0.78
sphingomyelin (d18:1/17:0, d17:1/18:0, d19:1/16:0)	0.94	0.98
hexadecasphingosine (d16:1)*	0.54	0.80

Plasma

Biochemical Name	KO/WT CTRL	KO/WT HF
N-palmitoyl-sphinganine (d18:0/16:0)	1	0.88
N-palmitoyl-sphingosine (d18:1/16:0)	0.06	0.05
N-palmitoyl-phytosphingosine (t18:0/16:0)	1	1
glycosyl-N-palmitoyl-sphingosine (d18:1/16:0)	0.15	0.1
palmitoyl dihydrosphingomyelin (d18:0/16:0)*	0.57	0.46
palmitoyl sphingomyelin (d18:1/16:0)	0.44	0.37
hydroxypalmitoyl sphingomyelin (d18:1/16:0(OH))**	0.59	0.65
sphingomyelin (d18:1/14:0, d16:1/16:0)*	0.28	0.29
sphingomyelin (d18:2/14:0, d18:1/14:1)*	0.62	0.9
sphingomyelin (d17:1/16:0, d18:1/15:0, d16:1/17:0)*	0.12	0.1
sphingomyelin (d18:2/16:0, d18:1/16:1)*	0.38	0.6
sphingomyelin (d18:1/17:0, d17:1/18:0, d19:1/16:0)	0.48	0.62

A

Biochemical Name	KO/WT CTRL	KO/WT HF
sphinganine	1.31	0.59
sphingadienine	0.96	1.36
N-stearoyl-sphinganine (d18:0/18:0)*	1.78	0.27
N-stearoyl-sphingosine (d18:1/18:0)*	1.40	0.95
N-arachidoyl-sphingosine (d18:1/20:0)*	1.07	0.94
N-behenoyl-sphingadienine (d18:2/22:0)*	0.78	1.33
ceramide (d18:1/17:0, d17:1/18:0)*	0.93	0.57
ceramide (d16:1/24:1, d18:1/22:1)*	0.75	0.67
ceramide (d18:2/24:1, d18:1/24:2)*	1.27	0.89
glycosyl-N-stearoyl-sphingosine (d18:1/18:0)	1.65	0.58
glycosyl-N-nervonoyl-sphingosine (d18:1/24:1)*	1.14	0.49
glycosyl ceramide (d18:1/20:0, d16:1/22:0)*	0.95	0.69
glycosyl ceramide (d16:1/24:1, d18:1/22:1)*	0.46	0.36
glycosyl ceramide (d18:2/24:1, d18:1/24:2)*	1.69	0.68
lactosyl-N-behenoyl-sphingosine (d18:1/22:0)*	1.26	1.10
lactosyl-N-nervonoyl-sphingosine (d18:1/24:1)*	2.83	0.53
behenoyl dihydrosphingomyelin (d18:0/22:0)*	1.22	0.99
sphingomyelin (d18:0/18:0, d19:0/17:0)*	1.40	0.53
sphingomyelin (d18:0/20:0, d16:0/22:0)*	1.59	0.46
stearoyl sphingomyelin (d18:1/18:0)	1.48	1.40
behenoyl sphingomyelin (d18:1/22:0)*	1.04	1.44
tricosanoyl sphingomyelin (d18:1/23:0)*	1.30	1.25
lignoceroyl sphingomyelin (d18:1/24:0)	1.09	1.38
sphingomyelin (d18:2/23:1)*	1.58	0.84
sphingomyelin (d18:1/18:1, d18:2/18:0)	1.51	1.07
sphingomyelin (d18:1/19:0, d19:1/18:0)*	0.91	1.00
sphingomyelin (d18:1/20:0, d16:1/22:0)*	1.17	1.24
sphingomyelin (d18:1/20:1, d18:2/20:0)*	1.16	1.56
sphingomyelin (d18:1/21:0, d17:1/22:0, d16:1/23:0)*	0.69	0.93
sphingomyelin (d18:2/21:0, d16:2/23:0)*	0.44	0.88
sphingomyelin (d18:1/22:1, d18:2/22:0, d16:1/24:1)*	0.80	1.30
sphingomyelin (d18:1/22:2, d18:2/22:1, d16:1/24:2)*	0.77	1.53
sphingomyelin (d18:2/23:0, d18:1/23:1, d17:1/24:1)*	0.92	1.05
sphingomyelin (d18:1/24:1, d18:2/24:0)*	1.58	1.06
sphingomyelin (d18:2/24:1, d18:1/24:2)*	1.65	1.24
sphingomyelin (d18:1/25:0, d19:0/24:1, d20:1/23:0, d19:1/24:0)*	1.19	1.28
sphingosine	1.30	0.92
hexadecasphingosine (d16:1)*	0.54	0.80
phytosphingosine	1.61	1.07

B

Biochemical Name	KO/WT CTRL	KO/WT HF
sphinganine	1.65	1.03
sphinganine-1-phosphate	0.78	0.85
N-behenoyl-sphingadienine (d18:2/22:0)*	0.25	1.27
ceramide (d18:1/20:0, d16:1/22:0, d20:1/18:0)*	0.38	0.65
ceramide (d16:1/24:1, d18:1/22:1)*	0.26	0.37
ceramide (d18:2/24:1, d18:1/24:2)*	0.38	0.48
glycosyl-N-stearoyl-sphingosine (d18:1/18:0)	0.74	0.42
glycosyl-N-behenoyl-sphingadienine (d18:2/22:0)*	0.51	1.14
glycosyl ceramide (d18:1/20:0, d16:1/22:0)*	0.54	0.55
glycosyl ceramide (d16:1/24:1, d18:1/22:1)*	0.44	0.28
glycosyl ceramide (d18:2/24:1, d18:1/24:2)*	0.79	0.55
behenoyl dihydrosphingomyelin (d18:0/22:0)*	0.95	0.85
sphingomyelin (d18:0/18:0, d19:0/17:0)*	1.14	1.06
sphingomyelin (d18:0/20:0, d16:0/22:0)*	1	0.48
stearoyl sphingomyelin (d18:1/18:0)	1	1.23
behenoyl sphingomyelin (d18:1/22:0)*	0.82	0.96
tricosanoyl sphingomyelin (d18:1/23:0)*	1.09	0.89
lignoceroyl sphingomyelin (d18:1/24:0)	0.98	1
sphingomyelin (d18:2/18:1)*	0.91	1.01
sphingomyelin (d18:2/23:1)*	0.73	0.65
sphingomyelin (d18:2/24:2)*	0.98	0.97
sphingomyelin (d18:1/18:1, d18:2/18:0)	0.89	1.14
sphingomyelin (d18:1/19:0, d19:1/18:0)*	0.61	0.61
sphingomyelin (d18:1/20:0, d16:1/22:0)*	0.87	0.91
sphingomyelin (d18:1/20:1, d18:2/20:0)*	0.71	1.06
sphingomyelin (d18:1/21:0, d17:1/22:0, d16:1/23:0)*	0.54	0.68
sphingomyelin (d18:2/21:0, d16:2/23:0)*	0.34	0.54
sphingomyelin (d18:1/22:1, d18:2/22:0, d16:1/24:1)*	0.66	0.99
sphingomyelin (d18:1/22:2, d18:2/22:1, d16:1/24:2)*	0.55	0.86
sphingomyelin (d18:2/23:0, d18:1/23:1, d17:1/24:1)*	0.72	0.7
sphingomyelin (d18:1/24:1, d18:2/24:0)*	1.03	0.64
sphingomyelin (d18:2/24:1, d18:1/24:2)*	0.93	0.85
sphingomyelin (d18:1/25:0, d19:0/24:1, d20:1/23:0, d19...	1.15	0.68
sphingosine	2.2	1.05
sphingosine 1-phosphate	1.02	1.04

Figure S4.6 Differential effects of CerS6 KO on the non-C_{16}-sphingolipids in liver (A) and plasma (B).

A

Sub-pathway	Biochemical Name	KO/WT CTRL	KO/WT HF
Short Chain Fatty Acid	butyrate (4:0)	2.45	1.04
Medium Chain Fatty Acids	(2 or 3)-decenoate (10:1n7 or n8)	1.65	0.60
	5-dodecenoate (12:1n7)	2.10	1.21
Long Chain Polyunsaturated Fatty Acids	tetradecadienoate (14:2)*	1.46	1.14
	hexadecatrienoate (16:3n3)	1.14	1.36
	heptadecatrienoate (17:3)*	0.96	1.30
	stearidonate (18:4n3)	0.96	1.37
	docosatrienoate (22:3n3)	1.12	1.55
	nisinate (24:6n3)	1.21	2.33
	docosatrienoate (22:3n6)*	1.49	1.97
	adrenate (22:4n6)	1.30	1.43
	docosapentaenoate (n6 DPA; 22:5n6)	1.68	2.65
	docosadienoate (22:2n6)	1.06	1.58
Fatty Acids Dicarboxylate	glutarate (C5-DC)	1.91	0.47
	hexadecanedioate (C16-DC)	1.99	1.01
	hexadecenedioate (C16:1-DC)*	1.59	0.74
	octadecenedioate (C18:1-DC)	1.57	1.03
	octadecadienedioate (C18:2-DC)*	1.88	1.33
	2-hydroxysebacate	2.33	0.92
Amino-Fatty Acids	N-acetyl-2-aminooctanoate*	1.91	0.98
	3-hydroxyhexanoate	1.51	0.64
	3-hydroxyoctanoate	1.30	0.96
Fatty Acids, Monohydroxy	3-hydroxydecanoate	1.31	1.10
	3-hydroxylaurate	1.27	1.22
	3-hydroxymyristate	1.08	1.20
	16-hydroxypalmitate	1.54	0.80
BCAA Metabolism	butyrylglycine	1.17	0.97
	propionylcarnitine (C3)	2.75	1.42
Acyl-glycine	N-octanoylglycine	1.18	2.38
	palmitoylcarnitine (C16)	2.06	1.13
	stearoylcarnitine (C18)	1.85	1.02
Acyl-Carnitines	lignoceroylcarnitine (C24)*	1.27	0.78
	linoleoylcarnitine (C18:2)*	1.57	0.90
	arachidonoylcarnitine (C20:4)	1.38	0.96
	adipoylcarnitine (C6-DC)	1.43	0.77
	pimeloylcarnitine/3-methyladipoylcarnitine (C7-DC)	3.04	0.53
Ketone bodies	3-hydroxybutyrate (BHBA)	1.44	0.67
	palmitoylcholine	1.56	0.88
	oleoylcholine	1.58	1.38
Acyl-Cholines	palmitoleoylcholine	1.53	1.94
	linoleoylcholine*	1.84	1.73
	stearoylcholine*	1.58	0.61

B

Sub-pathway	Biochemical Name	KO/WT CTRL	KO/WT HF
Short Chain Fatty Acid	butyrate/isobutyrate (4:0)	2.02	0.89
Medium Chain Fatty Acid	caprylate (8:0)	0.8	1.09
	(2 or 3)-decenoate (10:1n7 or n8)	1.13	0.74
Long Chain Saturated Fatty Acid	nonadecanoate (19:0)	0.85	0.76
	palmitoleate (16:1n7)	0.74	1.13
Long Chain Monounsaturated Fatty Acid	eicosenoate (20:1)	0.72	0.82
Fatty Acid	erucate (22:1n9)	0.64	0.4
	nervonate (24:1n9)*	0.88	0.4
	docosapentaenoate (n3 DPA; 22:5n3)	0.7	1.05
Long Chain Polyunsaturated	docosapentaenoate (n6 DPA; 22:5n6)	1.11	1.57
Fatty Acid (n3 and n6)	docosadienoate (22:2n6)	0.93	0.86
	glutarate (C5-DC)	1.84	1.21
	3-methylglutarate/2-methylglutarate	0.65	2
	adipate (C6-DC)	0.6	2.26
Fatty Acid, Dicarboxylate	3-hydroxyadipate*	0.62	0.28
	suberate (C8-DC)	1.01	0.75
	sebacate (C10-DC)	1.41	0.91
	tetradecanedioate (C14-DC)	1.28	1.59
	tetradecadienedioate (C14:2-DC)*	1.44	0.98
Fatty Acid, Amino	2-aminoheptanoate	1.04	0.56
	N-acetyl-2-aminooctanoate*	1.03	0.72
	2-hydroxydecanoate	1.48	0.91
	3-hydroxyhexanoate	0.94	0.88
	3-hydroxyoctanoate	1.19	0.56
Fatty Acid, Monohydroxy	3-hydroxydecanoate	1.22	0.88
	3-hydroxysebacate	1.72	0.7
	3-hydroxylaurate	1.31	0.58
	3-hydroxymyristate	1.07	0.73
	3-hydroxyoleate*	0.99	0.86
	5-hydroxyhexanoate	1.81	0.56
	16-hydroxypalmitate	0.95	0.84
Fatty Acid, Dihydroxy	2S,3R-dihydroxybutyrate	0.7	0.8
	3,4-dihydroxybutyrate	0.84	0.8
	myristoylcarnitine (C14)	0.81	0.89
	palmitoylcarnitine (C16)	0.79	0.76
Fatty Acid Metabolism (Acyl Carnitine,)	margaroylcarnitine (C17)*	0.69	0.81
Long Chain Saturated	stearoylcarnitine (C18)	0.84	0.83
	arachidoylcarnitine (C20)*	0.87	0.73
	behenoylcarnitine (C22)*	0.74	0.87
	lignoceroylcarnitine (C24)*	0.57	0.82
	myristoleoylcarnitine (C14:1)*	0.91	0.75
Fatty Acid Metabolism (Acyl Carnitine,	palmitoleoylcarnitine (C16:1)*	0.77	0.89
Monounsaturated)	oleoylcarnitine (C18:1)	0.84	0.87
	eicosenoylcarnitine (C20:1)*	0.84	0.83
	nervonoylcarnitine (C24:1)*	1.12	0.59
Fatty Acid Metab. (Acyl Carn. Polyunsat.)	linoleoylcarnitine (C18:2)*	1	0.76
Fatty Acid Metabolism (Acyl Carnitine)	pimeloylcarnitine/3-methyladipoylcarnitine (C7-DC)	4.14	0.28
Fatty Acid Metabolism (Acyl Carnitine,	3-hydroxypalmitoylcarnitine	0.68	0.6
Hydroxy)	3-hydroxyoleoylcarnitine	0.74	0.83
Ketone Bodies	3-hydroxybutyrate (BHBA)	1.33	0.46
Fatty Acid Metabolism (Acyl Choline)	palmitoylcholine	1.21	0.08
	linoleoylcholine*	1.21	0.06
	arachidonoylcholine	1.2	0.08

Figure S4.7 Differential effects of CerS6 KO on the free and conjugated fatty acids in liver (A) and plasma (B).

A

Sub-pathway	Biochemical Name	KO/WT CTRL	KO/WT HF
Phosphatidylcholine (PC)	1-myristoyl-2-palmitoyl-GPC (14:0/16:0)	1.06	1.19
	1-myristoyl-2-arachidonoyl-GPC (14:0/20:4)*	0.91	1.44
	1-palmitoyl-2-arachidonoyl-GPC (16:0/20:4n6)	1.00	1.11
	1-palmitoleoyl-2-linoleoyl-GPC (16:1/18:2)*	0.93	1.27
	1-palmitoleoyl-2-linolenoyl-GPC (16:1/18:3)*	0.83	1.42
	1,2-dilinoleoyl-GPC (18:2/18:2)	0.96	1.22
	1-linoleoyl-2-linolenoyl-GPC (18:2/18:3)*	1.14	1.56
	1-linoleoyl-2-arachidonoyl-GPC (18:2/20:4n6)*	0.85	1.43
Phosphatidylethanolamine (PE)	1-oleoyl-2-linoleoyl-GPE (18:1/18:2)*	1.12	1.22
	1-oleoyl-2-arachidonoyl-GPE (18:1/20:4)*	1.11	1.16
	1-oleoyl-2-docosahexaenoyl-GPE (18:1/22:6)*	1.09	1.13
	1,2-dilinoleoyl-GPE (18:2/18:2)*	1.13	1.20
	1-linoleoyl-2-arachidonoyl-GPE (18:2/20:4)*	1.05	1.28
Glycosyl PE	1-palmitoyl-2-oleoyl-glycosyl-GPE (16:0/18:1)**	1.03	2.13
	1-palmitoyl-2-linoleoyl-glycosyl-GPE (16:0/18:2)**	1.16	1.47
	1-palmitoyl-2-arachidonoyl-glycosyl-GPE (16:0/20:4)**	0.99	1.19
	1-palmitoyl-2-docosahexaenoyl-glycosyl-GPE (16:0/22:6)**	0.98	1.29
	1-stearoyl-2-linoleoyl-glycosyl-GPE (18:0/18:2)**	0.99	1.21
	1-stearoyl-2-arachidonoyl-glycosyl-GPE (18:0/20:4)**	0.92	1.07
	1-stearoyl-2-docosahexaenoyl-glycosyl-GPE (18:0/22:6)**	0.92	1.18
Phosphatidylserine	1-stearoyl-2-oleoyl-GPS (18:0/18:1)	1.20	0.88
Phosphatidylglycerol	1-palmitoyl-2-linoleoyl-GPG (16:0/18:2)	0.90	1.32
Phosphatidylinositol (PI)	1-stearoyl-2-linoleoyl-GPI (18:0/18:2)	0.73	1.32

B

Sub-pathway	Biochemical Name	KO/WT CTRL	KO/WT HF
Phosphatidylcholine (PC)	1-myristoyl-2-arachidonoyl-GPC (14:0/20:4)*	0.56	1.39
	1,2-dipalmitoyl-GPC (16:0/16:0)	0.8	1.02
	1-palmitoyl-2-palmitoleoyl-GPC (16:0/16:1)*	0.58	0.99
	1-palmitoyl-2-stearoyl-GPC (16:0/18:0)	0.64	1.01
	1-palmitoyl-2-oleoyl-GPC (16:0/18:1)	0.76	0.93
	1-palmitoyl-2-linoleoyl-GPC (16:0/18:2)	0.86	1.03
	1-palmitoyl-2-gamma-linolenoyl-GPC (16:0/18:3n6)*	0.7	1.08
	1-palmitoyl-2-arachidonoyl-GPC (16:0/20:4n6)	0.75	1.01
	1-palmitoyl-2-docosahexaenoyl-GPC (16:0/22:6)	0.79	0.97
	1-palmitoleoyl-2-linoleoyl-GPC (16:1/18:2)*	0.74	0.94
	1-palmitoleoyl-2-linolenoyl-GPC (16:1/18:3)*	0.64	1.09
	1-stearoyl-2-oleoyl-GPC (18:0/18:1)	0.66	0.82
	1-stearoyl-2-linoleoyl-GPC (18:0/18:2)*	0.79	0.92
	1-stearoyl-2-arachidonoyl-GPC (18:0/20:4)	0.7	0.83
	1-stearoyl-2-docosahexaenoyl-GPC (18:0/22:6)	0.72	0.72
	1-oleoyl-2-linoleoyl-GPC (18:1/18:2)*	0.79	1.04
	1,2-dilinoleoyl-GPC (18:2/18:2)	0.82	1.1
	1-linoleoyl-2-arachidonoyl-GPC (18:2/20:4n6)*	0.66	1.2
Phosphatidylethanolamine (PE)	1-palmitoyl-2-linoleoyl-GPE (16:0/18:2)	1.04	0.65
	1-palmitoyl-2-arachidonoyl-GPE (16:0/20:4)*	0.97	0.67
	1-palmitoyl-2-docosahexaenoyl-GPE (16:0/22:6)*	0.93	0.58
	1-stearoyl-2-linoleoyl-GPE (18:0/18:2)*	0.88	0.71
	1-stearoyl-2-arachidonoyl-GPE (18:0/20:4)	0.89	0.65
	1-stearoyl-2-docosahexaenoyl-GPE (18:0/22:6)*	0.97	0.56
	1-oleoyl-2-linoleoyl-GPE (18:1/18:2)*	1	0.75
	1-oleoyl-2-arachidonoyl-GPE (18:1/20:4)*	0.96	0.73
	1-oleoyl-2-docosahexaenoyl-GPE (18:1/22:6)*	0.99	0.64
Phosphatidylinositol (PI)	1-palmitoyl-2-linoleoyl-GPI (16:0/18:2)	0.93	1.58
	1-stearoyl-2-linoleoyl-GPI (18:0/18:2)	0.82	1.66
	1-stearoyl-2-arachidonoyl-GPI (18:0/20:4)	0.86	1.07
	1-oleoyl-2-arachidonoyl-GPI (18:1/20:4)*	1	1.27

Figure S4.8 Differential effects of CerS6 KO on the phospholipids in liver (A) and plasma (B).

A

SubPathway	Biochemical Name	KO/WT CTRL	KO/WT HF
Lysophospholipids	1-palmitoleoyl-GPC (16:1)*	0.81	1.44
	2-palmitoleoyl-GPC (16:1)*	0.72	1.43
Plasmalogens	1-(1-enyl-palmitoyl)-2-oleoyl-GPE (P-16:0/18:1)*	1.43	0.67
	1-(1-enyl-stearoyl)-2-oleoyl-GPE (P-18:0/18:1)	1.70	0.45
	1-(1-enyl-stearoyl)-2-arachidonoyl-GPE (P-18:0/20:4)*	1.40	0.91
Monoglyceride	glycerophosphoglycerol	0.95	1.41
	2-arachidonoylglycerol (20:4)	1.17	1.67
Diacylglycerols	stearoyl-arachidonoyl-glycerol (18:0/20:4) [2]*	1.15	1.29
	oleoyl-arachidonoyl-glycerol (18:1/20:4) [2]*	1.07	1.49
	linoleoyl-arachidonoyl-glycerol (18:2/20:4) [1]*	2.57	1.81
	linoleoyl-arachidonoyl-glycerol (18:2/20:4) [2]*	1.47	1.67
	linoleoyl-docosahexaenoyl-glycerol (18:2/22:6) [2]*	1.28	1.42
	palmitoyl-docosahexaenoyl-glycerol (16:0/22:6) [1]*	1.31	0.55
	stearoyl-linoleoyl-glycerol (18:0/18:2) [2]*	0.95	0.74
	linoleoyl-linolenoyl-glycerol (18:2/18:3) [2]*	0.62	1.18

SubPathway	Biochemical Name	KO/WT	KO/WT HF
Docosanoid	14-HDoHE/17-HDoHE	1.36	0.62
Eicosanoid	prostaglandin F2alpha	1.30	0.36
	6-keto prostaglandin F1alpha	CTRL 1.24	0.62
	12-HEPE	1.13	0.61
	12-HETE	1.43	0.72
	15-HETE	1.09	0.60
	12-HHTrE	1.30	0.48

B

Sub-pathway	Biochemical Name	KO/WT CTRL	KO/WT HF
Glycerolipid Metabolism	glycerol	1.06	1.19
	glycerol 3-phosphate	1.46	0.95
	glycerophosphoglycerol	0.8	1.24
Monoacylglycerol	1-palmitoleoylglycerol (16:1)*	0.36	0.7
	1-oleoylglycerol (18:1)	0.41	0.64
	1-linoleoylglycerol (18:2)	0.43	0.67
	1-linolenoylglycerol (18:3)	0.4	0.68
	1-dihomo-linolenylglycerol (20:3)	0.44	0.44
	1-arachidonylglycerol (20:4)	0.63	0.68
	1-docosahexaenoylglycerol (22:6)	0.61	0.51
	2-palmitoleoylglycerol (16:1)*	0.31	1
	2-oleoylglycerol (18:1)	0.37	0.75
	2-linoleoylglycerol (18:2)	0.41	0.73
	2-arachidonoylglycerol (20:4)	0.42	0.62
	2-docosahexaenoylglycerol (22:6)*	0.6	0.41
Diacylglycerol	diacylglycerol (16:1/18:2 [2], 16:0/18:3 [1])*	0.48	1
	oleoyl-linoleoyl-glycerol (18:1/18:2) [1]	0.65	0.56
	oleoyl-linoleoyl-glycerol (18:1/18:2) [2]	0.63	0.53
	oleoyl-arachidonoyl-glycerol (18:1/20:4) [1]*	0.82	0.48
	oleoyl-arachidonoyl-glycerol (18:1/20:4) [2]*	0.89	0.48
	linoleoyl-arachidonoyl-glycerol (18:2/20:4) [1]*	1.01	0.77
	linoleoyl-arachidonoyl-glycerol (18:2/20:4) [2]*	0.81	0.79
	linoleoyl-docosahexaenoyl-glycerol (18:2/22:6) [2]*	0.77	0.43

Sub-pathway	Biochemical Name	KO/WT CTRL	KO/WT HF
Docosanoid	14-HDoHE/17-HDoHE	1.04	1.07
Eicosanoid	12-HEPE	0.73	1.09
	12-HETE	1.32	1.24
	12-HHTrE	2.78	1.58

Figure S4.9 Differential effects of CerS6 KO on the glycerolipids in liver (A) and plasma (B).

114

A

SubPathway	Biochemical Name	KO/WT CTRL	KO/WT HF
Glycolysis, Gluconeogenesis, and Pyruvate Metabolism	glucose	0.86	1.47
	fructose-6-phosphate	0.65	1.03
	2,3-diphosphoglycerate	1.11	0.58
	dihydroxyacetone phosphate (DHAP)	0.44	1.04
	2-phosphoglycerate	1.42	0.63
	pyruvate	0.77	1.18
	lactate	0.96	1.31
Penthose Phosphate Pathway	ribose 1-phosphate	0.57	0.99
	erythrose 4-phosphate	0.36	1.05
Penthose metabolism	ribose	1.06	1.85
	ribitol	0.80	1.28
	ribulose/xylulose	0.84	1.52
	arabitol/xylitol	0.94	1.26
	arabonate/xylonate	0.77	1.06
	sedoheptulose	0.92	1.74
	ribulonate/xylulonate/lyxonate*	0.74	1.28
Glycogen Metabolism	maltohexaose	1.14	2.14
	maltopentaose	0.93	1.37
	maltotetraose	0.71	1.91
	maltotriose	0.85	2.23
	maltose	1.11	2.31
Fructose, Mannose, Galactose Metabolism	fructose	0.88	2.10
	mannitol/sorbitol	0.65	1.91
	mannose	0.87	1.49
	galactonate	1.04	0.44

B

Sub-pathway	Biochemical Name	KO/WT CTRL	KO/WT HF
Glycolysis, Gluconeogenesis, and Pyruva	1,5-anhydroglucitol (1,5-AG)	0.86	0.85
	glucose	0.84	1.26
	fructose 1,6-diphosphate/glucose 1,6-diphosphate/myo-i	2.75	1.91
	2,3-diphosphoglycerate	3.05	5.35
	3-phosphoglycerate	1.57	1.6
	pyruvate	1.01	1.41
	lactate	1.09	1.27
	glycerate	1.19	1.03
Pentose Phosphate Pathway	ribose 1-phosphate	3.42	0.68
Pentose Metabolism	ribose	2.5	0.79
	ribitol	1.28	1.13
	ribulonate/xylulonate/lyxonate*	0.92	1.33
Disaccharides and Oligosaccharides	sucrose	1.71	0.78
Fructose, Mannose and Galactose Metab	mannitol/sorbitol	0.67	1.56
	mannose	0.73	0.97
	galactonate	1.4	0.51

C

SubPathway	Biochemical Name	KO/WT CTRL	KO/WT HF
TCA Cycle	citrate	1.06	0.39
	aconitate [cis or trans]	1.33	0.34
	isocitrate	0.90	0.52
	tricarballylate	1.35	0.81

Sub-pathway	Biochemical Name	KO/WT CTRL	KO/WT HF
	citrate	0.91	1.38
	aconitate [cis or trans]	1.03	1.33
	isocitrate	1.4	1.83
	alpha-ketoglutarate	1.35	2.16
TCA Cycle	succinate	1.33	1.14
	fumarate	1.62	2.45
	malate	1.45	2.03

Figure S4.10 Mice show differential response of carbohydrate metabolites in liver (A, C) and plasma (B, D).

Sub Pathway	Biochemical Name	KO/WT CTRL	KO/WT HF
	glycine	1.04	1.19
	dimethylglycine	1.18	0.65
Glycine, Serine, Threonine Metabolism	betaine	1.60	0.87
	serine	1.08	1.30
	threonine	1.05	1.27
Alanine and Aspartate Metabolism	alanine	1.00	1.32
	asparagine	1.11	1.27
	glutamate	0.96	1.25
	glutamine	0.83	0.69
Glutamate Metabolism	N-acetylglutamine	0.65	0.71
	4-hydroxyglutamate	1.16	0.49
	N-acetyl-aspartyl-glutamate (NAAG)	0.94	1.16
	S-1-pyrroline-5-carboxylate	1.06	1.42
	histidine	0.98	1.34
	N-acetylhistidine	0.84	0.95
	N-acetyl-1-methylhistidine*	0.65	0.80
Histidine Metabolism	formiminoglutamate	1.55	2.30
	imidazole lactate	0.77	0.96
	anserine	0.99	1.33
	1-methylhistamine	2.66	0.31
	1-methyl-4-imidazoleacetate	0.90	0.30
	1-ribosyl-imidazoleacetate*	0.61	0.63
	lysine	0.99	1.22
	N6-acetyllysine	1.07	1.25
	fructosyllysine	0.93	1.56
Lysine Metabolism	N2-acetyl,N6,N6-dimethyllysine	0.69	0.73
	2-aminoadipate	2.24	0.40
	glutarylcarnitine (C5-DC)	2.20	1.05
	5-aminovalerate	2.24	0.48
	N,N,N-trimethyl-5-aminovalerate	1.27	0.59
	phenylalanine	1.03	1.28
Phenylalanine Metabolism	1-carboxyethylphenylalanine	1.01	1.73
	phenyllactate (PLA)	0.82	1.42
	phenethylamine	1.32	0.50
	2-hydroxyphenylacetate	1.58	1.65
	tyrosine	1.03	1.36
	1-carboxyethyltyrosine	1.09	1.63
	phenol sulfate	1.48	1.66
Tyrosine Metabolism	phenol glucuronide	1.24	4.38
	4-methoxyphenol sulfate	2.06	1.38
	O-methyltyrosine	0.95	1.40
	4-hydroxycinnamate sulfate	4.60	0.45
	tryptophan	1.04	1.29
	kynurenine	1.74	1.89
Tryptophan Metabolism	kynurenate	2.15	1.21
	anthranilate	1.45	1.47
	xanthurenate	1.88	1.50
	tryptamine	0.38	0.59

SubPathway	Biochemical Name	KO/WT CTRL	KO/WT HF
	leucine	1.00	1.25
	1-carboxyethylleucine	0.91	1.69
	isovalerylglycine	1.42	1.37
	isovalerylcarnitine (C5)	2.04	0.72
	beta-hydroxyisovalerate	1.60	0.92
	beta-hydroxyisovaleroylcarnitine	1.52	1.02
Leucine, Isoleucine and Valine	isoleucine	1.03	1.21
Metabolism	1-carboxyethylisoleucine	1.09	1.66
	2-methylbutyrylcarnitine (C5)	4.64	0.62
	2-methylbutyrylglycine	1.52	0.81
	tiglylcarnitine (C5:1-DC)	3.63	0.97
	ethylmalonate	0.83	1.00
	methylsuccinate	0.90	0.19
	methylsuccinoylcarnitine	1.08	0.19
	valine	1.07	1.33
	1-carboxyethylvaline	1.02	1.66
	isobutyrylcarnitine (C4)	4.25	0.63
	methionine	1.10	1.23
	S-methylmethionine	1.66	1.44
	S-adenosylmethionine (SAM)	0.55	0.71
	S-adenosylhomocysteine (SAH)	0.88	1.06
Methionine, Cysteine and Taurine	homocysteine	1.31	1.78
Metabolism	N-acetylcysteine	1.00	1.18
	S-methylcysteine	1.01	0.70
	cystine	2.37	1.62
	hypotaurine	1.36	1.34
	taurine	0.91	0.96
	succinoyltaurine	0.73	0.68
	taurocyamine	1.02	0.41
	argininosuccinate	1.01	1.71
	urea	1.16	1.27
	ornithine	1.13	1.35
Urea Cycle; Arginine and Proline	3-amino-2-piperidone	1.08	1.43
Metabolism	2-oxoarginine*	0.95	1.45
	citrulline	1.16	1.42
	homocitrulline	0.66	0.58
	proline	1.03	1.27
	N2,N5-diacetylornithine	0.81	2.00
	N-acetylhomocitrulline	0.58	0.41
Creatine Metabolism	creatine	1.34	1.06
	putrescine	1.20	0.65
Polyamine Metabolism	N-acetyl-isoputreanine	0.79	0.42
	(N(1) + N(8))-acetylspermidine	1.11	0.61
	5-methylthioadenosine (MTA)	0.71	0.80
	glutathione, reduced (GSH)	0.64	0.64
Glutathione Metabolism	glutathione, oxidized (GSSG)	0.96	1.17
	cysteine-glutathione disulfide	1.50	1.56
	S-lactoylglutathione	0.52	0.91
	4-hydroxy-nonenal-glutathione	0.68	0.41

Figure S4.11 CerS6 KO livers had significant diet-dependent changes in amino acid metabolism.

Sub-pathway	Biochemical Name	KO/WT CTRL	KO/WT HF
Glycine, Serine and Threonine Metabolism	glycine	1.2	1.22
	sarcosine	1.32	0.76
	dimethylglycine	1.38	0.52
	betaine	1.56	1.01
Histidine Metabolism	1-methylhistidine	0.73	0.85
	N-acetylhistidine	1.05	0.75
	N-acetyl-1-methylhistidine*	0.96	0.7
	trans-urocanate	1.93	1.28
	histamine	0.58	0.76
	1-methylhistamine	1.86	0.7
	1-methyl-4-imidazoleacetate	1.1	0.27
	1-methyl-5-imidazoleacetate	1.09	0.49
	1-ribosyl-imidazoleacetate*	0.74	0.6
Phenylalanine Metabolism	phenylalanine	1.15	1.04
	N-acetylphenylalanine	1.28	1.03
	1-carboxyethylphenylalanine	1.12	1.43
	phenylpyruvate	1.15	1.44
	phenyllactate (PLA)	0.78	1.4
	phenylacetate	1.66	1.51
	4-hydroxyphenylacetate	0.93	2.27
Tyrosine metabolism	tyrosine	1.39	1.45
	N-acetyltyrosine	2	2.1
	1-carboxyethyltyrosine	1.17	1.64
	4-hydroxyphenylpyruvate	1.25	1.47
	3-(4-hydroxyphenyl)lactate	1.32	1.14
	phenol sulfate	1.21	1.69
	phenol glucuronide	1.92	2.95
	N-formylphenylalanine	1.21	1.46
	4-hydroxycinnamate sulfate	4.51	0.96
	4-hydroxyphenylacetate sulfate	1.23	1.88
	thyroxine	0.97	1.4
Tryptophan metabolism	tryptophan	1.01	1.23
	kynurenate	1.8	1.36
	serotonin	2.49	1.7
	indoleacrylate	2.71	0.76
	indolepropionate	3.68	0.99
	indoleacetylglycine	1.56	0.86

Sub-pathway	Biochemical Name	KO/WT CTRL	KO/WT HF
	alpha-hydroxyisocaproate	1.1	1.38
	isovalerate (i5:0)	2.99	1.11
	3-methylcrotonylglycine	1.66	1.17
	beta-hydroxyisovalerate	2.04	0.96
Leucine, Isoleucine and Valine	1-carboxyethylisoleucine	1.11	1.62
Metabolism	2-methylbutyrylglycine	1.58	1.34
	tigloylglycine	1.73	1.65
	3-hydroxy-2-ethylpropionate	0.67	0.81
	1-carboxyethylvaline	1.03	1.42
	isobutyrylcarnitine (C4)	1.41	1.06
	isobutyrylglycine	1.15	1.32
	2,3-dihydroxy-2-methylbutyrate	0.89	0.53
	methionine	1.04	1.24
	N-formylmethionine	1.62	1.09
Methionine, Cysteine, SAM and	S-methylmethionine	3.35	0.74
Taurine Metabolism	methionine sulfone	1.62	0.57
	alpha-ketobutyrate	0.32	0.55
	cysteine	0.89	1.46
	S-methylcysteine	0.91	0.58
	S-methylcysteine sulfoxide	1.04	0.45
	hypotaurine	2.3	1.8
	homocitrulline	1.52	0.2
	dimethylarginine (SDMA + ADMA)	1.08	0.71
	N-delta-acetylornithine	1.42	0.94
Urea cycle; Arginine and Proline	N2,N5-diacetylornithine	1.66	1.08
Metabolism	pro-hydroxy-pro	1.31	0.96
	N-methylproline	0.96	1.38
	N-monomethylarginine	0.92	0.55
	N-acetylhomocitrulline	1.02	0.23
	N-acetylputrescine	1.27	0.73
Polyamine Metabolism	N-acetyl-isoputreanine	1.63	0.53
	spermidine	1.77	1.17
	(N(1) + N(8))-acetylspermidine	1.12	0.48
	5-methylthioadenosine (MTA)	1.29	0.99
	4-acetamidobutanoate	1.15	0.73
Guanidino and Acetamido Metab	4-guanidinobutanoate	1.63	2.09
	glutathione, oxidized (GSSG)	1.99	1.38
Glutathione Metabolism	cysteinylglycine disulfide*	0.68	0.5
	5-oxoproline	1.35	1.1
	2-aminobutyrate	0.75	0.66
	2-hydroxybutyrate/2-hydroxyisobutyrate	0.72	0.55
	ophthalmate	1.83	0.76

Figure S4.12 CerS6 KO plasma had significant diet-dependent changes in amino acid metabolism.

A

SubPathway	Biochemical Name	KO/WT LF	KO/WT HF
Primary Bile Acid Metabolism	cholate	3.13	1.82
	glycocholate	33.69	3.38
	taurocholate	4.31	1.53
	chenodeoxycholate	2.23	1.41
	chenodeoxycholic acid sulfate (1)	3.63	2.03
	taurochenodeoxycholate	7.86	1.45
	beta-muricholate	2.27	1.05
	alpha-muricholate	3.21	1.38
	tauro-beta-muricholate	59.88	0.93
	glyco-beta-muricholate**	69.21	0.67
	cholate sulfate	18.45	1.57
Secondary Bile Acid Metabolism	deoxycholate	2.23	2.64
	taurodeoxycholate	4.14	2.31
	taurodeoxycholic acid (12 or 24)-sulfate*	4.11	0.79
	6-beta-hydroxylithocholate	3.79	2.87
	12-ketolithocholate	3.99	1.77
	taurolithocholate	10.37	2.43
	ursodeoxycholate	2.23	1.32
	tauroursodeoxycholate	34.83	1.14
	6-oxolithocholate	3.21	4.39
	hyocholate	4.07	1.02
	hyodeoxycholate	2.68	3.48
	taurohyodeoxycholic acid	86.12	0.84
	3-dehydrocholate	3.44	1.87
	taurochenodeoxycholic acid (7 or 24)-sulfate	4.12	1.00

B

Sub-pathway	Biochemical Name	KO/WT LF	KO/WT HF
Primary Bile Acid Metabolism	cholate	83.68	21.91
	glycocholate	4.4	1.51
	taurocholate	13.27	6.72
	taurochenodeoxycholate	8.39	10.43
	beta-muricholate	19.92	4.47
	alpha-muricholate	123.59	23.55
	tauro-beta-muricholate	64.31	13.39
Secondary Bile Acid Metabolism	glyco-beta-muricholate**	7.22	1
	deoxycholate	3.3	4.37
	taurodeoxycholate	2.36	7.55
	ursodeoxycholate	14.71	3.73
	tauroursodeoxycholate	6.54	6.11
	6-oxolithocholate	6.95	7.83
	taurohyodeoxycholic acid	2.36	5.9
	7-ketodeoxycholate	51.71	6.65

Figure S4.13 CerS6 KO mice had significant genotype- and diet-dependent alterations in bile acid metabolism in liver (A) and plasma (B).

CHAPTER 5: FOLIC ACID SUPPLEMENTATION SHAPES PLASMA SPHINGOLIPID PROFILES OF MICE FED HIGH FAT DIET

Introduction

Ceramides are a class of bioactive lipids within the sphingolipid family. Ceramides can be synthesized *de novo* in the ER beginning with the condensation of palmitoyl-CoA and serine [95] and ending with the attachment of an acyl chain via Ceramide Synthase (CerS) enzymes. There are six isoforms of the CerS, each possessing a unique affinity for specific acyl chains used to synthesize ceramides [99]. CerS6 is expressed in low levels in most tissues and produces $C_{14:0}$- and $C_{16:0}$-ceramides [99]. Ceramides are considered a hub of sphingolipid metabolism because they can be further converted to other sphingolipid species including sphingomyelins and hexosyl-ceramides by the attachment of a phosphocholine or sugar headgroup, respectively [1]. While serving structural roles in the cell membranes, along with sphingomyelins and glycosyl-ceramides, ceramides also respond to many extracellular and intracellular stimuli including UV radiation, ionizing radiation, endotoxins, cytokines, and chemotherapeutic agents [12, 92, 144-149]. Similarly, HexCer have been implicated in cellular signaling [314] and are thought to contribute to the development of IR [315, 316] and atherosclerosis [317]. As it relates to nutrient stress, sphingolipids have been studied for their role in response to folate stress, synthetic retinoids, vitamin E metabolites, and choline and magnesium withdrawal [7-10, 12].

Ceramides have been considered as potential biomarkers for several disease states. They have been individually assessed and linked to the outcomes and, based on select ceramide species levels, ceramide risk scores have been derived. A study investigating two large cohorts

122

found 11 distinct plasma ceramides and 1 plasma dihydroceramide that were predictive of major adverse cardiovascular events in patients with previous myocardial infarction [211]. Several groups have proposed to use a combined ceramide risk score for cardiovascular events based on the values of $C_{16:0}$-Cer, $C_{18:0}$-Cer, $C_{24:1}$-Cer and $C_{24:0}$-Cer [215-219]. However, these studies only showed associations to specified outcomes and provided little mechanistic understanding of how ceramides may contribute to development and progression of disease. While the link between diet and cardiovascular disease is well established, the understanding of how short- and long-term dietary patterns affect ceramide levels and how that contributes to disease progression is missing.

Our lab has previously established the role of ceramides in response to nutrient stress, specifically low folate conditions. Folate is a B-vitamin found in green leafy vegetables and fortified foods. Mandatory fortification with FA, the synthetic form of folate, began in the US in the 1990s to reduce the incidence of neural tube defects [39]. However in recent years, large epidemiological studies have found increased incidences of certain types of cancer after the introduction of mandatory fortification [45, 318] . Folate metabolism has also been connected to alterations in lipid metabolism, with conflicting results in both rodents and humans pointing to both beneficial effect and potentially negative effect on lipid metabolism when diets were supplemented with folic acid [48, 54, 55, 68, 69, 72, 319]. We have shown in cell culture that folate withdrawal from media or ectopic expression of folate-regulatory enzyme ALDH1L1 results in a significant increase of CerS6 expression and levels of C_{16}-Cer [12]. We also investigated this relationship in a mouse model to determine whether the folate stress similarly elevates $C_{16:0}$-Cer levels in mouse liver. While we did not find a significant increase in hepatic $C_{16:0}$-Cer levels in mice fed a folate deficient diet, many sphingolipid species were changed due

to lack of dietary folate (Ceramide Synthase 6 mediates sex-specific metabolic response to dietary folic acid supplementation, *Molecular Metabolism,* under revision).

In the present study, we sought to assess how the long-term exposure to low or high dietary FA influences plasma ceramide levels in mice consuming a high fat diet and to evaluate the role of CerS6 in response to dietary alterations. We <u>hypothesized</u> that low dietary FA will elevate ceramide levels in response to nutrient stress with specific increases in C_{16}-Cer, whereas high dietary FA will exert a beneficial effect on sphingolipid metabolism by decreasing the concentrations of lipotoxic ceramide species.

Materials and Methods

Animal husbandry

All experiments were approved by the Institutional Animal Care and Use committee (IACUC) at the North Carolina Research Campus (NCRC). CerS6 KO mice were a generous gift from Dr. Ogretmen and were further backcrossed for at least 11 generations to C57BL/6NHsd mice from Envigo (Indianapolis, IN). Male and female mice heterozygous for CerS6 were bred to obtain CerS6 KO and WT littermates that were randomized to dietary groups at weaning. This study was part of a larger studying using the CerS6 KO model and as such, western blot confirmation of CerS6 protein in WT mice only can be found in Figure S4.1. Animals were group-housed in microisolator cages under standard conditions (12h light/dark cycle, temperature- and humidity-controlled conditions), and received *ad libitum* access to water and one of three purified synthetic diets. The protein sources (casein and L-cystine) were consistent across diets, as were sources of carbohydrate (corn starch, sucrose, maltodextrin) and fat (soybean oil and lard). All diets had high levels of fat: 58% of caloric value was from fat. The diets differed only in their folic acid content: 0 ppm in folate deficient diet (FD); 2 ppm in control folate diet (Ctrl); and 12 ppm in folate over-supplemented diet (FS). Diet information is

provided in Table S5.1. Mice were placed on one of the diets at weaning and weighed each week for 16 weeks. All mice were fasted for 4 hours and body composition was assessed prior to euthanasia.

Body composition

Body composition (lean and fat mass) was assessed before animals were placed on diet and before necropsy using the EchoMRI-130 Body Composition Analyzer.

LC-MS/MS analysis of sphingolipids

Lipids from 75µL plasma were extracted [320] and the sphingolipid levels were measured by HPLC-MS/MS using methodology as previously described by the MUSC Lipidomics Shared Resource [252].

Statistical analysis

For statistical analysis of differences between two groups Student's t-test was performed using GraphPad software. For the statistical analysis of differences between three or more groups, one-way ANOVA was used with Sidak's multiple comparisons test to determine differences between specific groups. Results were determined to be statistically significantly different at $p < 0.05$.

Results

CerS6 KO mice accumulate less fat and gain less weight on high fat diet with additional effect of FA that differs between males and females

Since the goal of our study was investigation of the effects of both low and high levels of FA on a high fat background, we conducted weekly monitoring of animal weight and measured body composition before and at the end of dietary exposure. Male WT mice, after 16 weeks on any level of dietary folate, weighed significantly more than their CerS6 KO counterparts (Fig 5.1A). Additionally, the FD diet resulted in WT mice gaining significantly more weight than

those on Ctrl diet, but FS diet showed no significant difference from Ctrl in post-diet body weight (Fig 5.1A). However, when the changes in body weight were evaluated, both WT FD and WT FS mice gained significantly more weight than those on the Ctrl folate diet indicating a negative effect of both low and high folate levels in combination with high fat (Fig 5.1A). As hypothesized, all WT mice gained significantly more weight than the KO counterparts, in agreement with previous reports [205]. CerS6 KO mice also gained less weight on the FS diet reaching statistical significance only when compared to the FD diet. Measurements of fat mass showed significantly higher percent for WT mice on the FD and FS diets compared to corresponding groups of KO mice, but no significant difference was found between WT and KO mice on the Ctrl diet (Fig 5.1A).
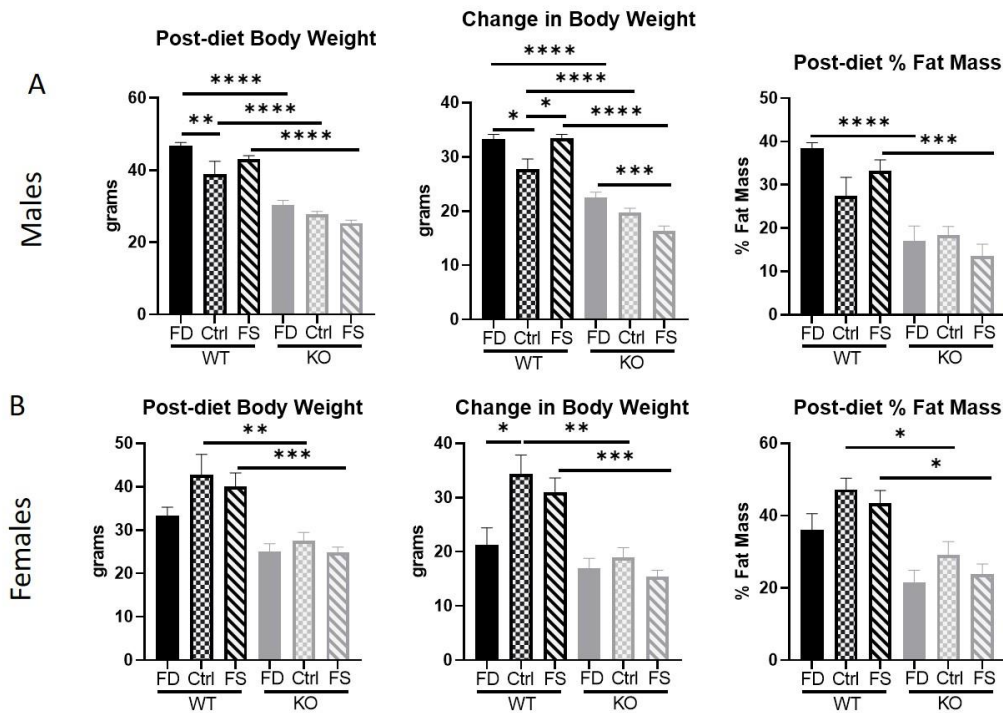

Figure 5.1 Low folic acid affected body weight in male WT mice (A) but did not affect female (B) or CerS6 KO mice. Data presented as mean $\pm$ SEM, n=3-6. Solid bars, FD diet; Checkered bars, Control diet. Striped bars, FS diet. WT shown in black and KO shown in grey. *, p<0.05; **, p<0.01; ***, p<0.001; ****, p<0.0001, determined by One-way ANOVA with Sidak's multiple comparisons test

Female mice exhibited a completely different pattern of weight gain and body composition response to dietary FA levels than males (Fig 5.1B). Wild-type females on the Ctrl and FS diet weighed more after 16 weeks on the diets compared to KO mice but this was not the case for the mice on the FD diet. Similarly, only WT mice on the Ctrl and FS diet had significantly more weight gain than their KO counterparts. Additionally, the WT Ctrl females gained significantly more weight than the WT FD mice, the opposite of what was seen in males. Similar to post-diet body weight, measures of post-diet % fat mass revealed a significant difference only between WT and KO on the Ctrl and FS diets indicating a potentially protective effect of the FD diet in females.

Plasma ceramides demonstrated sex differences in response to folate supplementation

Since plasma ceramides have been evaluated as possible biomarkers for disease states, we assessed plasma ceramides and other sphingolipids in order to determine how they respond to dietary intervention. In male WT mice, the FD diet elevated both C_{16}-dhCer and C_{16}-Cer, but not C_{14}-Cer, while CerS6 KO mice were protected from increases in these species (Fig 5.2A). There were several Cer species that demonstrated a U-shaped response to FA, with increased levels on both the FD and FS diets in WT mice (Fig 5.2B). Interestingly, the CerS6 KO mice on these diets were protected from significant increases indicating that CerS6 affects more than just C_{14}- and C_{16}-Cer in the plasma.
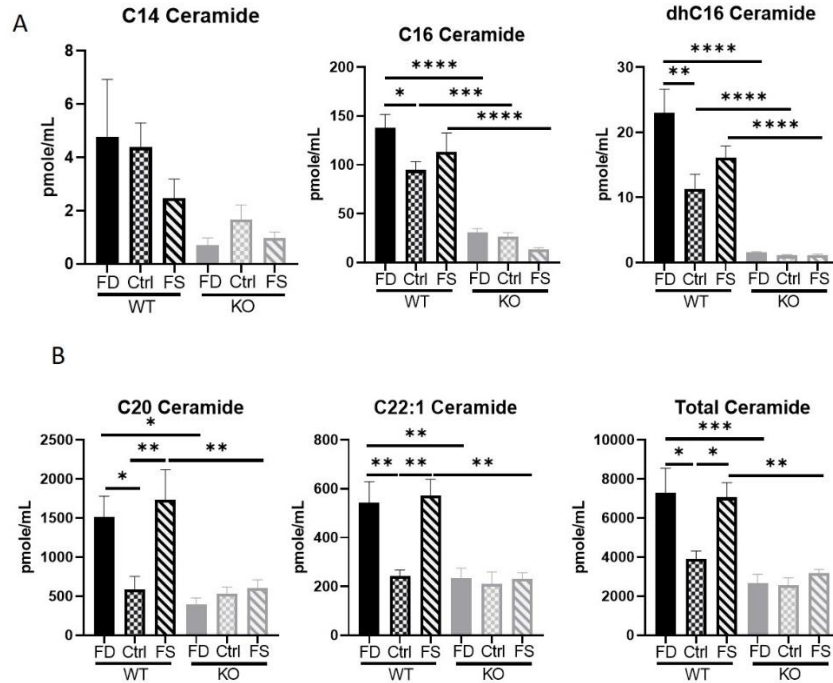
Figure 5.2 In WT males, both plasma CerS6-produced ceramides (A) and very-long-chain ceramides (B) demonstrate U-shaped response to FA. Data presented as mean $\pm$ SEM, n=3-5. Solid bars, FD diet; Checkered bars, Control diet. Striped bars, FS diet. WT shown in black and KO shown in grey. *, p<0.05; **, p<0.01; ***, p<0.001; ****, p<0.0001, determined by One-way ANOVA with Sidak's multiple comparisons test

Female mice had a different response to the FA content in their diet (Fig 5.3). C_{16}-Cer was elevated in animals on Ctrl and FS diets, but not on FD diet. There was no difference in C_{16}-dhCer concentrations in female WT mice, but the CerS6 KO mice were protected from C_{16}-Cer accumulation similar to male CerS6 KO mice. $C_{24:0}$- and total ceramides were also elevated in the WT Ctrl mice but overall, there were few changes in plasma ceramides due to dietary folic acid.
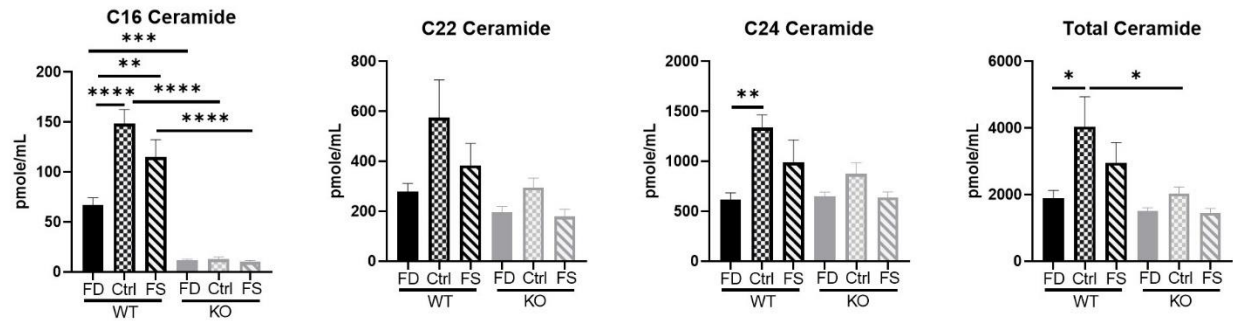
Figure 5.3 Female mice demonstrated bell-shaped response to FA and were more resistant to changes in ceramides. Data presented as mean $\pm$ SEM, n=3-5. Solid bars, FD diet; Checkered bars, Control diet. Striped bars, FS diet. WT shown in black and KO shown in grey. *, $p<0.05$; **, $p<0.01$; ***, $p<0.001$; ****, $p<0.0001$, determined by One-way ANOVA with Sidak's multiple comparisons test

Plasma sphingomyelins increase on folate-deficient diet in males but not in females

Ceramides are at the center of sphingolipid metabolism and serve as precursors for complex sphingolipids [1] with sphingomyelin being one of them. Sphingomyelins are formed from ceramides via the transfer of a phosphocholine head group from phosphatidylcholine. In male mice, sphingomyelin species produced from CerS6-specific ceramides were the most significantly changed species (Fig 5.4).
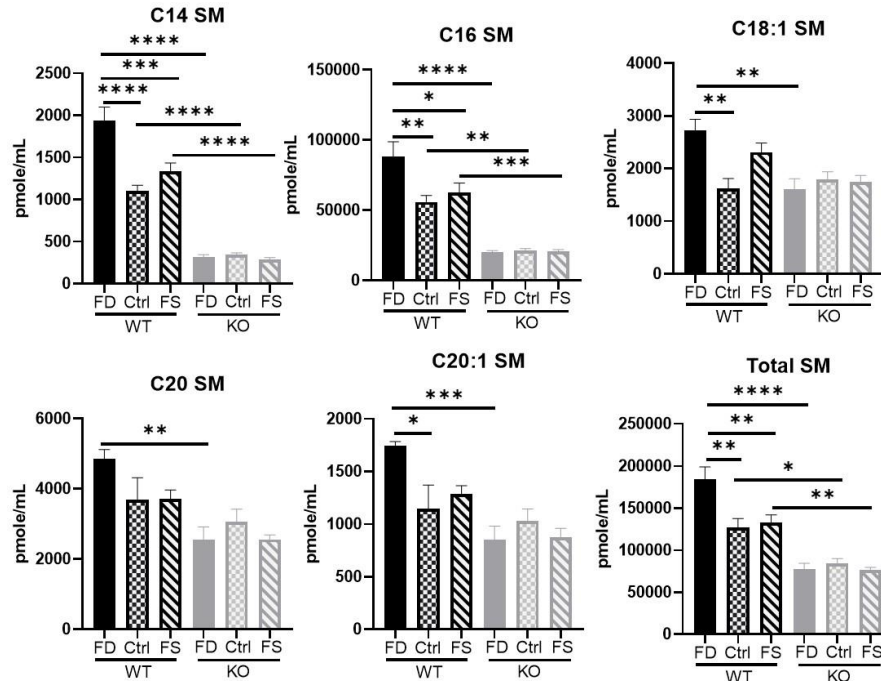
Figure 5.4 FD diet elevated SM species in WT male mice. Data presented as mean $\pm$ SEM, n=5. Solid bars, FD diet; Checkered bars, Control diet. Striped bars, FS diet. WT shown in black and KO shown in grey. *, $p<0.05$; **, $p<0.01$; ***, $p<0.001$; ****, $p<0.0001$, determined by One-way ANOVA with Sidak's multiple comparisons test

C$_{14}$-SM was elevated in WT FD compared to WT Ctrl and FS mice (75% and 45% respectively) and CerS6 KO mice had significantly lower levels of this SM (69-83%) on all diets. Similar response was seen for C$_{16}$-SM and total SM levels. On the FD diet, C$_{18:1}$-, C$_{20:0}$-, and C$_{20:1}$-SM were significantly higher in WT compared to the CerS6 KO FD mice. Overall, male CerS6 KO mice tended to have lower levels of most SM species but these differences were not statistically significant.

In female WT mice, C$_{14}$- and C$_{16}$- and total SM were significantly elevated on the Ctrl and FS diets compared to FD diet, but no FA effect was seen among the KO mice on any diets (Fig 5.5). However, other SM species, including C$_{22}$-, C$_{24}$- and C$_{26}$-SM, were higher in CerS6 KO compared to WT mice on the Ctrl and FS diets. On the contrary, male CerS6 KO mice did

not have any SM species that was higher in KO than in WT animals, further underscoring

differences between sexes in response to dietary folic acid.
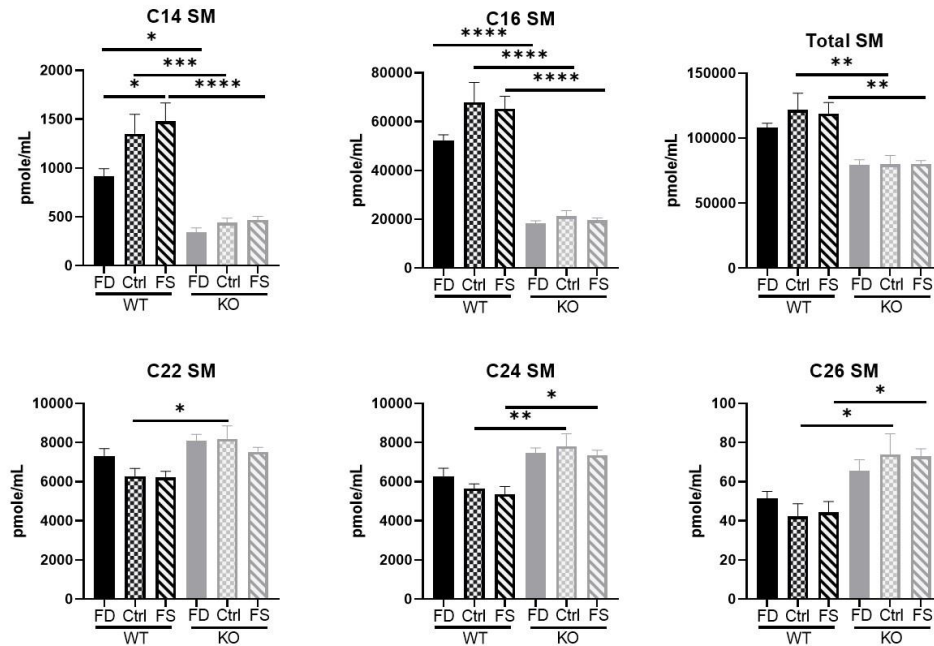
Figure 5.5 Female mice demonstrated fewer changes in SM species however some were increased due to absence of CerS6. Data presented as mean $\pm$ SEM, n=5. Solid bars, FD diet; Checkered bars, Control diet. Striped bars, FS diet. WT shown in black and KO shown in grey. *, p<0.05; **, p<0.01; ***, p<0.001; ****, p<0.0001, determined by One-way ANOVA with Sidak's multiple comparisons test

Hexosyl-Ceramides were elevated on both low and high FA diets in males only

Hexosyl-ceramides, including glucosyl- and galactosyl-ceramides, represent another

group of complex sphingolipids made via the addition of a glucose or galactose headgroup to

ceramide, respectively. As ceramides can be shunted to the synthesis of HexCer species, the

plasma HexCer levels may also be important determinants of sphingolipid balance in response to

nutrient stress. Similar to the aforementioned sphingolipids, C_{16}-HexCer was significantly lower

in CerS6 KO mice irrespective of dietary FA (Fig 5.6).
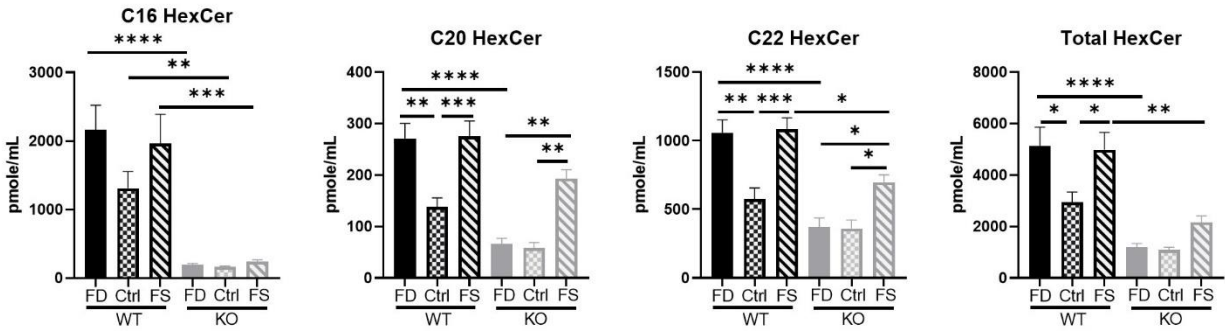
Figure 5.6 Plasma HexCer species increased in response to low and high folate in male WT mice. Data presented as mean $\pm$ SEM, n=5. Solid bars, FD diet; Checkered bars, Control diet. Striped bars, FS diet. WT shown in black and KO shown in grey. *, $p<0.05$; **, $p<0.01$; ***, $p<0.001$; ****, $p<0.0001$, determined by One-way ANOVA with Sidak's multiple comparisons test

The FD and FS diets in WT mice increased the levels of C_{16}-HexCer compared to Ctrl diet (however not reaching statistical significance), while increases for C_{20}-, C_{22}-, and Total HexCer were significant. Interestingly, CerS6 KO mice on the FS diet exhibited significantly increased plasma levels of C_{20}-, C_{22}- and total HexCer, whereas the KO mice on the other two diets did not.

Hexosyl-Ceramides in female WT mice reflected the levels of ceramides (Fig 5.7) with significantly higher levels on the Ctrl diet but no significant difference between FD and FS diets. Additionally, C_{16}-HexCer at all FA levels were higher in WT mice compared to KO mice. C_{22}- and Total HexCer levels were the highest in WT Ctrl mice. Moreover, C_{22}-HexCer were the highest in KO FS animals, similar to males but overall, there were fewer changes in HexCer species in females, in line with all previously discussed sphingolipids, thus demonstrating resistance to change in response to diet.
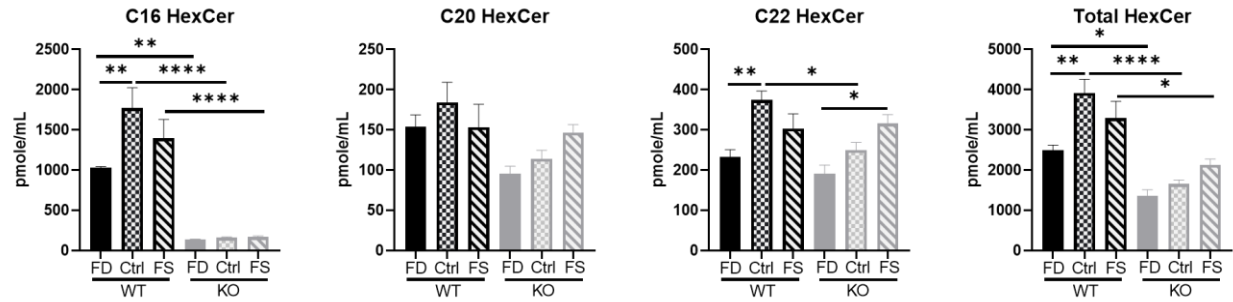
Figure 5.7 FD diet prevented accumulation of several HexCer species in female mice. Data presented as mean $\pm$ SEM, n=5. Solid bars, FD diet; Checkered bars, Control diet. Striped bars, FS diet. WT shown in black and KO shown in grey. *, $p<0.05$; **, $p<0.01$; ***, $p<0.001$; ****, $p<0.0001$, determined by One-way ANOVA with Sidak's multiple comparisons test

Discussion

In this study, we evaluated the sphingolipid response to both low and high FA on the background of high dietary fat consumption in WT and CerS6 KO mice. Overall, our results confirmed the central hypothesis that dietary folate stress will result in sphingolipid changes mediated by CerS6 and C_{16}-Cer. Several ceramide species, C_{20}- and $C_{22:1}$-Cer, were increased in plasma of male mice, along with C_{16}-Cer and C_{16}-dhCer, resulting in approximately 2.5-fold increase in Total Cer levels (Fig 5.2). Contrary to our expectations, mice on FS diet also had elevated C_{16}-Cer and C_{16}-dhCer which did not reach statistical significance as well as 2.5-3-fold increase in C_{20}- and $C_{22:1}$-Cer (Fig 5.2). This U-shape response of C_{16}-, as well as of C_{20}- and $C_{22:1}$-Cer was mediated by CerS6, because CerS6 KO mice did not show such response to dietary FA changes. Importantly, while C_{16}-Cer and C_{16}-dhCer levels were 4-10-fold lower in KO plasma compared to WT and did not change in response to dietary FA, the C_{20}- and $C_{22:1}$-Cer did not differ significantly between WT control and KO plasma on any diet. This response pattern indicates that FA itself did not affect CerS4-generated ceramides in the absence of CerS6 but the FA-induced increase in CerS4 products was due to CerS6. Heterodimerization of CerS6 with CerS2 and CerS5 with alteration of their activities has been demonstrated [133], but effects on

133

CerS4 are not known. Since acyl chain specificities of CerS4 and CerS2 overlap with regard to C_{22}-acyl-CoA, it is possible that $C_{22:1}$-Cer increase could be driven by CerS6 heterodimerization with CerS2 [44]. Any upregulation of ceramides in males was abrogated by CerS6 KO, underscoring the role of CerS6 as a mediator of dietary response.

Remarkably, response to alterations of dietary FA in females was completely different than in males. Both FD and FS diets reduced C_{16}-, C_{22}-, C_{24}- and total Cer levels in WT mice (bell shape, Fig 5.3). Moreover, along with about 6-10-fold lower levels of C_{16}-Cer in CerS6 KO plasma compared to WT, the C_{22}-, C_{24}- and Total Cer were at about the same levels in WT and KO mice on the FD diet, but 2-3 times higher in WT compared to KO samples on control and FS diets. Thus, the response of C_{16}-Cer to FD and FS diets was mediated by CerS6, however for the other species, relationship is not clear. Another important difference between two sexes was 3.5 and ~ 2-fold difference in total Cer levels between sexes on FD and FS diets respectively, with relatively similar levels on Ctrl diet. Altogether, our data indicate that female mice respond differently to FA intake on HF diet than male mice and that CerS6 may have a less significant role in controlling plasma sphingolipid profiles of female mice, thus making them less sensitive to dietary alterations. A protective effect from obesity and metabolic syndrome has been reported in several studies investigating female mice or male mice given estrogen and their response to dietary interventions including dietary restriction [321], high-fat diet [322, 323], and protein dilution [324].

Plasma sphingomyelin levels also responded to change in folate supplementation and the response to FA was also different in males and females (Fig 5.4, Fig 5.5). In WT male mice, response of SM species to FA was reminiscent of the ceramide response. Lack of response to folate and 4-6-times lower levels of C_{14}- and C_{16}-sphingomyelins in CerS6 KO mice are

consistent with our hypothesis that CerS6 mediates adaptation to dietary folate in whole animal. C_{18}- and C_{20}-SM which demonstrated an increase in response to low dietary FA in WT mice did not show significant differences between WT mice on Ctrl diet or in KO mice on any diet. This indicates that changes observed in response to low FA in WT animals are caused by response of CerS6. In female mice, plasma SM were not changed by folate supplementation, with exception of C_{14}-SM, which was lower on FD diet and increased with increase in FA (Fig 5.5). Significantly lower plasma levels of C_{14}- and C_{16}-SM (3-4-fold) in KO mice compared to WT point to CerS6-produced ceramides as the main contributors to the plasma sphingomyelin pools. Interestingly, levels of C_{22}-, C_{24}- and C_{26}-SM were higher in KO versus WT females and did not show response to dietary FA for either genotype. These data indicate that female plasma sphingomyelins are less responsive to dietary effects.

Hexosyl-Ceramides, representing combined pools of glucosyl- and galactosyl-ceramides, were changed with alterations in dietary FA and these changes followed the changing patterns of corresponding ceramides in male and female WT mice. Male WT mice demonstrated a U-shaped response to increasing levels of FA. Interestingly, KO male mice also showed response to dietary FA, but only to high folate supplementation. At the same time, female WT mice showed bell-shaped response to dietary FA, while in KO mice HexCer levels showed direct correlation with dietary FA such that as FA levels increased, so did the concentration of several HexCer species. While the mechanisms for significant increase of HexCer at high folate levels are not known, it is possible that the excess FA combined with HFD is causing alterations in glucose metabolism. Previous work from our lab exploring the effects of low and high FA diets in mice found altered carbohydrate metabolism as well as significantly increased levels of UDP-glucose (a substrate for glucosyl-ceramide biosynthesis) in CerS6 KO mice (data not published). Folic acid

supplementation has also been found to yield beneficial effects on blood glucose levels and insulin resistance in rat [325] and mouse studies [326]. DNA methylation and transcriptional regulation of genes involved in insulin signaling have been proposed as putative mechanisms linking folic acid and glucose metabolism [53]. It is also possible that HexCer species are less toxic compared to ceramides and conversion of ceramides to HexCer species protects tissues from deleterious effects of ceramide.

Our experiments also showed that male KO mice weighed significantly less than their WT controls, regardless of FA intake. Additionally, consumption of a diet that was lacking folate (FD) or too high in folate (FS) led to additional weight gain over the duration of the study. Interestingly, the low folate diet also led to increased weight gain in CerS6 KO mice which was not expected. Previous studies have demonstrated that CerS5 or CerS6 knockout in mice, or pharmacological inhibition of $C_{16:0}$-Cer, conferred protection from weight gain when fed a HF diet [4, 173, 205], which we expected to be more important in determining body weight FA content. Additionally, a previous study investigating dietary folic acid on a lower fat diet did not show any differences due to low folic acid in liver tissue of CerS6 KO mice (Ceramide Synthase 6 mediates sex-specific metabolic response to dietary folic acid supplementation, *Molecular Metabolism,* under revision). The combination of high fat content and low FA likely worked synergistically in regulation of body weight leading to increased weight gain even in CerS6 KO mice. Results presented herein show that low folate causes increase in weight gain in both WT and CerS6 KO male mice while high FA consumption increases body weight in WT mice only. It is likely that the FD and FS diets affect additional metabolic pathways supporting increased weight gain, including through AMPK, NADPH oxidase and acyl carnitine levels [54, 55, 72, 76], however absence of these effects in CerS6 KO mice indicates that ceramides may also be

involved in responding to high folic acid consumption. The effect of folic acid combined with high fat diet consumption was quite different in female mice. The low (FD) folate diet prevented weight gain in female WT mice, while over-supplementation (FS) did not affect weight gain. No effect of folic acid on body weight was found in CerS6 KO mice indicating that in females CerS6 plays a critical role in fat metabolism and storage and this regulation is highly sex-dependent.

Conclusion

Folate has been linked to lipid metabolism, but the results have been conflicting in rodent models. In human studies, obese patients are reported to have low folate levels in circulation [58-60], independent of dietary intake [61] and studies have found an inverse association between serum folate levels and BMI [62]. Low maternal folate levels were also associated with an increased risk of obesity and IR and type 2 diabetes in the offspring later in life [63, 64]. In human studies, FA supplementation has been found to decrease insulin resistance and plasma levels of homocysteine while improving blood glucose control in obese patients with type 2 diabetes [65-67]. Thus, decreased folate levels may affect susceptibility to metabolic syndrome [68, 69]. Though the mechanisms of these effects are not established, our data implicate sphingolipids as potential mediators of folate status effects on lipid metabolism and body composition. These findings also underscore the need to better understand both short and long-term dietary factors that alter sphingolipid levels, especially as they are being increasingly considered as biomarkers and components of risk scores for diseases [211, 215, 216, 218, 219, 327]. More importantly, dietary effects should be investigated in each sex separately and reference values for plasma ceramides should be determined for each sex in order to properly

evaluate the validity of plasma sphingolipids as biomarkers. Ceramides have been found to be modified by gastric bypass surgery [220], aerobic exercise [221] and statin use [217, 222] but there is a need to establish how sensitive the sphingolipid pools are to diet composition.

Supplementary Materials

Diet Number (Teklad)	TD.180092	TD.180093	TD.180094
Diet Name	FD	Ctrl	FS
Ingredient (g/kg)			
Caseine, Vitamin-Free	195.0	195.0	195.0
L-Cystine	3.0	3.0	3.0
Corn Starch	34.237	34.237	34.237
Sucrose	210.0	200.251	200.241
Maltodextrin	130.0	130.0	130.0
Soybean Oil	60.0	60.0	60.0
Lard	280.0	280.0	280.0
Cellulose	50.0	50.0	50.0
Mineral Mix (AIN-93G-MX (94046))	35.0	35.0	35.0
TBHQ, antioxidant	0.012	0.012	0.012
Vitamin Mix (AIN-93-VX (94047))		10.0	10.0
Niacin	0.03		
Calcium Pantothenate	0.016		
Pyridoxine HCl	0.007		
Thiamin (81%)	0.006		
Riboflavin	0.006		
Biotin	0.0002		
Vitamin B12 in mannitol (0.1% trituration)	0.025		
Vitamin E (DL-alpha tocopheryl acetate (500 IU/g)	0.15		
Vitamin A, palmitate (500,000 IU/g)	0.008		
Vitamin D3, cholecalciferol (500,000 IU/g)	0.002		
Vitamin K1, phylloquinone	0.0008		
Folic Acid			0.01
Choline Bitartrate	2.5	2.5	2.5
% kcal from protein	**13.6**	**13.6**	**13.6**
% kcal from carbohydrate	**28.3**	**28.3**	**28.3**
% kcal from fat	**58.2**	**58.2**	**58.2**
kcal/g	**5.3**	**5.3**	**5.3**

Table S5.1 Diet composition

CHAPTER 6: SYNTHESIS

The focus of this dissertation was to evaluate the changes in sphingolipid pools as a result of changes in dietary fat and folic acid consumption. Upon short-term dietary consumption of low FA, many changes were observed in sphingolipids and several other lipid classes. Interestingly, the levels of FA in diet significantly impacted the concentrations of other vitamins, including fat-soluble vitamins in both WT and CerS6 KO mice in a sex-dependent manner (Ch. III). Many phenotypic and biochemical changes we observed differed according to sex, but there were significant differences due to changes in dietary FA concentrations, even under short-term FA exposure on a relatively low-fat diet. We next challenged WT and CerS6 KO mice by feeding them a high fat diet for 16 weeks to assess long-term effects of dietary intervention (Ch. IV). CerS6 KO mice were protected from diet-induced weight gain, hepatic lipid droplet accumulation, and from elevation of many plasma sphingolipid species, not just those with C_{14} and C_{16} backbones. This indicates a strong contribution of CerS6 to the sphingolipid profiles of plasma, as opposed to CerS5, which also produces C_{14} and C_{16} sphingolipids. Finally, the mice were challenged by a combination of HFD and low or high FA intake to assess how FA may alter sphingolipid levels in the presence of a high fat diet (Ch. V). Both male and female CerS6 KO mice were protected from weight gain and accumulation of some sphingolipid species as seen in the previous study. However, male and female WT mice differed in their response to FA with females demonstrating decreased weight gain when fed the FD diet whereas males were similarly sensitive to low or high FA with both significantly elevating plasma sphingolipid levels and some measures of body composition. Taken together, the work in this dissertation provides

strong evidence that hepatic and plasma sphingolipid pools are sensitive to both short- and long-term dietary intake of folic acid and fat and that this response differs depending on sex.

Contributions to Sphingolipid Field

This dissertation contributes to the growing field of sphingolipid metabolism in several areas. First, we have established that sphingolipids are involved in nutrient sensing and response in a whole-animal model. Much of the work investigating specific sphingolipid response to nutrient presence or withdrawal have been performed using *in vitro* methods. While this can provide detailed, mechanistic data, the results are difficult to translate to humans. In the present studies, we demonstrated that sphingolipids, specifically ceramides, sphingomyelins, and glucosyl-/galactosyl-ceramides respond to changes in both dietary folic acid and fat content. Additionally, the studies were both short term (4 week) and longer-term (16 week) interventions, indicating that sphingolipids respond early (in less than four weeks) and these metabolic changes persist over the course of dietary exposure. We also demonstrated that FA affects sphingolipid metabolism when combined with HFD. Both low and high dietary folic acid raised several plasma sphingolipid species, which has been associated with increased risk of diseases, thus underscoring the importance of detailed evaluation of the effects of FA over-supplementation. Given that this work implicates sphingolipids as a possible connecting pathway between folate and lipid metabolism, future studies can include sphingolipid measurements to better assess how folate affects lipid metabolism.

Second, we have provided compelling data, including lipidomics, gene expression, and metabolomics, to demonstrate that male and female mice differ significantly in their response to dietary fat and FA. The differences in sphingolipid response to dietary intervention between sexes highlights the need to establish reference values for sphingolipids, specifically ceramides, if they are going to be utilized as biomarkers for disease states. An additional unexpected finding

141

was that the concentrations of other vitamins were altered in response to dietary intervention with FA and that this response differed between males and females. This finding was not anticipated, and our experiments were not designed to fully address or elucidate the possible mechanisms by which FA is affecting other vitamins, but they do provide clear data that warrant future studies investigating metabolic relationships between different vitamins.

Finally, we have contributed knowledge regarding the function of one of the isoforms of Ceramide Synthases, specifically CerS6. There are only a handful of studies that have utilized a knockout mouse model to understand the function of CerS6 in specific contexts. Here we have characterized the CerS6 KO mouse in its response to dietary changes by evaluating indirect calorimetry, gene expression, liver and plasma metabolome, and specific sphingolipid profiles. These data provide more insight into the role of CerS6 and its products in responding to dietary intervention and how those changes define sphingolipid balance. Our data will be used to inform future studies investigating the role of CerS6, as well as sphingolipids in general, in nutrient response, regulation of metabolism in different tissues, and how the balance of sphingolipids in liver and plasma affects physiological functions.

Strengths and Limitations

Our studies possess several strengths in their design, enabling the potential to draw relevant conclusions. First, the use of a genetic mouse model allows for characterization of CerS6 without the side effects that accompany drug treatment, which was previously the best way of suppressing CerS activity. Knocking out CerS6 in the entire body also gives a better picture of ceramide metabolism at a broad level as ceramide pools from other tissues cannot compensate for the lack of C_{14}- and C_{16}-ceramides. Additionally, the use of dietary intervention studies for both short and long durations provide valuable insight into changes that occur due to long-term consumption of low or high FA and also informs on the acute effects and

compensatory changes in a short-term nutrient stress. The use of different diets to capture a range of macronutrient and micronutrient intake allowed for a better understanding of the role of CerS6 in responding to both dietary fat and FA intake, especially considering that human consumption of both fat and FA varies greatly. The metabolic profiling we undertook is also a strength of this study. Calorimetry data was not included in several studies investigating the relationship between ceramides and metabolic measures [4, 173, 232]. However we were able to measure energy expenditure, respiratory exchange ratio and food intake to gain a better understanding of whole body mouse metabolism in our knockout model, which is a step further than the previous study which also investigated CerS6 KO mice on a high fat diet [205]. Additionally, the metabolomics analysis for both liver and plasma tissues provides a much more complete picture of metabolism by focusing on the primary metabolizing organ, the liver, and the circulating plasma which delivers nutrients to all other tissues in the body. Further precise characterization of this mouse model was achieved through targeted measurement of three sphingolipid pools - ceramides, sphingomyelins, and hexosyl-ceramides - which provides more specific and informative data about changes in sphingolipids due to nutrient stress as opposed to just assessing ceramide profile alone.

However, these studies do have some limitations. Mouse models do not perfectly translate to human conditions or metabolism. The whole-body CerS6 KO mouse model allowed us to examine the effects of total ablation of CerS6 and consequently significantly lower C_{16}-Cer levels, however the use of tissue-specific knockout would have been useful in assessing changes due to nutrient stress in each tissue. This would have enabled us to draw more specific conclusions about the utilization of folate and consequences of alterations in dietary folate as it relates to sphingolipid metabolism in specific tissues. An additional limitation of these studies

143

was the missing lactosyl-ceramide measurements. While we did measure glucosyl- and galactosyl-ceramide, lactosyl-ceramides are an additional pool that should be considered. Inhibition of glycosphingolipid synthesis has been found to reduce measures of atherosclerosis, including arterial stiffness, and lactosyl-ceramide levels were 3-fold higher in rabbits fed a Western diet for 90 days [303]. Finally, the use of an extremely high fat diet as the one used in this study is not translatable in most cases [313]. Human consumption patterns, behaviors, and decisions are extremely complex, and these features cannot be captured in a controlled mouse study; however, we can still draw from these studies in order to inform human studies.

Future Directions

Specifically related to this dissertation and the data presented herein, future work includes transcriptomics analysis of liver tissue to shed light on the mechanisms underlying our findings. Additionally, quantifying both mRNA and protein expression of CerS isoforms in several tissues will be extremely useful in understanding CerS distribution as a result of our dietary intervention and also will add to the literature seeking to characterize CerS in mice.

While the field of sphingolipid metabolism is diverse, there are three specific areas this field should address that are related to the nutrition-sphingolipid connection we established in this dissertation. First, we need to better understand how sphingolipids respond to diet both in terms of specific nutrients and dietary patterns. Despite dietary intake of ceramides being relatively low compared to endogenous synthesis, these studies, in addition to others, demonstrate that hepatic and plasma ceramides respond to diet. Therefore, it is possible that there are dietary components or overall dietary patterns that may be more beneficial and improve ceramide profiles. One priority within this endeavor should be an assessment of how fatty acid composition affects sphingolipid metabolites. Ceramide, the hub of sphingolipid metabolism, is synthesized from palmitate and serine and the increased availability of palmitate from diet is

associated with obesity and IR [328, 329]. Therefore, this step in the biosynthetic pathway is relevant for investigation of whether the dietary interventions could reduce levels of ceramides by modulating availability of palmitate. Studies investigating the types of fatty acids (saturated versus unsaturated) that are used in the diet could also provide relevant information about differential effects in systemic or tissue ceramide levels as saturated fatty acids are required for synthesis of the sphingosine backbone of ceramide [136]. Additionally, gaining a better understanding of how sphingolipid pools respond to dietary components including vitamins and minerals, especially those often supplemented in humans, would provide valuable information about how diet can influence sphingolipid metabolism.

Second, large-scale studies should be conducted to establish reference values for ceramide species. A growing number of studies are investigating possible associations between sphingolipids and risk for diseases, however, there are currently no established values for plasma concentrations of specific sphingolipids. They are also not used as biomarkers at this time, but there is a growing conversation about their potential usefulness in this area. Therefore, the goal in this regard is to establish reference values of species of interest in the population, including stratification by sex, ethnicity, and age, with studies including relevant dietary information as well.

Third, more studies should investigate the contribution of other CerS isoforms in mediating the effects of diet. While our studies specifically investigated Ceramide Synthase 6, it is well-established that CerS isoforms heterodimerize and therefore other CerS are likely affected by the absence of CerS6 protein. Additionally, as ceramide inhibitors or drugs that interfere with sphingolipid metabolism gain attention and begin to be tested and developed as therapeutics, it is imperative to have a better grasp on the dynamics of sphingolipid metabolism in terms of protein

expression, metabolite levels, and fluxes between sphingolipid pools. If a CerS6 inhibitor is developed and proven to be effective in reducing the lipotoxic C_{16}-ceramide levels, a better understanding of the other isoforms and the relationship between proteins and metabolites will ultimately provide better information for managing ceramide concentrations, in addition to any possible consequences of changes in diet.

REFERENCES

1.   Hannun, Y.A. and L.M. Obeid, *Many ceramides.* The Journal of biological chemistry, 2011. **286**(32): p. 27855-27862.

2.   Meeusen, J.W., et al., *Plasma Ceramides.* Arterioscler Thromb Vasc Biol, 2018. **38**(8): p. 1933-1939.

3.   Separovic, D., et al., *Altered Levels of Serum Ceramide, Sphingosine and Sphingomyelin Are Associated with Colorectal Cancer: A Retrospective Pilot Study.* Anticancer Res, 2017. **37**(3): p. 1213-1218.

4.   Raichur, S., et al., *The role of C16:0 ceramide in the development of obesity and type 2 diabetes: CerS6 inhibition as a novel therapeutic approach.* Mol Metab, 2019. **21**: p. 36-50.

5.   Liu, Q., et al., *Chemical synthesis and functional characterization of a new class of ceramide analogues as anti-cancer agents.* Bioorg Med Chem, 2019. **27**(8): p. 1489-1496.

6.   Chaurasia, B. and S.A. Summers, *Ceramides - Lipotoxic Inducers of Metabolic Disorders.* Trends Endocrinol Metab, 2015. **26**(10): p. 538-550.

7.   Altura, B.M., et al., *Short-term magnesium deficiency upregulates sphingomyelin synthase and p53 in cardiovascular tissues and cells: relevance to the de novo synthesis of ceramide.* Am J Physiol Heart Circ Physiol, 2010. **299**: p. H2046-H2055.

8.   Morrill, G.A., et al., *Mg2+ modulates membrane sphingolipid and lipid second messenger levels in vascular smooth muscle cells.* FEBS Lett, 1998. **440**(1-2): p. 167-71.

9.   McIlroy, G.D., et al., *Fenretinide mediated retinoic acid receptor signalling and inhibition of ceramide biosynthesis regulates adipogenesis, lipid accumulation, mitochondrial function and nutrient stress signalling in adipocytes and adipose tissue.* Biochem Pharmacol, 2016. **100**: p. 86-97.

10.   Palau, V.E., et al., *gamma-Tocotrienol induces apoptosis in pancreatic cancer cells by upregulation of ceramide synthesis and modulation of sphingolipid transport.* BMC Cancer, 2018. **18**(1): p. 564.

11.   Choi, S., et al., *Myristate-induced endoplasmic reticulum stress requires ceramide synthases 5/6 and generation of C14-ceramide in intestinal epithelial cells.* FASEB J, 2018. **32**(10): p. 5724-5736.

12.   Hoeferlin, L.A., et al., *Folate stress induces apoptosis via p53-dependent de novo ceramide synthesis and up-regulation of ceramide synthase 6.* The Journal of biological chemistry, 2013. **288**(18): p. 12880-12890.

13.   Strickland, K.C., N.I. Krupenko, and S.A. Krupenko, *Molecular mechanisms underlying the potentially adverse effects of folate.* Clinical chemistry and laboratory medicine, 2013. **51**(3): p. 607-616.

14.   Scaglione, F. and G. Panzavolta, *Folate, folic acid and 5-methyltetrahydrofolate are not the same thing.* Xenobiotica, 2014. **44**(5): p. 480-8.

15.   Suh, J.R., A.K. Herbig, and P.J. Stover, *New perspectives on folate catabolism.* Annu Rev Nutr, 2001. **21**: p. 255-82.

16.   Sanderson, P., et al., *Folate bioavailability: UK Food Standards Agency workshop report.* Br J Nutr, 2003. **90**(2): p. 473-9.

17.   da Silva, R.P., et al., *Novel insights on interactions between folate and lipid metabolism.* BioFactors (Oxford, England), 2014. **40**(3): p. 277-283.

18.   Ebara, S., *Nutritional role of folate.* Congenit Anom (Kyoto), 2017. **57**(5): p. 138-141.

19.   Jhaveri, M.S., C. Wagner, and J.B. Trepel, *Impact of extracellular folate levels on global gene expression.* Mol Pharmacol, 2001. **60**(6): p. 1288-95.

20.   Katula, K.S., A.N. Heinloth, and R.S. Paules, *Folate deficiency in normal human fibroblasts leads to altered expression of genes primarily linked to cell signaling, the cytoskeleton and extracellular matrix.* J Nutr Biochem, 2007. **18**(8): p. 541-52.

21.   Zhu, H., et al., *Differentially expressed genes in embryonic cardiac tissues of mice lacking Folr1 gene activity.* BMC Dev Biol, 2007. **7**: p. 128.

22.   Blount, B.C., et al., *Folate deficiency causes uracil misincorporation into human DNA and chromosome breakage: implications for cancer and neuronal damage.* Proc Natl Acad Sci U S A, 1997. **94**(7): p. 3290-5.

23.   Kim, Y.I., et al., *Folate deficiency in rats induces DNA strand breaks and hypomethylation within the p53 tumor suppressor gene.* Am J Clin Nutr, 1997. **65**(1): p. 46-52.

24.   Bohnsack, B.L. and K.K. Hirschi, *Nutrient regulation of cell cycle progression.* Annu Rev Nutr, 2004. **24**: p. 433-53.

25.   Fournier, I., et al., *Folate deficiency alters melatonin secretion in rats.* J Nutr, 2002. **132**(9): p. 2781-4.

26.   Champier, J., et al., *Folate depletion changes gene expression of fatty acid metabolism, DNA synthesis, and circadian cycle in male mice.* Nutrition research (New York, N.Y.), 2012. **32**(2): p. 124-132.

27.   Graham, I.M., et al., *Plasma homocysteine as a risk factor for vascular disease. The European Concerted Action Project.* JAMA, 1997. **277**(22): p. 1775-81.

28.   Bistulfi, G., et al., *Mild folate deficiency induces genetic and epigenetic instability and phenotype changes in prostate cancer cells.* BMC biology, 2010. **8**: p. 6-7007-8-6.

29.   Yi, P., et al., *Increase in plasma homocysteine associated with parallel increases in plasma S-adenosylhomocysteine and lymphocyte DNA hypomethylation.* J Biol Chem, 2000. **275**(38): p. 29318-23.

30.   Crider, K.S., et al., *Folate and DNA methylation: a review of molecular mechanisms and the evidence for folate's role.* Adv Nutr, 2012. **3**(1): p. 21-38.

31.   Christensen, K.E., et al., *Steatosis in mice is associated with gender, folate intake, and expression of genes of one-carbon metabolism.* J Nutr, 2010. **140**(10): p. 1736-41.

32.   Kitami, T., et al., *Gene-environment interactions reveal a homeostatic role for cholesterol metabolism during dietary folate perturbation in mice.* Physiological genomics, 2008. **35**(2): p. 182-190.

33.   van Gool, J.D., et al., *Folic acid and primary prevention of neural tube defects: A review.* Reprod Toxicol, 2018. **80**: p. 73-84.

34.   Liu, Z., et al., *Multiple B-vitamin inadequacy amplifies alterations induced by folate depletion in p53 expression and its downstream effector MDM2.* International journal of cancer, 2008. **123**(3): p. 519-525.

35.   Halsted, C.H., *The intestinal absorption of dietary folates in health and disease.* J Am Coll Nutr, 1989. **8**(6): p. 650-8.

36.   Wei, M.M. and J.F. Gregory, 3rd, *Organic Acids in Selected Foods Inhibit Intestinal Brush Border Pteroylpolyglutamate Hydrolase in Vitro: Potential Mechanism Affecting the Bioavailability of Dietary Polyglutamyl Folate.* J Agric Food Chem, 1998. **46**(1): p. 211-219.

37.   Christensen, K.E., et al., *High folic acid consumption leads to pseudo-MTHFR deficiency, altered lipid metabolism, and liver injury in mice.* Am J Clin Nutr, 2015. **101**(3): p. 646-58.

38.   Bailey, S.W. and J.E. Ayling, *The extremely slow and variable activity of dihydrofolate reductase in human liver and its implications for high folic acid intake.* Proc Natl Acad Sci U S A, 2009. **106**(36): p. 15424-9.

39.   Crider, K.S., L.B. Bailey, and R.J. Berry, *Folic acid food fortification-its history, effect, concerns, and future directions.* Nutrients, 2011. **3**(3): p. 370-84.

40.   Bailey, R.L., et al., *Total folate and folic acid intake from foods and dietary supplements in the United States: 2003-2006.* Am J Clin Nutr, 2010. **91**(1): p. 231-7.

41.   Bailey, R.L., et al., *Total folate and folic acid intakes from foods and dietary supplements of US children aged 1-13 y.* Am J Clin Nutr, 2010. **92**(2): p. 353-8.

42.   Yeung, L.F., et al., *Contributions of enriched cereal-grain products, ready-to-eat cereals, and supplements to folic acid and vitamin B-12 usual intake and folate and vitamin B-12 status in US children: National Health and Nutrition Examination Survey (NHANES), 2003-2006.* Am J Clin Nutr, 2011. **93**(1): p. 172-85.

43.   Lucock, M., *Folic acid: nutritional biochemistry, molecular biology, and role in disease processes.* Mol Genet Metab, 2000. **71**(1-2): p. 121-38.

44.   Figueiredo, J.C., et al., *Folic acid and risk of prostate cancer: results from a randomized clinical trial.* Journal of the National Cancer Institute, 2009. **101**(6): p. 432-435.

45.   Ebbing, M., et al., *Cancer incidence and mortality after treatment with folic acid and vitamin B12.* JAMA, 2009. **302**(19): p. 2119-26.

46.   Sauer, J., J.B. Mason, and S.W. Choi, *Too much folate: a risk factor for cancer and cardiovascular disease?* Curr Opin Clin Nutr Metab Care, 2009. **12**(1): p. 30-6.

47.   Hollinger, J.L., et al., *In vitro studies of 5, 10-methylenetetrahydrofolate reductase: inhibition by folate derivatives, folate antagonists, and monoamine derivatives.* J Neurochem, 1982. **38**(3): p. 638-42.

48.   Kelly, K.B., et al., *Excess Folic Acid Increases Lipid Storage, Weight Gain, and Adipose Tissue Inflammation in High Fat Diet-Fed Rats.* Nutrients, 2016. **8**(10).

49.   Morris, M.S., et al., *Circulating unmetabolized folic acid and 5-methyltetrahydrofolate in relation to anemia, macrocytosis, and cognitive test performance in American seniors.* Am J Clin Nutr, 2010. **91**(6): p. 1733-44.

50.   Troen, A.M., et al., *Unmetabolized folic acid in plasma is associated with reduced natural killer cell cytotoxicity among postmenopausal women.* J Nutr, 2006. **136**(1): p. 189-94.

51.   Smith, A.D., Y.I. Kim, and H. Refsum, *Is folic acid good for everyone?* Am J Clin Nutr, 2008. **87**(3): p. 517-33.

52.   Ulrich, C.M. and J.D. Potter, *Folate supplementation: too much of a good thing?* Cancer Epidemiol Biomarkers Prev, 2006. **15**(2): p. 189-93.

53.   Li, W., et al., *Folic acid supplementation alters the DNA methylation profile and improves insulin resistance in high-fat-diet-fed mice.* J Nutr Biochem, 2018. **59**: p. 76-83.

54.   Sid, V., et al., *Folic acid supplementation during high-fat diet feeding restores AMPK activation via an AMP-LKB1-dependent mechanism.* Am J Physiol Regul Integr Comp Physiol, 2015. **309**(10): p. R1215-25.

55.   Sarna, L.K., et al., *Folic acid supplementation attenuates high fat diet induced hepatic oxidative stress via regulation of NADPH oxidase.* Can J Physiol Pharmacol, 2012. **90**(2): p. 155-65.

56.   Gavrilova, O., et al., *Liver peroxisome proliferator-activated receptor gamma contributes to hepatic steatosis, triglyceride clearance, and regulation of body fat mass.* J Biol Chem, 2003. **278**(36): p. 34268-76.

57.   Sie, K.K., et al., *Effect of maternal and postweaning folic acid supplementation on global and gene-specific DNA methylation in the liver of the rat offspring.* Mol Nutr Food Res, 2013. **57**(4): p. 677-85.

58.   Mojtabai, R., *Body mass index and serum folate in childbearing age women.* Eur J Epidemiol, 2004. **19**(11): p. 1029-36.

59.   da Silva, V.R., et al., *Obesity affects short-term folate pharmacokinetics in women of childbearing age.* Int J Obes (Lond), 2013. **37**(12): p. 1608-10.

60.   Xia, M.F., et al., *Serum folic acid levels are associated with the presence and severity of liver steatosis in Chinese adults.* Clin Nutr, 2018. **37**(5): p. 1752-1758.

61.   Mahabir, S., et al., *Measures of adiposity and body fat distribution in relation to serum folate levels in postmenopausal women in a feeding study.* Eur J Clin Nutr, 2008. **62**(5): p. 644-50.

62.   Hirsch, S., et al., *Serum folate and homocysteine levels in obese females with non-alcoholic fatty liver.* Nutrition, 2005. **21**(2): p. 137-41.

63.   Sinclair, K.D., et al., *DNA methylation, insulin resistance, and blood pressure in offspring determined by maternal periconceptional B vitamin and methionine status.* Proc Natl Acad Sci U S A, 2007. **104**(49): p. 19351-6.

64.   Xie, R.H., et al., *Maternal folate status and obesity/insulin resistance in the offspring: a systematic review.* Int J Obes (Lond), 2016. **40**(1): p. 1-9.

65.   Dehkordi, E.H., et al., *Effect of folic acid on homocysteine and insulin resistance of overweight and obese children and adolescents.* Adv Biomed Res, 2016. **5**: p. 88.

66.   Gargari, B.P., V. Aghamohammadi, and A. Aliasgharzadeh, *Effect of folic acid supplementation on biochemical indices in overweight and obese men with type 2 diabetes.* Diabetes Res Clin Pract, 2011. **94**(1): p. 33-8.

67.   Solini, A., E. Santini, and E. Ferrannini, *Effect of short-term folic acid supplementation on insulin sensitivity and inflammatory markers in overweight subjects.* Int J Obes (Lond), 2006. **30**(8): p. 1197-202.

68.   Setola, E., et al., *Insulin resistance and endothelial function are improved after folate and vitamin B12 therapy in patients with metabolic syndrome: relationship between homocysteine levels and hyperinsulinemia.* Eur J Endocrinol, 2004. **151**(4): p. 483-9.

69.   Hayden, M.R. and S.C. Tyagi, *Homocysteine and reactive oxygen species in metabolic syndrome, type 2 diabetes mellitus, and atheroscleropathy: the pleiotropic effects of folate supplementation.* Nutr J, 2004. **3**: p. 4.

70.   Mierzecki, A., et al., *Influence of folic acid supplementation on coagulation, inflammatory, lipid, and kidney function parameters in subjects with low and moderate content of folic acid in the diet.* Kardiol Pol, 2015. **73**(4): p. 280-6.

71.   Hales, C.M., et al., *Differences in Obesity Prevalence by Demographic Characteristics and Urbanization Level Among Adults in the United States, 2013-2016.* JAMA, 2018. **319**(23): p. 2419-2429.

72.   Dahlhoff, C., et al., *Methyl-donor supplementation in obese mice prevents the progression of NAFLD, activates AMPK and decreases acyl-carnitine levels.* Mol Metab, 2014. **3**(5): p. 565-80.

73.   Sid, V., et al., *High-fat diet consumption reduces hepatic folate transporter expression via nuclear respiratory factor-1.* J Mol Med (Berl), 2018. **96**(11): p. 1203-1213.

74.   Burdge, G.C., et al., *Folic acid supplementation during the juvenile-pubertal period in rats modifies the phenotype and epigenotype induced by prenatal nutrition.* J Nutr, 2009. **139**(6): p. 1054-60.

75.   Walker, A.K., et al., *A conserved SREBP-1/phosphatidylcholine feedback circuit regulates lipogenesis in metazoans.* Cell, 2011. **147**(4): p. 840-52.

76.   McNeil, C.J., et al., *Disruption of lipid metabolism in the liver of the pregnant rat fed folate-deficient and methyl donor-deficient diets.* Br J Nutr, 2008. **99**(2): p. 262-71.

77.   Levy, M. and A.H. Futerman, *Critical Review: Mammalian Ceramide Synthases.* Life, 2010. **62**(5): p. 347-356.

78.   Hannun, Y.A. and L.M. Obeid, *Principles of bioactive lipid signalling: lessons from sphingolipids.* Nature reviews.Molecular cell biology, 2008. **9**(2): p. 139-150.

79.   Maceyka, M. and S. Spiegel, *Sphingolipid metabolites in inflammatory disease.* Nature, 2014. **510**(7503): p. 58-67.

80.   Mullen, T.D., Y.A. Hannun, and L.M. Obeid, *Ceramide synthases at the centre of sphingolipid metabolism and biology.* The Biochemical journal, 2012. **441**(3): p. 789-802.

81.   van Meer, G. and H. Sprong, *Membrane lipids and vesicular traffic.* Curr Opin Cell Biol, 2004. **16**(4): p. 373-8.

82.   Schiffmann, S., et al., *Ceramide metabolism in mouse tissue.* The international journal of biochemistry & cell biology, 2013. **45**(8): p. 1886-1894.

83.   Haughey, N.J., et al., *Roles for dysfunctional sphingolipid metabolism in Alzheimer's disease neuropathogenesis.* Biochim Biophys Acta, 2010. **1801**(8): p. 878-86.

84.   Petrache, I., et al., *Ceramide synthases expression and role of ceramide synthase-2 in the lung: insight from human lung cells and mouse models.* PLoS One, 2013. **8**(5): p. e62968.

85.   Yamashita, T., et al., *A vital role for glycosphingolipid synthesis during development and differentiation.* Proc Natl Acad Sci U S A, 1999. **96**(16): p. 9142-7.

86.   Hojjati, M.R., Z. Li, and X.C. Jiang, *Serine palmitoyl-CoA transferase (SPT) deficiency and sphingolipid levels in mice.* Biochim Biophys Acta, 2005. **1737**(1): p. 44-51.

87.   Wang, X., et al., *Mitochondrial degeneration and not apoptosis is the primary cause of embryonic lethality in ceramide transfer protein mutant mice.* J Cell Biol, 2009. **184**(1): p. 143-58.

88.   Taha, T.A., T.D. Mullen, and L.M. Obeid, *A house divided: ceramide, sphingosine, and sphingosine-1-phosphate in programmed cell death.* Biochim Biophys Acta, 2006. **1758**(12): p. 2027-36.

89.   Futerman, A.H. and Y.A. Hannun, *The complex life of simple sphingolipids.* EMBO Rep, 2004. **5**(8): p. 777-82.

90.   Guillas, I., et al., *C26-CoA-dependent ceramide synthesis of Saccharomyces cerevisiae is operated by Lag1p and Lac1p.* EMBO J, 2001. **20**(11): p. 2655-65.

91.   Schorling, S., et al., *Lag1p and Lac1p are essential for the Acyl-CoA-dependent ceramide synthase reaction in Saccharomyces cerevisae.* Mol Biol Cell, 2001. **12**(11): p. 3417-27.

92.   Hannun, Y.A. and L.M. Obeid, *The Ceramide-centric universe of lipid-mediated cell regulation: stress encounters of the lipid kind.* J Biol Chem, 2002. **277**(29): p. 25847-50.

93.   Mandon, E.C., et al., *Subcellular localization and membrane topology of serine palmitoyltransferase, 3-dehydrosphinganine reductase, and sphinganine N-acyltransferase in mouse liver.* J Biol Chem, 1992. **267**(16): p. 11144-8.

94.   Hirschberg, K., J. Rodger, and A.H. Futerman, *The long-chain sphingoid base of sphingolipids is acylated at the cytosolic surface of the endoplasmic reticulum in rat liver.* Biochem J, 1993. **290 (Pt 3**): p. 751-7.

95.   Futerman, A.H. and H. Riezman, *The ins and outs of sphingolipid synthesis.* Trends Cell Biol, 2005. **15**(6): p. 312-8.

96.   Hartmann, D., et al., *The equilibrium between long and very long chain ceramides is important for the fate of the cell and can be influenced by co-expression of CerS.* Int J Biochem Cell Biol, 2013. **45**(7): p. 1195-203.

97.   Venkataraman, K., et al., *Upstream of growth and differentiation factor 1 (uog1), a mammalian homolog of the yeast longevity assurance gene 1 (LAG1), regulates N-stearoyl-sphinganine (C18-(dihydro)ceramide) synthesis in a fumonisin B1-independent manner in mammalian cells.* J Biol Chem, 2002. **277**(38): p. 35642-9.

98.   Riebeling, C., et al., *Two mammalian longevity assurance gene (LAG1) family members, trh1 and trh4, regulate dihydroceramide synthesis using different fatty acyl-CoA donors.* J Biol Chem, 2003. **278**(44): p. 43452-9.

99. Mizutani, Y., A. Kihara, and Y. Igarashi, *Mammalian Lass6 and its related family members regulate synthesis of specific ceramides.* Biochem J, 2005. **390**(Pt 1): p. 263-71.

100. Stancevic, B. and R. Kolesnick, *Ceramide-rich platforms in transmembrane signaling.* FEBS Lett, 2010. **584**(9): p. 1728-40.

101. Kitatani, K., J. Idkowiak-Baldys, and Y.A. Hannun, *The sphingolipid salvage pathway in ceramide metabolism and signaling.* Cell Signal, 2008. **20**(6): p. 1010-8.

102. Yu, J., et al., *JNK3 signaling pathway activates ceramide synthase leading to mitochondrial dysfunction.* J Biol Chem, 2007. **282**(35): p. 25940-9.

103. Boot, R.G., et al., *Identification of the non-lysosomal glucosylceramidase as beta-glucosidase 2.* J Biol Chem, 2007. **282**(2): p. 1305-12.

104. Milhas, D., C.J. Clarke, and Y.A. Hannun, *Sphingomyelin metabolism at the plasma membrane: implications for bioactive sphingolipids.* FEBS Lett, 2010. **584**(9): p. 1887-94.

105. Mao, C. and L.M. Obeid, *Ceramidases: regulators of cellular responses mediated by ceramide, sphingosine, and sphingosine-1-phosphate.* Biochim Biophys Acta, 2008. **1781**(9): p. 424-34.

106. Pewzner-Jung, Y., et al., *A critical role for ceramide synthase 2 in liver homeostasis: I. alterations in lipid metabolic pathways.* J Biol Chem, 2010. **285**(14): p. 10902-10.

107. Pewzner-Jung, Y., S. Ben-Dor, and A.H. Futerman, *When do Lasses (longevity assurance genes) become CerS (ceramide synthases)?: Insights into the regulation of ceramide synthesis.* J Biol Chem, 2006. **281**(35): p. 25001-5.

108. Lahiri, S. and A.H. Futerman, *LASS5 is a bona fide dihydroceramide synthase that selectively utilizes palmitoyl-CoA as acyl donor.* J Biol Chem, 2005. **280**(40): p. 33735-8.

109. Turpin-Nolan, S.M., et al., *CerS1-Derived C18:0 Ceramide in Skeletal Muscle Promotes Obesity-Induced Insulin Resistance.* Cell Rep, 2019. **26**(1): p. 1-10 e7.

110. Kumagai, K., et al., *CERT mediates intermembrane transfer of various molecular species of ceramides.* J Biol Chem, 2005. **280**(8): p. 6488-95.

111. Holmes, R.S., K.A. Barron, and N.I. Krupenko, *Ceramide Synthase 6: Comparative Analysis, Phylogeny and Evolution.* Biomolecules, 2018. **8**(4).

112. Laviad, E.L., et al., *Characterization of ceramide synthase 2: tissue distribution, substrate specificity, and inhibition by sphingosine 1-phosphate.* J Biol Chem, 2008. **283**(9): p. 5677-84.

113. Min, J., et al., *(Dihydro)ceramide synthase 1 regulated sensitivity to cisplatin is associated with the activation of p38 mitogen-activated protein kinase and is abrogated by sphingosine kinase 1.* Mol Cancer Res, 2007. **5**(8): p. 801-12.

114. Koybasi, S., et al., *Defects in cell growth regulation by C18:0-ceramide and longevity assurance gene 1 in human head and neck squamous cell carcinomas.* J Biol Chem, 2004. **279**(43): p. 44311-9.

115. Cai, X.F., et al., *Molecular cloning, characterisation and tissue-specific expression of human LAG3, a member of the novel Lag1 protein family.* DNA Seq, 2003. **14**(2): p. 79-86.

116. Spassieva, S.D., et al., *Disruption of ceramide synthesis by CerS2 down-regulation leads to autophagy and the unfolded protein response.* Biochem J, 2009. **424**(2): p. 273-83.

117. Pewzner-Jung, Y., et al., *A critical role for ceramide synthase 2 in liver homeostasis: II. insights into molecular changes leading to hepatopathy.* J Biol Chem, 2010. **285**(14): p. 10911-23.

118. Mizutani, Y., A. Kihara, and Y. Igarashi, *LASS3 (longevity assurance homologue 3) is a mainly testis-specific (dihydro)ceramide synthase with relatively broad substrate specificity.* Biochem J, 2006. **398**(3): p. 531-8.

119. Rabionet, M., et al., *Male germ cells require polyenoic sphingolipids with complex glycosylation for completion of meiosis: a link to ceramide synthase-3.* J Biol Chem, 2008. **283**(19): p. 13357-69.

120. Coderch, L., et al., *Ceramides and skin function.* Am J Clin Dermatol, 2003. **4**(2): p. 107-29.

121. Wang, G., et al., *Long-chain ceramide is elevated in presenilin 1 (PS1M146V) mouse brain and induces apoptosis in PS1 astrocytes.* Glia, 2008. **56**(4): p. 449-56.

122. Ebel, P., et al., *Inactivation of ceramide synthase 6 in mice results in an altered sphingolipid metabolism and behavioral abnormalities.* The Journal of biological chemistry, 2013. **288**(29): p. 21433-21447.

123. Senkal, C.E., et al., *Antiapoptotic roles of ceramide-synthase-6-generated C16-ceramide via selective regulation of the ATF6/CHOP arm of ER-stress-response pathways.* FASEB J, 2010. **24**(1): p. 296-308.

124. Mesicek, J., et al., *Ceramide synthases 2, 5, and 6 confer distinct roles in radiation-induced apoptosis in HeLa cells.* Cell Signal, 2010. **22**(9): p. 1300-7.

125. Schull, S., et al., *Cytochrome c oxidase deficiency accelerates mitochondrial apoptosis by activating ceramide synthase 6.* Cell death & disease, 2015. **6**: p. e1691.

126. Sridevi, P., et al., *Stress-induced ER to Golgi translocation of ceramide synthase 1 is dependent on proteasomal processing.* Exp Cell Res, 2010. **316**(1): p. 78-91.

127. Sridevi, P., et al., *Ceramide synthase 1 is regulated by proteasomal mediated turnover.* Biochim Biophys Acta, 2009. **1793**(7): p. 1218-27.

128. Ben-David, O., et al., *Encephalopathy caused by ablation of very long acyl chain ceramide synthesis may be largely due to reduced galactosylceramide levels.* J Biol Chem, 2011. **286**(34): p. 30022-33.

129. Sassa, T., T. Hirayama, and A. Kihara, *Enzyme Activities of the Ceramide Synthases CERS2-6 Are Regulated by Phosphorylation in the C-terminal Region.* J Biol Chem, 2016. **291**(14): p. 7477-87.

130. Raichur, S., et al., *CerS2 Haploinsufficiency Inhibits beta-Oxidation and Confers Susceptibility to Diet-Induced Steatohepatitis and Insulin Resistance.* Cell Metab, 2014. **20**(5): p. 919.

131. Fresques, T., et al., *Regulation of ceramide synthase by casein kinase 2-dependent phosphorylation in Saccharomyces cerevisiae.* J Biol Chem, 2015. **290**(3): p. 1395-403.

132. Muir, A., et al., *TORC2-dependent protein kinase Ypk1 phosphorylates ceramide synthase to stimulate synthesis of complex sphingolipids.* Elife, 2014. **3**.

133.   Laviad, E.L., et al., *Modulation of ceramide synthase activity via dimerization.* J Biol Chem, 2012. **287**(25): p. 21025-33.

134.   Lahiri, S. and A.H. Futerman, *The metabolism and function of sphingolipids and glycosphingolipids.* Cell Mol Life Sci, 2007. **64**(17): p. 2270-84.

135.   Mullen, T.D., et al., *Selective knockdown of ceramide synthases reveals complex interregulation of sphingolipid metabolism.* Journal of lipid research, 2011. **52**(1): p. 68-77.

136.   Holland, W.L., et al., *Inhibition of ceramide synthesis ameliorates glucocorticoid-, saturated-fat-, and obesity-induced insulin resistance.* Cell Metab, 2007. **5**(3): p. 167-79.

137.   Henry, B., et al., *Acid sphingomyelinase.* Handb Exp Pharmacol, 2013(215): p. 77-88.

138.   Cyster, J.G. and S.R. Schwab, *Sphingosine-1-phosphate and lymphocyte egress from lymphoid organs.* Annu Rev Immunol, 2012. **30**: p. 69-94.

139.   Rivera, J., R.L. Proia, and A. Olivera, *The alliance of sphingosine-1-phosphate and its receptors in immunity.* Nat Rev Immunol, 2008. **8**(10): p. 753-63.

140.   Pattingre, S., et al., *Ceramide-induced autophagy: to junk or to protect cells?* Autophagy, 2009. **5**(4): p. 558-60.

141.   Guillas, I., et al., *Human homologues of LAG1 reconstitute Acyl-CoA-dependent ceramide synthesis in yeast.* J Biol Chem, 2003. **278**(39): p. 37083-91.

142.   Stiban, J., R. Tidhar, and A.H. Futerman, *Ceramide synthases: roles in cell physiology and signaling.* Adv Exp Med Biol, 2010. **688**: p. 60-71.

143.   Goldkorn, T. and S. Filosto, *Lung injury and cancer: Mechanistic insights into ceramide and EGFR signaling under cigarette smoke.* Am J Respir Cell Mol Biol, 2010. **43**(3): p. 259-68.

144.   Andrieu-Abadie, N., et al., *Ceramide in apoptosis signaling: relationship with oxidative stress.* Free Radic Biol Med, 2001. **31**(6): p. 717-28.

145. Birbes, H., et al., *Selective hydrolysis of a mitochondrial pool of sphingomyelin induces apoptosis.* FASEB J, 2001. **15**(14): p. 2669-79.

146. Haimovitz-Friedman, A., R.N. Kolesnick, and Z. Fuks, *Ceramide signaling in apoptosis.* Br Med Bull, 1997. **53**(3): p. 539-53.

147. Kolesnick, R., *Signal transduction through the sphingomyelin pathway.* Mol Chem Neuropathol, 1994. **21**(2-3): p. 287-97.

148. Pandey, S., R.F. Murphy, and D.K. Agrawal, *Recent advances in the immunobiology of ceramide.* Exp Mol Pathol, 2007. **82**(3): p. 298-309.

149. Ravid, T., et al., *Ceramide accumulation precedes caspase-3 activation during apoptosis of A549 human lung adenocarcinoma cells.* Am J Physiol Lung Cell Mol Physiol, 2003. **284**(6): p. L1082-92.

150. Grosch, S., S. Schiffmann, and G. Geisslinger, *Chain length-specific properties of ceramides.* Progress in lipid research, 2012. **51**(1): p. 50-62.

151. Panjarian, S., et al., *De novo N-palmitoylsphingosine synthesis is the major biochemical mechanism of ceramide accumulation following p53 up-regulation.* Prostaglandins Other Lipid Mediat, 2008. **86**(1-4): p. 41-8.

152. Hartmann, D., et al., *Long chain ceramides and very long chain ceramides have opposite effects on human breast and colon cancer cell growth.* Int J Biochem Cell Biol, 2012. **44**(4): p. 620-8.

153. Holland, W.L., et al., *Lipid-induced insulin resistance mediated by the proinflammatory receptor TLR4 requires saturated fatty acid-induced ceramide biosynthesis in mice.* J Clin Invest, 2011. **121**(5): p. 1858-70.

154. Hamada, Y., et al., *Involvement of de novo ceramide synthesis in pro-inflammatory adipokine secretion and adipocyte-macrophage interaction.* The Journal of nutritional biochemistry, 2014. **25**(12): p. 1309-1316.

155. Ogretmen, B. and Y.A. Hannun, *Biologically active sphingolipids in cancer pathogenesis and treatment.* Nat Rev Cancer, 2004. **4**(8): p. 604-16.

156.   Schenck, M., et al., *Ceramide: physiological and pathophysiological aspects.* Arch Biochem Biophys, 2007. **462**(2): p. 171-5.

157.   Hait, N.C., et al., *Sphingosine kinases, sphingosine 1-phosphate, apoptosis and diseases.* Biochim Biophys Acta, 2006. **1758**(12): p. 2016-26.

158.   Yacoub, A., et al., *PERK-dependent regulation of ceramide synthase 6 and thioredoxin play a key role in mda-7/IL-24-induced killing of primary human glioblastoma multiforme cells.* Cancer Res, 2010. **70**(3): p. 1120-9.

159.   Senkal, C.E., et al., *Alteration of ceramide synthase 6/C16-ceramide induces activating transcription factor 6-mediated endoplasmic reticulum (ER) stress and apoptosis via perturbation of cellular Ca2+ and ER/Golgi membrane network.* J Biol Chem, 2011. **286**(49): p. 42446-58.

160.   Yun, S.H., et al., *By activating Fas/ceramide synthase 6/p38 kinase in lipid rafts, stichoposide D inhibits growth of leukemia xenografts.* Oncotarget, 2015. **6**(29): p. 27596-612.

161.   Novgorodov, S.A., et al., *Developmentally regulated ceramide synthase 6 increases mitochondrial Ca2+ loading capacity and promotes apoptosis.* J Biol Chem, 2011. **286**(6): p. 4644-58.

162.   Tirodkar, T.S., et al., *Expression of Ceramide Synthase 6 Transcriptionally Activates Acid Ceramidase in a c-Jun N-terminal Kinase (JNK)-dependent Manner.* J Biol Chem, 2015. **290**(21): p. 13157-67.

163.   Sassa, T., et al., *A shift in sphingolipid composition from C24 to C16 increases susceptibility to apoptosis in HeLa cells.* Biochim Biophys Acta, 2012. **1821**(7): p. 1031-7.

164.   Liu, X., et al., *Acid ceramidase inhibition: a novel target for cancer therapy.* Front Biosci, 2008. **13**: p. 2293-8.

165.   Williams, B., et al., *A novel role for ceramide synthase 6 in mouse and human alcoholic steatosis.* FASEB J, 2018. **32**(1): p. 130-142.

166. Reichel, M., et al., *Chronic Psychosocial Stress in Mice Is Associated With Increased Acid Sphingomyelinase Activity in Liver and Serum and With Hepatic C16:0-Ceramide Accumulation.* Front Psychiatry, 2018. **9**: p. 496.

167. Erez-Roman, R., R. Pienik, and A.H. Futerman, *Increased ceramide synthase 2 and 6 mRNA levels in breast cancer tissues and correlation with sphingosine kinase expression.* Biochem Biophys Res Commun, 2010. **391**(1): p. 219-23.

168. Schiffmann, S., et al., *Ceramide synthases and ceramide levels are increased in breast cancer tissue.* Carcinogenesis, 2009. **30**(5): p. 745-52.

169. Turpin, S.M., et al., *Obesity-induced CerS6-dependent C16:0 ceramide production promotes weight gain and glucose intolerance.* Cell metabolism, 2014. **20**(4): p. 678-686.

170. Adams, J.M., 2nd, et al., *Ceramide content is increased in skeletal muscle from obese insulin-resistant humans.* Diabetes, 2004. **53**(1): p. 25-31.

171. Haus, J.M., et al., *Plasma ceramides are elevated in obese subjects with type 2 diabetes and correlate with the severity of insulin resistance.* Diabetes, 2009. **58**(2): p. 337-43.

172. Eisinger, K., et al., *Lipidomic analysis of the liver from high-fat diet induced obese mice identifies changes in multiple lipid classes.* Exp Mol Pathol, 2014. **97**(1): p. 37-43.

173. Gosejacob, D., et al., *Ceramide Synthase 5 Is Essential to Maintain C16:0-Ceramide Pools and Contributes to the Development of Diet-induced Obesity.* J Biol Chem, 2016. **291**(13): p. 6989-7003.

174. Frangioudakis, G., et al., *Saturated- and n-6 polyunsaturated-fat diets each induce ceramide accumulation in mouse skeletal muscle: reversal and improvement of glucose tolerance by lipid metabolism inhibitors.* Endocrinology, 2010. **151**(9): p. 4187-96.

175. Chavez, J.A. and S.A. Summers, *A ceramide-centric view of insulin resistance.* Cell Metab, 2012. **15**(5): p. 585-94.

176. Ussher, J.R., et al., *Inhibition of de novo ceramide synthesis reverses diet-induced insulin resistance and enhances whole-body oxygen consumption.* Diabetes, 2010. **59**(10): p. 2453-64.

177. Hammerschmidt, P., et al., *CerS6-Derived Sphingolipids Interact with Mff and Promote Mitochondrial Fragmentation in Obesity.* Cell, 2019. **177**(6): p. 1536-1552 e23.

178. Sako, Y. and V.E. Grill, *A 48-hour lipid infusion in the rat time-dependently inhibits glucose-induced insulin secretion and B cell oxidation through a process likely coupled to fatty acid oxidation.* Endocrinology, 1990. **127**(4): p. 1580-9.

179. Zhou, Y.P. and V.E. Grill, *Long-term exposure of rat pancreatic islets to fatty acids inhibits glucose-induced insulin secretion and biosynthesis through a glucose fatty acid cycle.* J Clin Invest, 1994. **93**(2): p. 870-6.

180. McGarry, J.D. and R.L. Dobbins, *Fatty acids, lipotoxicity and insulin secretion.* Diabetologia, 1999. **42**(2): p. 128-38.

181. Kelpe, C.L., et al., *Palmitate inhibition of insulin gene expression is mediated at the transcriptional level via ceramide synthesis.* J Biol Chem, 2003. **278**(32): p. 30015-21.

182. Ritz-Laser, B., et al., *Glucose-induced preproinsulin gene expression is inhibited by the free fatty acid palmitate.* Endocrinology, 1999. **140**(9): p. 4005-14.

183. Shimabukuro, M., et al., *Lipoapoptosis in beta-cells of obese prediabetic fa/fa rats. Role of serine palmitoyltransferase overexpression.* J Biol Chem, 1998. **273**(49): p. 32487-90.

184. Shimabukuro, M., et al., *Fatty acid-induced beta cell apoptosis: a link between obesity and diabetes.* Proc Natl Acad Sci U S A, 1998. **95**(5): p. 2498-502.

185. Maedler, K., et al., *Distinct effects of saturated and monounsaturated fatty acids on beta-cell turnover and function.* Diabetes, 2001. **50**(1): p. 69-76.

186. El-Assaad, W., et al., *Saturated fatty acids synergize with elevated glucose to cause pancreatic beta-cell death.* Endocrinology, 2003. **144**(9): p. 4154-63.

187. Sjoholm, A., *Ceramide inhibits pancreatic beta-cell insulin production and mitogenesis and mimics the actions of interleukin-1 beta.* FEBS Lett, 1995. **367**(3): p. 283-6.

188. Bikman, B.T. and S.A. Summers, *Ceramides as modulators of cellular and whole-body metabolism.* J Clin Invest, 2011. **121**(11): p. 4222-30.

189.   de Mello, V.D., et al., *Link between plasma ceramides, inflammation and insulin resistance: association with serum IL-6 concentration in patients with coronary heart disease.* Diabetologia, 2009. **52**(12): p. 2612-5.

190.   Gill, J.M. and N. Sattar, *Ceramides: a new player in the inflammation-insulin resistance paradigm?* Diabetologia, 2009. **52**(12): p. 2475-7.

191.   Gao, S., et al., *Important roles of brain-specific carnitine palmitoyltransferase and ceramide metabolism in leptin hypothalamic control of feeding.* Proc Natl Acad Sci U S A, 2011. **108**(23): p. 9691-6.

192.   Inokuchi, J., *Insulin resistance as a membrane microdomain disorder.* Biol Pharm Bull, 2006. **29**(8): p. 1532-7.

193.   Kabayama, K., et al., *TNFalpha-induced insulin resistance in adipocytes as a membrane microdomain disorder: involvement of ganglioside GM3.* Glycobiology, 2005. **15**(1): p. 21-9.

194.   Villa, N.Y., et al., *Sphingolipids function as downstream effectors of a fungal PAQR.* Mol Pharmacol, 2009. **75**(4): p. 866-75.

195.   Holland, W.L. and P.E. Scherer, *PAQRs: a counteracting force to ceramides?* Mol Pharmacol, 2009. **75**(4): p. 740-3.

196.   Kupchak, B.R., et al., *Antagonism of human adiponectin receptors and their membrane progesterone receptor paralogs by TNFalpha and a ceramidase inhibitor.* Biochemistry, 2009. **48**(24): p. 5504-6.

197.   Holland, W.L., et al., *Receptor-mediated activation of ceramidase activity initiates the pleiotropic actions of adiponectin.* Nat Med, 2011. **17**(1): p. 55-63.

198.   Junkin, K.A., et al., *Resistin acutely impairs insulin-stimulated glucose transport in rodent muscle in the presence, but not absence, of palmitate.* Am J Physiol Regul Integr Comp Physiol, 2009. **296**(4): p. R944-51.

199.   Stratford, S., D.B. DeWald, and S.A. Summers, *Ceramide dissociates 3'-phosphoinositide production from pleckstrin homology domain translocation.* Biochem J, 2001. **354**(Pt 2): p. 359-68.

200. Powell, D.J., et al., *Ceramide disables 3-phosphoinositide binding to the pleckstrin homology domain of protein kinase B (PKB)/Akt by a PKCzeta-dependent mechanism.* Mol Cell Biol, 2003. **23**(21): p. 7794-808.

201. Bourbon, N.A., L. Sandirasegarane, and M. Kester, *Ceramide-induced inhibition of Akt is mediated through protein kinase Czeta: implications for growth arrest.* J Biol Chem, 2002. **277**(5): p. 3286-92.

202. Fox, T.E., et al., *Ceramide recruits and activates protein kinase C zeta (PKC zeta) within structured membrane microdomains.* J Biol Chem, 2007. **282**(17): p. 12450-7.

203. Summers, S.A., et al., *Regulation of insulin-stimulated glucose transporter GLUT4 translocation and Akt kinase activity by ceramide.* Mol Cell Biol, 1998. **18**(9): p. 5457-64.

204. Stratford, S., et al., *Regulation of insulin action by ceramide: dual mechanisms linking ceramide accumulation to the inhibition of Akt/protein kinase B.* J Biol Chem, 2004. **279**(35): p. 36608-15.

205. Turpin, S.M., et al., *Obesity-induced CerS6-dependent C16:0 ceramide production promotes weight gain and glucose intolerance.* Cell Metab, 2014. **20**(4): p. 678-86.

206. Koves, T.R., et al., *Mitochondrial overload and incomplete fatty acid oxidation contribute to skeletal muscle insulin resistance.* Cell Metab, 2008. **7**(1): p. 45-56.

207. Boslem, E., et al., *A lipidomic screen of palmitate-treated MIN6 beta-cells links sphingolipid metabolites with endoplasmic reticulum (ER) stress and impaired protein trafficking.* Biochem J, 2011. **435**(1): p. 267-76.

208. Yen, C.L., M.H. Mar, and S.H. Zeisel, *Choline deficiency-induced apoptosis in PC12 cells is associated with diminished membrane phosphatidylcholine and sphingomyelin, accumulation of ceramide and diacylglycerol, and activation of a caspase.* FASEB J, 1999. **13**(1): p. 135-42.

209. Park, W.J., et al., *Hepatic fatty acid uptake is regulated by the sphingolipid acyl chain length.* Biochim Biophys Acta, 2014. **1841**(12): p. 1754-66.

210. Russo, S.B., et al., *Ceramide synthase 5 mediates lipid-induced autophagy and hypertrophy in cardiomyocytes.* J Clin Invest, 2012. **122**(11): p. 3919-30.

211. de Carvalho, L.P., et al., *Plasma Ceramides as Prognostic Biomarkers and Their Arterial and Myocardial Tissue Correlates in Acute Myocardial Infarction.* JACC Basic Transl Sci, 2018. **3**(2): p. 163-175.

212. Siddique, M.M., et al., *Dihydroceramides: From Bit Players to Lead Actors.* J Biol Chem, 2015. **290**(25): p. 15371-9.

213. Schissel, S.L., et al., *Rabbit aorta and human atherosclerotic lesions hydrolyze the sphingomyelin of retained low-density lipoprotein. Proposed role for arterial-wall sphingomyelinase in subendothelial retention and aggregation of atherogenic lipoproteins.* J Clin Invest, 1996. **98**(6): p. 1455-64.

214. Marathe, S., et al., *Human vascular endothelial cells are a rich and regulatable source of secretory sphingomyelinase. Implications for early atherogenesis and ceramide-mediated cell signaling.* J Biol Chem, 1998. **273**(7): p. 4081-8.

215. Cheng, J.M., et al., *Plasma concentrations of molecular lipid species in relation to coronary plaque characteristics and cardiovascular outcome: Results of the ATHEROREMO-IVUS study.* Atherosclerosis, 2015. **243**(2): p. 560-6.

216. Laaksonen, R., et al., *Plasma ceramides predict cardiovascular death in patients with stable coronary artery disease and acute coronary syndromes beyond LDL-cholesterol.* Eur Heart J, 2016. **37**(25): p. 1967-76.

217. Tarasov, K., et al., *Molecular lipids identify cardiovascular risk and are efficiently lowered by simvastatin and PCSK9 deficiency.* J Clin Endocrinol Metab, 2014. **99**(1): p. E45-52.

218. Wang, D.D., et al., *Plasma Ceramides, Mediterranean Diet, and Incident Cardiovascular Disease in the PREDIMED Trial (Prevencion con Dieta Mediterranea).* Circulation, 2017. **135**(21): p. 2028-2040.

219. Havulinna, A.S., et al., *Circulating Ceramides Predict Cardiovascular Outcomes in the Population-Based FINRISK 2002 Cohort.* Arterioscler Thromb Vasc Biol, 2016. **36**(12): p. 2424-2430.

220. Huang, H., et al., *Gastric bypass surgery reduces plasma ceramide subspecies and improves insulin sensitivity in severely obese patients.* Obesity (Silver Spring), 2011. **19**(11): p. 2235-40.

221. Bergman, B.C., et al., *Serum sphingolipids: relationships to insulin sensitivity and changes with exercise in humans.* Am J Physiol Endocrinol Metab, 2015. **309**(4): p. E398-408.

222. Ng, T.W., et al., *Dose-dependent effects of rosuvastatin on the plasma sphingolipidome and phospholipidome in the metabolic syndrome.* J Clin Endocrinol Metab, 2014. **99**(11): p. E2335-40.

223. Hicks, A.A., et al., *Genetic determinants of circulating sphingolipid concentrations in European populations.* PLoS Genet, 2009. **5**(10): p. e1000672.

224. Mehrabian, M., et al., *Genetic control of HDL levels and composition in an interspecific mouse cross (CAST/Ei x C57BL/6J).* J Lipid Res, 2000. **41**(12): p. 1936-46.

225. Good, D.A., et al., *Noncoding Variations in the Gene Encoding Ceramide Synthase 6 are Associated with Type 2 Diabetes in a Large Indigenous Australian Pedigree.* Twin Res Hum Genet, 2019. **22**(2): p. 79-87.

226. Hannun, Y.A. and L.M. Obeid, *Sphingolipids and their metabolism in physiology and disease.* Nat Rev Mol Cell Biol, 2018. **19**(3): p. 175-191.

227. Castro, B.M., M. Prieto, and L.C. Silva, *Ceramide: a simple sphingolipid with unique biophysical properties.* Prog Lipid Res, 2014. **54**: p. 53-67.

228. Goni, F.M., J. Sot, and A. Alonso, *Biophysical properties of sphingosine, ceramides and other simple sphingolipids.* Biochem Soc Trans, 2014. **42**(5): p. 1401-8.

229. Stith, J.L., F.N. Velazquez, and L.M. Obeid, *Advances in determining signaling mechanisms of ceramide and role in disease.* J Lipid Res, 2019. **60**(5): p. 913-918.

230. Hannun, Y.A. and L.M. Obeid, *Principles of bioactive lipid signalling: lessons from sphingolipids.* Nat Rev Mol Cell Biol, 2008. **9**(2): p. 139-50.

231. Ogretmen, B., *Sphingolipid metabolism in cancer signalling and therapy.* Nat Rev Cancer, 2018. **18**(1): p. 33-50.

232. Chaurasia, B., et al., *Targeting a ceramide double bond improves insulin resistance and hepatic steatosis.* Science, 2019. **365**(6451): p. 386-392.

233. Mullen, T.D., Y.A. Hannun, and L.M. Obeid, *Ceramide synthases at the centre of sphingolipid metabolism and biology.* Biochem J, 2012. **441**(3): p. 789-802.

234. Poss, A.M., W.L. Holland, and S.A. Summers, *Risky lipids: refining the ceramide score that measures cardiovascular health.* Eur Heart J, 2019.

235. Snider, J.M., C. Luberto, and Y.A. Hannun, *Approaches for probing and evaluating mammalian sphingolipid metabolism.* Anal Biochem, 2019. **575**: p. 70-86.

236. Zelnik, I.D., et al., *A Stroll Down the CerS Lane.* Adv Exp Med Biol, 2019. **1159**: p. 49-63.

237. Brachtendorf, S., K. El-Hindi, and S. Grosch, *Ceramide synthases in cancer therapy and chemoresistance.* Prog Lipid Res, 2019. **74**: p. 160-185.

238. Cingolani, F., A.H. Futerman, and J. Casas, *Ceramide synthases in biomedical research.* Chemistry and physics of lipids, 2016. **197**: p. 25-32.

239. Park, J.W., W.J. Park, and A.H. Futerman, *Ceramide synthases as potential targets for therapeutic intervention in human diseases.* Biochimica et biophysica acta, 2014. **1841**(5): p. 671-681.

240. Sofi, M.H., et al., *Ceramide synthesis regulates T cell activity and GVHD development.* JCI Insight, 2017. **2**(10).

241. Wegner, M.S., et al., *The enigma of ceramide synthase regulation in mammalian cells.* Prog Lipid Res, 2016. **63**: p. 93-119.

242. Hernandez-Corbacho, M.J., et al., *Tumor Necrosis Factor-alpha (TNFalpha)-induced Ceramide Generation via Ceramide Synthases Regulates Loss of Focal Adhesion Kinase (FAK) and Programmed Cell Death.* J Biol Chem, 2015. **290**(42): p. 25356-73.

243. Medici, V. and C.H. Halsted, *Folate, alcohol, and liver disease.* Mol Nutr Food Res, 2013. **57**(4): p. 596-606.

244. Strickland, K.C., N.I. Krupenko, and S.A. Krupenko, *Molecular mechanisms underlying the potentially adverse effects of folate.* Clin Chem Lab Med, 2013. **51**(3): p. 607-16.

245.   McNulty, H., et al., *Addressing optimal folate and related B-vitamin status through the lifecycle: health impacts and challenges.* Proc Nutr Soc, 2019. **78**(3): p. 449-462.

246.   Au, K.S., T.O. Findley, and H. Northrup, *Finding the genetic mechanisms of folate deficiency and neural tube defects-Leaving no stone unturned.* Am J Med Genet A, 2017. **173**(11): p. 3042-3057.

247.   Sid, V., Y.L. Siow, and K. O, *Role of folate in nonalcoholic fatty liver disease.* Can J Physiol Pharmacol, 2017. **95**(10): p. 1141-1148.

248.   Ducker, G.S. and J.D. Rabinowitz, *One-Carbon Metabolism in Health and Disease.* Cell Metab, 2017. **25**(1): p. 27-42.

249.   Fekry, B., et al., *Ceramide Synthase 6 Is a Novel Target of Methotrexate Mediating Its Antiproliferative Effect in a p53-Dependent Manner.* PLoSOne, 2016. **11**(1): p. e0146618.

250.   Oleinik, N.V., et al., *Rho GTPases RhoA and Rac1 Mediate Effects of Dietary Folate on Metastatic Potential of A549 Cancer Cells through the Control of Cofilin Phosphorylation.* J Biol Chem, 2014.

251.   Schmitz, J.C., et al., *Impact of dietary folic acid on reduced folates in mouse plasma and tissues. Relationship to dideazatetrahydrofolate sensitivity.* Biochem Pharmacol, 1994. **48**(2): p. 319-25.

252.   Bielawski, J., et al., *Comprehensive quantitative analysis of bioactive sphingolipids by high-performance liquid chromatography-tandem mass spectrometry.* Methods Mol Biol, 2009. **579**: p. 443-67.

253.   Evans, A.M., Bridgewater B.R., Liu Q., Mitchell M.W., Robinson R.J., Dai H., Stewart S.J., DeHaven C.D. and Miller L.A.D., *High Resolution Mass Spectrometry Improves Data Quantity and Quality as Compared to Unit Mass Resolution Mass Spectrometry in High-Throughput Profiling Metabolomics.* Metabolomics, 2014. **4**(2): p. 1-7.

254.   Oleinik, N.V., et al., *Rho GTPases RhoA and Rac1 mediate effects of dietary folate on metastatic potential of A549 cancer cells through the control of cofilin phosphorylation.* The Journal of biological chemistry, 2014. **289**(38): p. 26383-26394.

255. Hou, Z. and L.H. Matherly, *Biology of the major facilitative folate transporters SLC19A1 and SLC46A1.* Curr Top Membr, 2014. **73**: p. 175-204.

256. Matherly, L.H., Z. Hou, and Y. Deng, *Human reduced folate carrier: translation of basic biology to cancer etiology and therapy.* Cancer Metastasis Rev, 2007. **26**(1): p. 111-28.

257. Jiang, H., et al., *Sex-specific dysregulation of cysteine oxidation and the methionine and folate cycles in female cystathionine gamma-lyase null mice: a serendipitous model of the methylfolate trap.* Biol Open, 2015. **4**(9): p. 1154-62.

258. Lee, W.S., et al., *Effects of female sex hormones on folic acid-induced anti-angiogenesis.* Acta Physiol (Oxf), 2018. **222**(4): p. e13001.

259. Kopp, M., R. Morisset, and M. Rychlik, *Characterization and Interrelations of One-Carbon Metabolites in Tissues, Erythrocytes, and Plasma in Mice with Dietary Induced Folate Deficiency.* Nutrients, 2017. **9**(5).

260. Obeid, R., W. Holzgreve, and K. Pietrzik, *Is 5-methyltetrahydrofolate an alternative to folic acid for the prevention of neural tube defects?* J Perinat Med, 2013. **41**(5): p. 469-83.

261. Farrell, C.J., S.H. Kirsch, and M. Herrmann, *Red cell or serum folate: what to do in clinical practice?* Clin Chem Lab Med, 2013. **51**(3): p. 555-69.

262. Hartman, B.A., et al., *Neither folic acid supplementation nor pregnancy affects the distribution of folate forms in the red blood cells of women.* J Nutr, 2014. **144**(9): p. 1364-9.

263. Norheim, F., et al., *Genetic, dietary, and sex-specific regulation of hepatic ceramides and the relationship between hepatic ceramides and IR.* J Lipid Res, 2018. **59**(7): p. 1164-1174.

264. Couttas, T.A., et al., *Age-Dependent Changes to Sphingolipid Balance in the Human Hippocampus are Gender-Specific and May Sensitize to Neurodegeneration.* J Alzheimers Dis, 2018. **63**(2): p. 503-514.

265. Eberle, M., et al., *Regulation of ceramide synthase 6 in a spontaneous experimental autoimmune encephalomyelitis model is sex dependent.* Biochem Pharmacol, 2014. **92**(2): p. 326-35.

266.   Bouchon, B., J. Portoukalian, and H. Bornet, *Sex-specific difference of the galabiosylceramide level in the glycosphingolipids of human thyroid.* Biochim Biophys Acta, 1985. **836**(1): p. 143-52.

267.   Musso, G., et al., *Bioactive Lipid Species and Metabolic Pathways in Progression and Resolution of Nonalcoholic Steatohepatitis.* Gastroenterology, 2018. **155**(2): p. 282-302 e8.

268.   Mullen, T.D., et al., *Selective knockdown of ceramide synthases reveals complex interregulation of sphingolipid metabolism.* J Lipid Res, 2011. **52**(1): p. 68-77.

269.   Ganz, A.B., et al., *Genetic impairments in folate enzymes increase dependence on dietary choline for phosphatidylcholine production at the expense of betaine synthesis.* FASEB J, 2016. **30**(10): p. 3321-3333.

270.   Reo, N.V., M. Adinehzadeh, and B.D. Foy, *Kinetic analyses of liver phosphatidylcholine and phosphatidylethanolamine biosynthesis using (13)C NMR spectroscopy.* Biochim Biophys Acta, 2002. **1580**(2-3): p. 171-88.

271.   Siow, D.L. and B.W. Wattenberg, *Mammalian ORMDL proteins mediate the feedback response in ceramide biosynthesis.* J Biol Chem, 2012. **287**(48): p. 40198-204.

272.   Vacaru, A.M., et al., *Sphingomyelin synthase-related protein SMSr controls ceramide homeostasis in the ER.* J Cell Biol, 2009. **185**(6): p. 1013-27.

273.   Bourteele, S., et al., *Tumor necrosis factor induces ceramide oscillations and negatively controls sphingolipid synthases by caspases in apoptotic Kym-1 cells.* J Biol Chem, 1998. **273**(47): p. 31245-51.

274.   Deevska, G.M., et al., *Novel Interconnections in Lipid Metabolism Revealed by Overexpression of Sphingomyelin Synthase-1.* J Biol Chem, 2017. **292**(12): p. 5110-5122.

275.   van Meer, G., J. Wolthoorn, and S. Degroote, *The fate and function of glycosphingolipid glucosylceramide.* Philos Trans R Soc Lond B Biol Sci, 2003. **358**(1433): p. 869-73.

276.   Merrill, A.H., Jr., *Sphingolipid and glycosphingolipid metabolic pathways in the era of sphingolipidomics.* Chem Rev, 2011. **111**(10): p. 6387-422.

277.   Shayman, J.A., *Targeting Glucosylceramide Synthesis in the Treatment of Rare and Common Renal Disease.* Semin Nephrol, 2018. **38**(2): p. 183-192.

278.   Gaignard, P., et al., *Effect of Sex Differences on Brain Mitochondrial Function and Its Suppression by Ovariectomy and in Aged Mice.* Endocrinology, 2015. **156**(8): p. 2893-904.

279.   Kennedy, D.O., *B Vitamins and the Brain: Mechanisms, Dose and Efficacy--A Review.* Nutrients, 2016. **8**(2): p. 68.

280.   Moat, S.J., et al., *Effect of riboflavin status on the homocysteine-lowering effect of folate in relation to the MTHFR (C677T) genotype.* Clin Chem, 2003. **49**(2): p. 295-302.

281.   Pettus, B.J., et al., *The coordination of prostaglandin E2 production by sphingosine-1-phosphate and ceramide-1-phosphate.* Mol Pharmacol, 2005. **68**(2): p. 330-5.

282.   Li, X., K.A. Becker, and Y. Zhang, *Ceramide in redox signaling and cardiovascular diseases.* Cell Physiol Biochem, 2010. **26**(1): p. 41-8.

283.   Bose, R., et al., *Ceramide synthase mediates daunorubicin-induced apoptosis: an alternative mechanism for generating death signals.* Cell, 1995. **82**(3): p. 405-14.

284.   Hla, T. and R. Kolesnick, *C16:0-ceramide signals insulin resistance.* Cell metabolism, 2014. **20**(5): p. 703-705.

285.   Fekry, B., et al., *C16-ceramide is a natural regulatory ligand of p53 in cellular stress response.* Nat Commun, 2018. **9**(1): p. 4149.

286.   Fekry, B., et al., *CerS6 Is a Novel Transcriptional Target of p53 Protein Activated by Non-genotoxic Stress.* J Biochem, 2016. **291**(32): p. 16586-16596.

287.   Kim, M.H., et al., *Hepatic inflammatory cytokine production can be regulated by modulating sphingomyelinase and ceramide synthase 6.* Int J Mol Med, 2017. **39**(2): p. 453-462.

288.   Summers, S.A., *Ceramides in insulin resistance and lipotoxicity.* Prog Lipid Res, 2006. **45**(1): p. 42-72.

289. Havel, R.J., H.A. Eder, and J.H. Bragdon, *The distribution and chemical composition of ultracentrifugally separated lipoproteins in human serum.* J Clin Invest, 1955. **34**(9): p. 1345-53.

290. Quehenberger, O. and E.A. Dennis, *The human plasma lipidome.* N Engl J Med, 2011. **365**(19): p. 1812-23.

291. Licholai, J.A., et al., *Why Do Mice Overeat High-Fat Diets? How High-Fat Diet Alters the Regulation of Daily Caloric Intake in Mice.* Obesity (Silver Spring), 2018. **26**(6): p. 1026-1033.

292. Hu, S.W., L.; Togo, J.; Yang, D.; Xu, Y.; Wu, Y.; Douglas, A.; Speakman, J.R., *The carbohydrate-insulin model does not explain the impact of varying dietary macronutrients on the body weight and adiposity of mice.* Mol Metab, 2020. **32**: p. 27-43.

293. Senkal, C.E., et al., *Ceramide Is Metabolized to Acylceramide and Stored in Lipid Droplets.* Cell Metab, 2017. **25**(3): p. 686-697.

294. Tilg, H. and A.M. Diehl, *Cytokines in alcoholic and nonalcoholic steatohepatitis.* N Engl J Med, 2000. **343**(20): p. 1467-76.

295. Fucho, R., et al., *ASMase regulates autophagy and lysosomal membrane permeabilization and its inhibition prevents early stage non-alcoholic steatohepatitis.* J Hepatol, 2014. **61**(5): p. 1126-34.

296. Kasumov, T., et al., *Ceramide as a mediator of non-alcoholic Fatty liver disease and associated atherosclerosis.* PLoS One, 2015. **10**(5): p. e0126910.

297. Kurek, K., et al., *Inhibition of ceramide de novo synthesis reduces liver lipid accumulation in rats with nonalcoholic fatty liver disease.* Liver Int, 2014. **34**(7): p. 1074-83.

298. Holland, W.L. and S.A. Summers, *Sphingolipids, insulin resistance, and metabolic disease: new insights from in vivo manipulation of sphingolipid metabolism.* Endocr Rev, 2008. **29**(4): p. 381-402.

299. Kotronen, A., et al., *Comparison of lipid and fatty acid composition of the liver, subcutaneous and intra-abdominal adipose tissue, and serum.* Obesity (Silver Spring), 2010. **18**(5): p. 937-44.

300. Llacuna, L., et al., *Critical role of acidic sphingomyelinase in murine hepatic ischemia-reperfusion injury.* Hepatology, 2006. **44**(3): p. 561-72.

301. Teruel, T., R. Hernandez, and M. Lorenzo, *Ceramide mediates insulin resistance by tumor necrosis factor-alpha in brown adipocytes by maintaining Akt in an inactive dephosphorylated state.* Diabetes, 2001. **50**(11): p. 2563-71.

302. Cowart, L.A. and Y.A. Hannun, *Selective substrate supply in the regulation of yeast de novo sphingolipid synthesis.* J Biol Chem, 2007. **282**(16): p. 12330-40.

303. Chatterjee, S., et al., *Inhibition of glycosphingolipid synthesis ameliorates atherosclerosis and arterial stiffness in apolipoprotein E-/- mice and rabbits fed a high-fat and -cholesterol diet.* Circulation, 2014. **129**(23): p. 2403-13.

304. Chavez, J.A., et al., *Ceramides and glucosylceramides are independent antagonists of insulin signaling.* J Biol Chem, 2014. **289**(2): p. 723-34.

305. Fuller, M., *Sphingolipids: the nexus between Gaucher disease and insulin resistance.* Lipids Health Dis, 2010. **9**: p. 113.

306. Schooneman, M.G., et al., *Acylcarnitines: reflecting or inflicting insulin resistance?* Diabetes, 2013. **62**(1): p. 1-8.

307. Schooneman, M.G., et al., *Plasma acylcarnitines inadequately reflect tissue acylcarnitine metabolism.* Biochim Biophys Acta, 2014. **1841**(7): p. 987-94.

308. Calzada, E., O. Onguka, and S.M. Claypool, *Phosphatidylethanolamine Metabolism in Health and Disease.* Int Rev Cell Mol Biol, 2016. **321**: p. 29-88.

309. Patel, D. and S.N. Witt, *Ethanolamine and Phosphatidylethanolamine: Partners in Health and Disease.* Oxid Med Cell Longev, 2017. **2017**: p. 4829180.

310. Pettus, B.J., C.E. Chalfant, and Y.A. Hannun, *Sphingolipids in inflammation: roles and implications.* Curr Mol Med, 2004. **4**(4): p. 405-18.

311. Lamour, N.F. and C.E. Chalfant, *Ceramide-1-phosphate: the "missing" link in eicosanoid biosynthesis and inflammation.* Mol Interv, 2005. **5**(6): p. 358-67.

312. Hyde, R., et al., *Ceramide down-regulates System A amino acid transport and protein synthesis in rat skeletal muscle cells.* FASEB J, 2005. **19**(3): p. 461-3.

313. Speakman, J.R., *Use of high-fat diets to study rodent obesity as a model of human obesity.* Int J Obes (Lond), 2019. **43**(8): p. 1491-1492.

314. Ishibashi, Y., A. Kohyama-Koganeya, and Y. Hirabayashi, *New insights on glucosylated lipids: metabolism and functions.* Biochim Biophys Acta, 2013. **1831**(9): p. 1475-85.

315. Aerts, J.M., et al., *Pharmacological inhibition of glucosylceramide synthase enhances insulin sensitivity.* Diabetes, 2007. **56**(5): p. 1341-9.

316. Zhao, H., et al., *Inhibiting glycosphingolipid synthesis improves glycemic control and insulin sensitivity in animal models of type 2 diabetes.* Diabetes, 2007. **56**(5): p. 1210-8.

317. Bietrix, F., et al., *Inhibition of glycosphingolipid synthesis induces a profound reduction of plasma cholesterol and inhibits atherosclerosis development in APOE*3 Leiden and low-density lipoprotein receptor-/- mice.* Arterioscler Thromb Vasc Biol, 2010. **30**(5): p. 931-7.

318. Figueiredo, J.C., et al., *Folic acid and risk of prostate cancer: results from a randomized clinical trial.* J Natl Cancer Inst, 2009. **101**(6): p. 432-5.

319. Li, W., et al., *Folic acid prevents cardiac dysfunction and reduces myocardial fibrosis in a mouse model of high-fat diet-induced obesity.* Nutr Metab (Lond), 2017. **14**: p. 68.

320. Bligh, E.G. and W.J. Dyer, *A rapid method of total lipid extraction and purification.* Can J Biochem Physiol, 1959. **37**(8): p. 911-7.

321. Kane, A.E., et al., *Sex differences in the response to dietary restriction in rodents.* Curr Opin Physiol, 2018. **6**: p. 28-34.

322. Pettersson, U.S., et al., *Female mice are protected against high-fat diet induced metabolic syndrome and increase the regulatory T cell population in adipose tissue.* PLoS One, 2012. **7**(9): p. e46057.

323. Dakin, R.S., et al., *Estrogens protect male mice from obesity complications and influence glucocorticoid metabolism.* Int J Obes (Lond), 2015. **39**(10): p. 1539-47.

324.   Larson, K.R., et al., *Sex Differences in the Hormonal and Metabolic Response to Dietary Protein Dilution.* Endocrinology, 2017. **158**(10): p. 3477-3487.

325.   Cuthbert, C.E., J.E. Foster, and D.D. Ramdath, *A maternal high-fat, high-sucrose diet alters insulin sensitivity and expression of insulin signalling and lipid metabolism genes and proteins in male rat offspring: effect of folic acid supplementation.* Br J Nutr, 2017. **118**(8): p. 580-588.

326.   Zhao, M., et al., *Chronic folate deficiency induces glucose and lipid metabolism disorders and subsequent cognitive dysfunction in mice.* PLoS One, 2018. **13**(8): p. e0202910.

327.   Summers, S.A., *Could Ceramides Become the New Cholesterol?* Cell Metab, 2018. **27**(2): p. 276-280.

328.   Kusunoki, M., et al., *Relationship between serum concentrations of saturated fatty acids and unsaturated fatty acids and the homeostasis model insulin resistance index in Japanese patients with type 2 diabetes mellitus.* J Med Invest, 2007. **54**(3-4): p. 243-7.

329.   Puri, P., et al., *A lipidomic analysis of nonalcoholic fatty liver disease.* Hepatology, 2007. **46**(4): p. 1081-90.